EFFECT OF OPERATING CONDITIONS ON COLOR AND ANIONS REMOVAL FROM TEXTILE INDUSTRIAL EFFLUENT USING MEMBRANE DISTILLATION SYSTEM

Miss Pyae Phyo Kywe

จุฬาลงกรณ์มหาวิทยาลัย
CHULALONGKORN UNIVERSITY

A Thesis Submitted in Partial Fulfillment of the Requirements
for the Degree of Master of Engineering in Environmental Engineering
Department of Environmental Engineering
Faculty of Engineering
Chulalongkorn University
Academic Year 2018
Copyright of Chulalongkorn University

ผลของสภาวะการเดินระบบในการกำจัดสีและอิออนลบจากน้ำทิ้งอุตสาหกรรมฟอกย้อมโดยใช้ระบบเมมเบรนดิสทิลเลชั่น

น.ส.เป้ย โป คิว

Thesis Title   EFFECT OF OPERATING CONDITIONS ON COLOR
                      AND ANIONS REMOVAL FROM TEXTILE
                      INDUSTRIAL EFFLUENT USING MEMBRANE
                      DISTILLATION SYSTEM
By   Miss Pyae Phyo Kywe
Field of Study   Environmental Engineering
Thesis Advisor   Associate Professor CHAVALIT RATANATAMSKUL,
                      Ph.D.

          Accepted by the Faculty of Engineering, Chulalongkorn University in Partial
Fulfillment of the Requirement for the Master of Engineering

                      .... Dean of the Faculty of Engineering
                      (Professor SUPOT TEACHAVORASINSKUN, Ph.D.)

THESIS COMMITTEE
                      .... Chairman
                      (Assistant Professor SARUN TEJASEN, Ph.D.)
                      .... Thesis Advisor
                      (Associate Professor CHAVALIT RATANATAMSKUL,
                      Ph.D.)
                      .... Examiner
                      (Associate Professor VIBOON
                      SRICHAROENCHAIKUL, Ph.D.)
                      .... Examiner
                      (Jenyuk Lohwacharin, Ph.D.)
                      .... External Examiner
                      (Thanakorn Methatham, Ph.D.)

เปีย โป คิว :

ผลของสภาวะการเดินระบบในการกำจัดสีและอิออนลบจากน้ำทิ้งอุตสาหกรรมฟอกย้อมโดยใช้ระบบเมมเบรนดิส
ทิลเลชั่น. (EFFECT OF OPERATING CONDITIONS ON COLOR AND
ANIONS REMOVAL FROM TEXTILE INDUSTRIAL EFFLUENT
USING MEMBRANE DISTILLATION SYSTEM) อ.ที่ปรึกษาหลัก : ชวลิต
รัตนธรรมสกุล

ปัญหานึ่งในมลพิษหลักของน้ำเสียสิ่งทอได้แก่ปัญหาด้านสีและสารอินทรีย์
การพัฒนาระบบบำบัดน้ำเสียและการนำน้ำกลับมาใช้ใหม่ยังคงมีความท้าทาย เนื่องจากความขาดแคลนน้ำในโลก
ในกระบวนการบำบัดน้ำเสียจากโรงงานสิ่งทออาจมีทางเลือกหลายอย่าง
สำหรับงานวิจัยนี้การใช้เมมเบรนแบบการกลั่นน้ำเป็นแนวคิดหลักในการวิจัยนี้ จุดเด่นของระบบนี้คือลักษณะของเมมเบรน
พารามิเตอร์การทำงาน (อุณหภูมิและอัตราการไหล) และประสิทธิภาพในการบำบัด น้ำเสียจากโรงงานผลิตน้ำเสียสังเคราะห์
(Reactive Black-5 และ Reactive Blue-19) และน้ำทิ้งจากโรงงานอุตสาหกรรมสิ่งทอ
โดยงานวิจัยนี้ได้ศึกษาคุณสมบัติของเมมเบรนโดยเทคนิคกล้องจุลทรรศน์แบบส่องกราด การวัดมุมสัมผัส การวัดค่าศักย์ซีต้า
และความพรุนของเมมเบรน จากผลการศึกษาที่ได้พบว่า มุมการสัมผัสของเมมเบรนหลังการใช้งานมีค่ามากกว่า 90 องศา
แสดงให้เห็นว่าวัสดุยังคงมีคุณสมบัติไม่ชอบน้ำหลังการบำบัดและศักยภาพของซีตายังแสดงสมบัติของสารประกอบไอออนประ
จุลบที่ผิวหน้าน้ำอีก ด้วย ในแง่ของพารามิเตอร์การทำงาน อุณหภูมิของน้ำเข้าระบบ
และความเร็วในการไหลเวียนของของน้ำส่งผลต่อค่าฟลักซ์การซึมผ่านที่ได้ของเมมเบรน อุณหภูมิน้ำที่เพิ่มขึ้น (40°C,
50°Cและ 60°C) สามารถเพิ่มปริมาณการซึมผ่านของน้ำได้ถึงประมาณ 4 เท่าที่ 60°C เมื่อเทียบกับอุณหภูมิ 40°C
ความเร็วในการไหลเวียนของน้ำที่เพิ่มขึ้นสามารถให้ผลของการซึมผ่านของน้ำที่เพิ่มขึ้น (สูงสุด 80% และ 50% ที่ 0.15
m / s) มากกว่า 0.05 เมตร / วินาที ฟลักซ์ของน้ำเสียที่เกิดขึ้นจริงมีค่าน้อยกว่าน้ำเสียสังเคราะห์ประมาณ 48%
ภายใต้พารามิเตอร์ปฏิบัติการเดียวกัน ประสิทธิภาพในการกำจัดสีอยู่ในช่วง 96% ถึง 98%
แม้ว่าความเข้มข้นของสีในน้ำเสียจะเปลี่ยนแปลงไปก็ตาม การวิเคราะห์พารามิเตอร์อื่น ค่า pH การนำไฟฟ้า
ความเข้มข้นของแอนไอออนและสารอินทรีย์ TOC ถูกนำมาศึกษาในครั้งนี้
เช่นเดียวกับผลการเก็บรวบรวมพารามิเตอร์ของน้ำที่ซึมผ่านมีค่าต่ำกว่ามาตรฐานการบำบัดน้ำเสียจากโรงงานอุตสาหกรรม
กระทรวงอุตสาหกรรม 2560 ดังนั้นการใช้ระบบ DCMD
ร่วมกับพลังงานทดแทนจะสามารถเพิ่มประสิทธิภาพของการเตรียมเมมเบรนและการเดินระบบเมมเบรนแบบ DCMD
(ในแง่ของ spacers สภาพความขุ่นและวัสดุยื่อหุ้มเยื่อใหม่) และสภาวะของกระบวนการทำงาน เป็นต้น

สาขาวิชา	วิศวกรรมสิ่งแวดล้อม	ลายมือชื่อนิสิต ....
ปีการศึกษา	2561	ลายมือชื่อ อ.ที่ปรึกษาหลัก ....

5970481921 : MAJOR ENVIRONMENTAL ENGINEERING
KEYWORD: Cross-flow Velocity, Color removal, Feed Temperature, Direct Contact Membrane Distillation, Flux

Pyae Phyo Kywe : EFFECT OF OPERATING CONDITIONS ON COLOR AND ANIONS REMOVAL FROM TEXTILE INDUSTRIAL EFFLUENT USING MEMBRANE DISTILLATION SYSTEM. Advisor: Assoc. Prof. CHAVALIT RATANATAMSKUL, Ph.D.

One of the main pollution from textile wastewater is the dyeing wastewater containing color and organic matters. To develop wastewater treatment systems and to reuse the water are still challenged because of the scarcity of water in the world. Among the treatment methods of textile wastewater, membrane distillation was used as the concept of this research. The focus points of the direct contact membrane distillation system are the membrane characteristics, operating parameters (temperature and flow rate) and treatment efficiency. The synthetic dye wastewater (reactive black-5 and reactive blue-19) and real textile effluent were used as the feed wastewater. In this research, SEM imaging, the contact angle, the zeta potential and the porosity of the membrane were taken to investigate the membrane characteristics and the fouling conditions. The contact angle (greater than 90 degrees) showed that the material still had the hydrophobic properties after treatment and the zeta potential showed also the anions property of the material.

In terms of operating parameters, the feed temperature and flow rate can significantly affect the permeate flux. The increased feed temperature (40 °C, 50°C, and 60°C) can also increase the permeate flux up to about 4 times at 60°C, compared to that of 40°C. The increased cross-flow velocity can give the results of increased permeate flux (up to 80% and 50% at 0.15 m/s) more than 0.05 m/s. The flux of real wastewater is about 48% lesser than the synthetic wastewater under the same operating parameters. The color removal efficiency is in the range of 96% to 98%, although the feed color concentrations were changed. Another parameter analysis; pH, conductivity, anions, and TOC were also taken in this study. As with the collected results, the permeate water parameters are lower than the Industrial Effluent Standards B.E. 2560 by the Ministry of Industry. To use in the site and implement, the direct contact membrane distillation system should be considered with the renewable energy, the optimization of membrane preparations (spacers, fouling conditions and the novel membrane material) and the process conditions.

| Field of Study: | Environmental Engineering | Student's Signature .... |
| Academic Year: | 2018 | Advisor's Signature .... |

ACKNOWLEDGEMENTS

TABLE OF CONTENTS

Page

จุฬาลงกรณ์มหาวิทยาลัย

CHULALONGKORN UNIVERSITY

LIST OF TABLES

จุฬาลงกรณ์มหาวิทยาลัย
CHULALONGKORN UNIVERSITY

LIST OF FIGURES

Page

Nomenclature

B	Geometric factor
d_{max}	Pore size (m)
LEP	Liquid entry pressure (kPa)
T_f	Feed temperature (K)
T_p	Permeate temperature (K)
T_{mf}	Feed membrane temperature (K)
T_{mp}	Permeate membrane temperature (K)
TPC	Temperature Polarization Coefficient
J	Flux ($kg/m^2.hr$)
C_w	Overall mass transfer coefficient ($kg/m^2. s. Pa$)
P	Pressure (Pa)
X^w_f	Mole fraction of water
ΔT_{th}	Threshold temperature (K)
ΔH_v	Molar volume of vaporization of water
R	Real gas constant ($8.314472\ Jmol^{-1}K^{-1}$)
K_n	Knudsen's number
K_B	Boltzmann constant ($1.38\times10^{-23}\ JK^{-1}$)
D	Diffusivity coefficient ($m^2. s$)
P_{air}	Air pressure inside the pores (Pa)
Q_v	Latent heat transfer (W/m^2)
Q_c	Conduction heat transfer (W/m^2)
H	Effective heat transfer coefficient
h_f	Heat transfer coefficient from the feed
h_p	Heat transfer coefficient from the permeate
K_m	Thermal conductivity coefficient of membrane material
K_g	Thermal conductivity of gas diffusing in the membrane (W/m.K)
K_s	Thermal conductivity of membrane material (W/m.K)

d_h	Hydraulic diameter (m)
Nu	Nusselt number
Re	Reynolds number
Pr	Prandtl number
C_p	Specific heat capacity(J/kg.K)
k_f	Thermal conductivity (W/m.K)
v	Velocity (m/s)
PVDF	Polyvinylidene fluoride
MW	Molecular Weight (kg)

Greek Letters

γ	Liquid surface tension
Θ	Solid/ liquid contact angle
ε	Porosity (%)
τ	Tortuosity
α_f	Activity of water
λ	Mean free path (m)
σ	Collision diameter of the molecule (m)
μ	Viscosity (kg/m.s)
ρ_m	Density of membrane (kg/m^3)
ρ_p	Density of material (kg/m^3)

Subscripts and Superscripts

f	Feed side
p	Permeate side
m	Membrane surface
b	Bulk side
mf	Feed membrane surface
mp	Permeate membrane surface

CHAPTER 1

INTRODUCTION

1.1 Background

Nowadays the increased demand and growing scarcity of fresh water have been recognized to have significant impacts on the world. The development of wastewater treatment systems and water treatment are still needed to reuse water, disposal and get the clean water. Many researchers are trying to come out the efficient ways and methods.

Among the development methods, membrane processes are becoming popular. These processes are also included for wastewater treatment, water treatment and desalination water such as microfiltration (MF), ultrafiltration (UF), nanofiltration (NF), reverse osmosis (RO), electrodialysis (ED), capacitive deionization (CDI), etc. Most of the systems are using the transmembrane osmotic pressure as the driving force. Some of the driving forces are concentration, electrical or the chemical potential. As a new research, another type is the membrane distillation (MD). It is driven by the vapor partial pressure through a microporous hydrophobic membrane unlike the other types of former membranes. The hydrophobic property is that the vapor only can pass through the membrane and not liquid solution being distilled. The vapor from the hot side can permeate through the pores of the membrane to the permeate side because of the vapor pressure difference between these two sides.

Membrane Distillation has become the convenient way for the energy conservation method, like a solar energy system. Membrane Distillation (MD) has still a challenge for the treatment of industrial wastewater containing many chemical components. Moreover, the theory and models of membrane distillation (MD) are still under investigation; therefore, further studies should be investigated for a successful scale-up.

The objective of this work is to study the feasibility on the application of Membrane Distillation (MD) process for treatment of textile industrial wastewater in order to recycle and reuse of textile effluent.

1.2 Objectives

1. To investigate the effects of varied temperature and cross flow velocity on color and anions removal by direct contact membrane distillation process for the synthetic dyehouse wastewater (blue and black reactive dyes)

2. To investigate the effects of initial concentrations and pH on color and anions removal by direct contact membrane distillation process for the synthetic dyehouse wastewater (blue and black reactive dyes)

3. To investigate the fouling condition by the scaling status of Membrane Distillation system in treating the synthetic dyehouse wastewater (blue and black reactive dyes)

4. To know the feasibility of direct contact membrane distillation operation for color and anions removal from textile industrial effluent

1.3 Scope of Investigations

1. Using the lab scale direct contact membrane distillation reactor
2. Using two synthetic reactive dyes (reactive black 5 and reactive blue 19)
3. Using the cold bath, the condenser, the pressure gauge, the hot bath and the flat sheet hydrophobic PVDF membrane
4. Using the controlling parameters in terms of the feed temperature and the cross-flow velocity
5. Using the real textile effluent from a textile industry in Chonburi province

1.4 Experimental outcomes

1. Develop the direct contact membrane distillation system for effectively treatment of textile industrial effluent

2. Obtain the optimal operating condition in terms of the feed temperature and the cross- flow velocity for direct contact membrane distillation operation in treating textile effluent

CHAPTER 2

THEORIES AND LITERATUREREVIEWS

2.1 Membrane Process

At present, there are several types of membranes with different driving forces for water treatment. Types of various membrane processes are shown in Table 2.1.

Table 2.1 Several types of membrane processes with different driving forces

Membrane processes	Types of each membrane process
Pressure driven membrane process	Microfiltration, Ultrafiltration, Nanofiltration, Reverse Osmosis
Osmotically driven membrane process	Forward Osmosis
Thermally driven membrane process	Membrane Distillation, membrane contactor, thermo-osmosis
Electrically driven membrane process	Electrodialysis
Concentration driven membrane process	Pervaporation, Dialysis, Gas separation

2.2 Development of Membrane Distillation Process

Since 1963, membrane distillation (MD) was introduced, it has been developed in laboratory-scale for various purposes. In recent years, it gets an attention again in the academic field and for the commercial use. Some reports and researches came out for different uses and parameters of membrane distillation to be a practical usage on the ground.(Khayet, M., 2011)

Membrane Distillation (MD) is one of the non-isothermal membrane separation process from various membrane processes. The vapor pressure difference between the hydrophobic porous membrane surfaces makes the separation process possible.

Membrane distillation has been tested and researched in different fields e.g., desalination, food production, medical field. In the food industry, the concentration of food products or derivatives for fruit juice, flavor/aromatic compounds, liquid food and whey protein are also included. And other applications are the removal of ethanol and other volatile compounds from the fermentation broth. For the wastewater treatment, the wastewater is mainly included from the textile industry, olive mill, oil and gas industry, mining industry, dairy industry, coal gasification and rubber plant industry(Thomas, N. et al., 2017).

Membrane distillation are also researched to produce high purity water, concentration of ionic, colloid or other non-volatile aqueous solutions and removal of trace volatile organic compounds. The lower operating temperature than the conventional distillation process, the lower operating hydrostatic pressure than the pressure driven operating process, the less demanding membrane chemical properties and the high rejection factor achieved while containing no volatile solutes are as the advantages of MD. For the less use of energy, the waste heat and renewable energy sources can also be used and make the MD to combine with other processes (Khayet, M., 2011).

Depending on the types of separation by the heat and mass transfer, there are four configurations of membrane distillation; direct contact membrane distillation (DCMD), air-gap membrane distillation (AGMD), sweeping gas membrane distillation (SGMD) and vacuum membrane distillation (VMD).

Direct contact membrane distillation (DCMD) is mainly discussed in this research. It comprises three parts; hot feed side, non-wetted porous hydrophobic membrane material and the cold permeate side. The driving pressure is caused by the temperature difference between the hot side and the cold side. As a property of hydrophobicity, only vapor can pass through the media material.

2.3 Concept of Membrane distillation process

Membrane distillation process acts as a liquid-gas interface for the mass and heat transfer. The property of this membrane makes the physical barrier for the penetration of liquid into the membrane pores. For the condition of liquid-gas interface, the low thermal conductivity membrane is used for the efficient process.

The other physical characteristics of membranes like pore size, porosity and thickness are also needed to consider. The high permeability, high liquid entry pressure, low thermal conductivity, good chemical resistance and the heat stability are also counted for the efficient way (Belessiotis, V. et al., 2016).The liquid rejecting properties of membrane material (hydrophobic material) prevents the liquid penetrating into the pores, as the pressure of liquid does not exceed the minimum liquid entry pressure.

The generation of steam is not needed with too high energy consumption like the pervaporation process. The high pressure is also not considered like the reverse osmosis process. The energy consumption is convenient even with the waste energy (Jönsson, A. S. et al., 1985).

2.4 Membrane Distillation Configurations
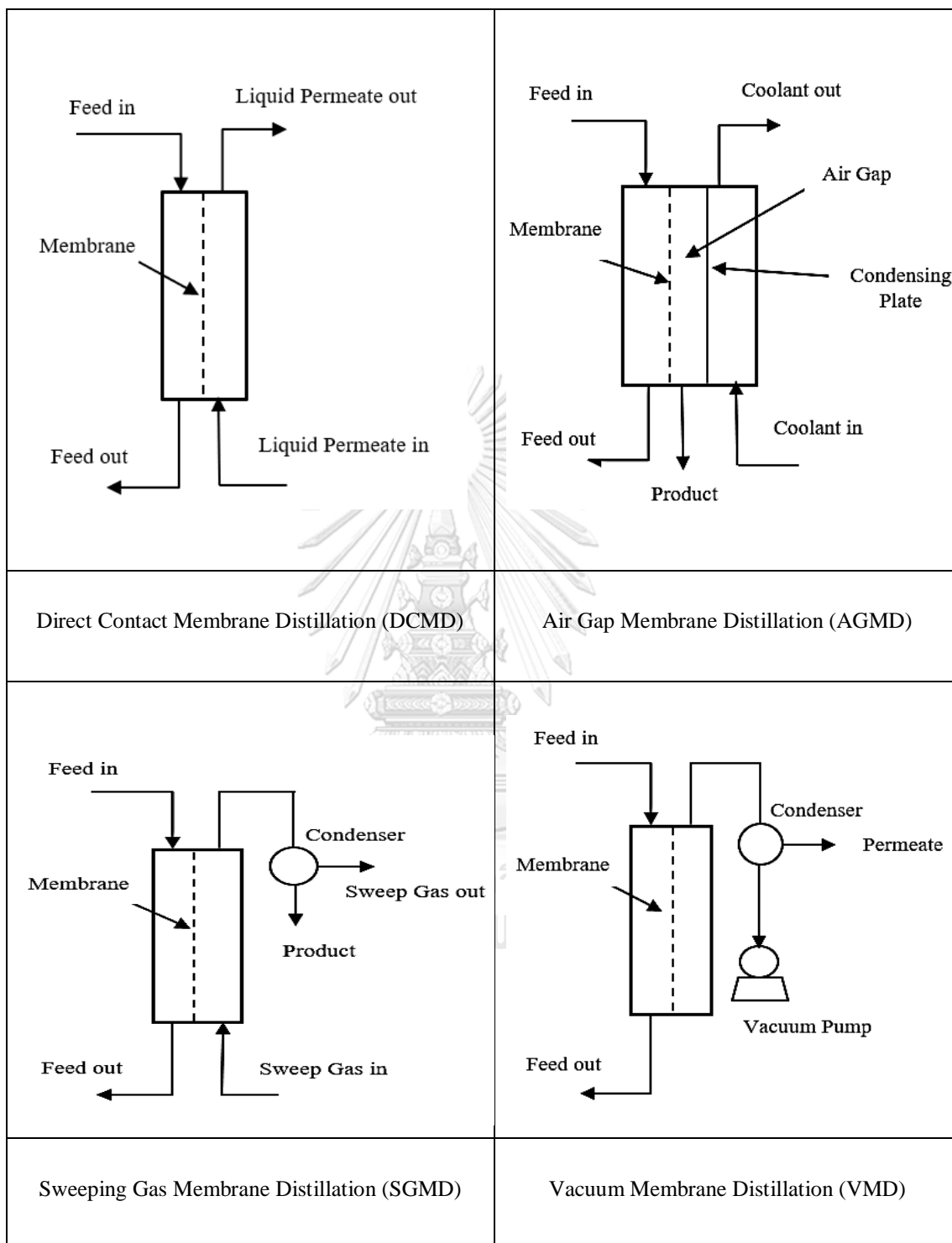
Figure 2.1 Membrane Distillation Configurations
(Ashoor, B. B. et al., 2016)

2.4.1 Direct Contact Membrane Distillation (DCMD)

This is the simplest configuration that can operate the separation process inside the MD module. The warm feed and permeate aqueous solution are directly contacted with the membrane. The transmembrane temperature difference is used as the driving force. The heat loss is occurred by conduction in this configure (Alkhudhiri, A. et al., 2012).

2.4.2 Air Gap Membrane Distillation (AGMD)

A stagnant air gap is added between the membrane and the condensation plate. According to this addition, the heat losses are reduced by air gap in this type. However, it can create the additional mass transfer resistance. Air-gap is around 2-10 mm (Onsekizoglu, P., 2012; Shirazi, A. et al., 2015).

2.4.3 Sweeping Gas Membrane Distillation (SGMD)

This configuration uses a cold inert gas to sweep the vapor at the permeate side and to carry the vapor molecules to the place where the condensation takes place. It is useful to remove volatile substances. Although it has a relatively low conductive heat loss, it is the least used system because of the operational cost of the external condensation system (Onsekizoglu, P., 2012).

2.4.4 Vacuum Membrane Distillation (VMD)

A vacuum is created at permeate side. In this type, the heat lost by conduction is negligible. The condensation takes place outside of the module like SGMD. It is useful for the separation of volatile solutions (Alkhudhiri, A. et al., 2012); (Shirazi, A. et al., 2015).

2.5 MD Membrane Characteristics

2.5.1 Membrane Materials

The membrane material must not be wetted and only vapor and non-condensable gases are present in the pores. The properties of membrane distillation (MD) material are with high water contact and maximum small pore size. The membrane material that is used in MD system is the hydrophobic material. The hydrophobic membranes are made from polytetrafluorethylene (PTFE), polyethylene (PE), polypropylene (PP) or polyvinylidene fluoride (PVDF). The membrane should

have low thermal conductivity and low resistance to mass transfer. It also has the resistance to chemicals (acids and bases) (El-Bourawi, M. S. et al., 2006; Alkhudhiri, A. et al., 2012).

2.5.2 Liquid Entry Pressure (LEP)

Liquid entry pressure is the minimum hydrostatic pressure which applies to the feed solution before it penetrates to the membrane pores. It is like a limitation of the hydrophobic forces to the membrane. LEP is different with each of the membrane material and prevents wetting of membrane.

$$LEP = \frac{-2B\gamma\cos(\theta)}{d_{max}} \qquad\qquad 2.1$$

B is the geometric factor by pore structure. The value is equal to 1 for the cylindrical pores. γ is the liquid surface tension, θ is the solid/ liquid contact angle and d_{max} is the pore size. For the high LEP, value can be obtained from the small maximum pore size and the high hydrophobicity (Belessiotis, V. et al., 2016).

2.5.3 Permeability

It is a function of applied temperature, membrane thickness, pore sizes, tortuosity, porosity, physical properties of the fluid, the geometry and its dimension and the average velocity of the fluid (Lawal, D. U. and Khalifa, A. E., 2014).

2.5.4 Membrane thickness

It is the predominant characteristic of the membrane for the obtaining flux amount. This is inversely proportional to the permeate flux. The thicker membrane having the higher amount of mass transfer resistance reduces to the permeate flux.

2.5.5 Membrane porosity

Porosity is one of the membrane characteristics that allows to pass the vapor through the pores of membrane. It is the ratio of the volume of pores to the volume of the membrane material. Higher porosity means that the membrane has a larger evaporation area.

$$\varepsilon = 1 - \frac{\rho_m}{\rho_p} \qquad\qquad 2.2$$

Where ε is the porosity, and ρ_m and ρ_p are the densities of membrane and material.

2.5.6   Membrane Tortuosity

It is the deviation of the pore structure. The expression is described as below (Srisurichan, S. et al., 2006).

$$\tau = \frac{(2 - \varepsilon)^2}{\varepsilon} \qquad\qquad 2.3$$

Where τ is the tortuosity and ε is the porosity.

2.5.7   Membrane mean pore size and distribution

Membrane pores are usually non-uniform. The permeate flux, the type of diffusion and the mechanism of mass transfer are dependent on the mean pore size and the mean free path through the membrane. The mean pore size is used to determine the flux. The use of mean pore size and pore size distribution are investigated for the flux. When the mean pore size is used, the prediction of flux should be taken carefully (Khayet, M. et al., 2004). But (Phattaranawik, J. et al., 2003) showed that the mean pore size and the distribution of pore size have the same effect on the transfer coefficient.

2.5.8   Temperature Polarization Coefficient (TPC)

The boundary layer of the membrane surface is a little different form the feed and permeate temperature. The temperature from the feed bulk (T_f) is higher than the temperature of the membrane surface of permeate side (T_{mf}) and the temperature of the membrane surface of permeate side (T_{mp}) is also higher than that of the permeate bulk (T_p). So, the temperature polarization is the ratio of the trans-membrane temperature difference to the bulk temperature difference (Martínez-Díez, L. and Vázquez-González, M. I., 1999). For the vapor pressure, the temperature on the surface is the function of driving force. The reducing TPC makes to increase the mass and heat flux. To improve the TPC, the flow design, the membrane

characteristics, the temperature difference and the spacers to promote can be controlled for the optimum flux (Manawi, Y. M. et al., 2014).
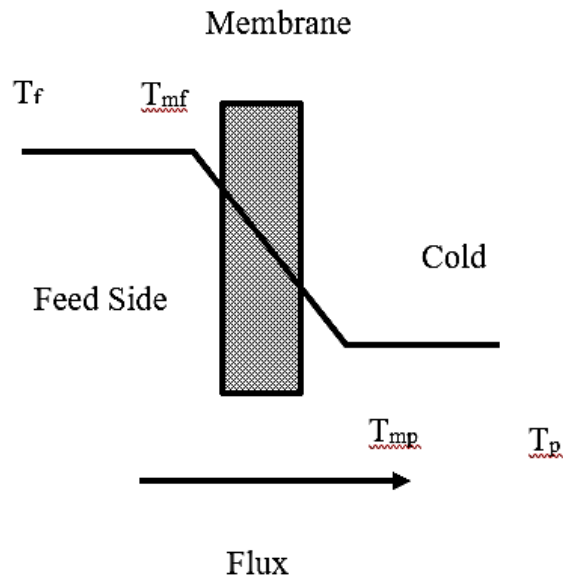
Figure 2.2 Heat Transfer Process in direct contact membrane distillation for Flux

The equation to calculate TPC can be shown in equation 2.4.

$$TPC = \frac{T_{mf}-T_{mp}}{T_f-T_p}$$
2.4

2.6 Mathematical Expressions of Direct Contact Membrane Distillation

Different technologies for the driving force can be used according to the types of membrane distillation. The side of the feed solution is similar, whereas the permeate side is changed for the different configurations.

During separation, the vapor from the feed side passes through the membrane pore and then condenses in the permeate side. According to the nature of the hydrophobic material, the liquid is prevented from passing through the membrane pores. The liquid-vapor interface occurs at the entrance and exit of the membrane surface. The main driving force for the direct contact membrane distillation (DCMD)

is the total partial vapor pressure at the feed and permeate of the pore ends caused by the temperature and concentration differences between the membrane surfaces (liquid-vapor interfaces). Temperature polarization coefficient and concentration polarization coefficient is for the mass transfer process of the direct contact membrane distillation (Martínez, L. and Rodríguez-Maroto, J. M., 2007).

The vaporization and the condensation take place with the temperature changes. So, the direct contact membrane distillation (DCMD) is the non-isothermal process. The heat of vaporization is considered for the changing from the liquid to the vapor at the interface of membrane feed side. When the vapor passed through the pore changes to the liquid at the interface of permeate membrane side, the heat of condensation is released. The conduction of heat transport also occurs while the vapor is passing through the pore of the membrane (Martínez, L. and Rodríguez-Maroto, J. M., 2007).

The following statements and the mathematical expressions are about the direct contact membrane distillation (DCMD) for the theoretical model. Both mass transfer and heat transfer processes take place simultaneously through the hydrophobic layer of membrane material.

2.6.1 Mass transfer

Mass transfer in direct contact membrane distillation makes the diffusion of vapor through the microporous material. The driving force for the direct contact membrane distillation (DCMD) is the partial vapor pressures through the membrane. The mass flux (J) is directly proportional to the vapor pressure difference through the membrane sides (Lawson, K. W. and Lloyd, D. R., 1997).

$$J \; \alpha \; \Delta P_m \qquad\qquad 2.5$$

The overall mass transfer coefficient dealing with the physical properties of membrane restricts the flux of membrane. The flux (J) depends on the overall mass transfer coefficient (membrane permeability) (C_w) and the pressure difference (ΔP_m).

$$J_w = C_w \Delta P_m \qquad\qquad 2.6$$

The transmembrane vapor pressure difference is expressed as;

$$\Delta P_m = P_{mf} - P_{mp} \qquad\qquad 2.7$$

The water vapor pressure in the membrane cannot be directly measured. So, the partial pressure difference is obtained by the transmembrane temperature difference. The vapor pressure difference through the membrane is below as; (Schofield, R. W. et al., 1987; Lawson, K. W. and Lloyd, D. R., 1997).

$$P_{mf} - P_{mp} = \left(\frac{dP}{dT}\right)(T_{mf} - T_{mp}) \qquad\qquad 2.8$$

The flux is obtained as with the temperature difference across the membrane for the pure water or very dilute and the bulk temperature difference $(T_f - T_p) \leq 10K$.

$$J_w = C_w \left[\frac{dP}{dT}\right](T_{mf} - T_{mp}) \qquad\qquad 2.9$$

For the more concentrated solution, the concentration of the solution makes the tension to the surface of the membrane and the reduction to the vapor pressure because of the dissolved species. The vapor partial pressure is modified by Raoult's law. According to the law, the driving force of the solution is obtained by the multiplying of the vapor pressure of the pure solvent at the same temperature and the mole fraction of the solvent. (Schofield, R. W. et al., 1987).

$$P_{solution} = P_{0(solvent)} \, x_{solvent} \qquad\qquad 2.10$$

$$P_{mf} - P_{mp} = \left(\frac{dP}{dT}\right)\left[(T_{mf} - T_{mp}) - \Delta T_{th}\right]x_f^w \alpha_f \qquad\qquad 2.11$$

The flux is varied by the concentration of the solution.

$$J_w = C_w \left[\frac{dP}{dT} \right] \left[(T_{mf} - T_{mp}) - \Delta T_{th} \right] x_f^w \alpha_f \qquad 2.12$$

x_f^w and α_f are the mole fraction of water and the activity of water. For the ideal aqueous solution, the flux is;

$$J_w = C_w \left[\frac{dP}{dT} \right] \left[(T_{mf} - T_{mp}) - \Delta T_{th} \right] \left(1 - x_f^{solute} \right) \qquad 2.13$$

(Schofield, R. W. et al., 1987)have showed that the threshold temperature, ΔT_{th}, is important for the concentrated solution.

$$\Delta T_{th} = \frac{RT^2}{M_w \Delta H_v} \frac{x_{mf} - x_{mp}}{1 - x_m} \qquad 2.14$$

$\frac{dP}{dT}$ can be evaluated with the T_m (average temperature in the membrane) by the Clausius-Clapeyron equation. The vapor pressure for the pure water at the temperature in the membrane; (Schofield, R. W. et al., 1987)

$$\left[\frac{dP}{dT} \right]_{T_m} = \left[\frac{\Delta H_v}{RT_m^2} P_{vapor} \right]_{T_m} \qquad 2.15$$

ΔH_v, the molar volume of vaporization of water is $\Delta H_v = 1.7535 T_m + 2024.3$

R is the real gas constant (8.314472 Jmol^{-1}K^{-1})

$$T_\mu = \frac{T_{\mu f} + T_{\mu \pi}}{2} \qquad 2.16$$

For the saturation water vapor pressure, Antoine equation can be used.

$$P_{vapor} = \exp\left(23.238 - \frac{3841}{T_m - 45} \right) \qquad 2.17$$

There is no significant concentration polarization near feed side of the membrane for the pure water. But for the concentrated solution or, the solution which contained one or more components, the concentration polarization is needed to consider on the feed side. The solute concentration near the membrane is getting higher than the feed side with the separation time going on. The overall mass transfer coefficient is increased, and the membrane material will be easily wetted by the high concentration nearby membrane. The resistances are dealing with the diffusivity type of different flows by the collisions between molecules and other molecules or pore wall of membrane. According to the overall of many researches, the diffusion through the membrane can be divided into the three mechanisms(Lawson, K. W. and Lloyd, D. R., 1997; Belessiotis, V. et al., 2016).

1. Knudsen type of flow model
2. Molecular Type of flow model
3. Transition type of flow model (Knudsen-molecular type of flow model)

The Knudsen's number (K_n) and the mean free path (λ) are used for choosing the flow type. The Knudsen's number is defined as the ratio of the mean free path of molecules to the pore size of the membrane.

$$K_n = \frac{\lambda}{d_p}$$
2.18

The mean free path is given as below;

$$\lambda = \frac{k_B T_m}{\sqrt{2} \pi P_m \sigma^2}$$
2.19

K_B is the Boltzmann constant 1.38×10^{-23} JK^{-1}. T_m and P_m are the absolute mean temperature (K) and pressure (Pa) in the membrane. The total pressure in membrane for the direct contact membrane distillation is 1 atm with neglecting of the viscous flow because the feed and permeate aqueous solution is contacting the membrane under the atmospheric condition (Khayet, M. et al., 2004). σ is the collision diameter of the molecule (2.61 A° for vapor water). (Lawson, K. W. and

Lloyd, D. R., 1997; Lawal, D. U. and Khalifa, A. E., 2014; Belessiotis, V. et al., 2016).

According to the Knudsen's number (K_n) and the mean free path (λ) values, the flow types are represented as;

$K_n > 1$ or $d_p < \lambda$ **(Knudsen type of flow model)**

The mean free path of water vapor molecules is larger than the membrane pore size. The collision between the molecules and the pore wall is mentioned in this flow type. The pore size is too small, so the collision between the molecules can be ignored. In this type, the collision between the molecules and the pore wall inside the membrane can be encountered. The coefficient will be dependent on the membrane pore geometry. (Schofield, R. W. et al., 1987; Lawson, K. W. and Lloyd, D. R., 1997; Ding, Z. et al., 2003; Khayet, M. et al., 2004; Alkhudhiri, A. et al., 2012; Lawal, D. U. and Khalifa, A. E., 2014)

$$C_w^{Kn} = \frac{2\pi}{3RT_m}\left(\frac{8RT_m}{\pi M_w}\right)^{1/2}\frac{r^3}{\tau\delta}$$

2.20

If the membrane pore size is considered to have a uniform distribution, the mean diameter of pore size can be used.(Phattaranawik, J. et al., 2003; Khayet, M. et al., 2004)

$$C_w^{Kn} = \frac{2\varepsilon r}{3RT_m\tau\delta}\left(\frac{8RT_m}{\pi M_w}\right)^{1/2}$$

2.21

$K_n < 0.01$ or $d_p > 100\lambda$ **(Molecular Type of flow model)**

The mean free path is smaller than the pore diameter size because the stationary air is trapped inside the pore. Having the air film inside the membrane pores makes the resistance of permeability by the ordinary molecular diffusion mode. The distribution and collision between molecules are considered in molecular type. The average mole fraction of air pressure within the pore is predominant.(Schofield,

R. W. et al., 1987; Lawson, K. W. and Lloyd, D. R., 1997; Khayet, M. et al., 2004; Alkhudhiri, A. et al., 2012; Belessiotis, V. et al., 2016)

$$C_w^D = \frac{\pi}{RT_m} \frac{PD}{P_{air}} \frac{r^2}{\tau\delta} \qquad 2.22$$

D is the diffusivity coefficient of water. P is the total pressure inside the membrane pore or the total pressure of the air and the water vapor inside the pore. P_{air} is the air pressure inside the pores.

If the uniform pore size is assumed, the equation is given as;(Khayet, M. et al., 2004)

$$C_w^D = \frac{\varepsilon}{\tau\delta} \frac{PD}{P_{air}} \frac{M}{RT_m} \qquad 2.23$$

The value of PD (Pa.m^{2}s^{-1}) of water- air is;(Phattaranawik, J. et al., 2003)

$$PD = 1.895 \times 10^{-5} T_m^{2.072} \qquad 2.24$$

$0.01 < K_n < 1$ or $\lambda < d_p < 100\lambda$ **(Transition type of flow model)**

The transition condition between the Knudsen type and the molecular type. The collision takes place between both molecule-molecule and molecule-pore wall. The vapor diffusion also passes through the stagnant air inside the membrane pore. (Khayet, M. et al., 2004; Belessiotis, V. et al., 2016)

$$C_w^c = \frac{\pi}{RT} \frac{1}{\tau\delta} \left[\left(\frac{2}{3} \left(\frac{8RT}{\pi M_w} \right)^{1/2} r^3 \right)^{-1} + \left(\frac{PD}{P_a} r^2 \right)^{-1} \right]^{-1} \qquad 2.25$$

For the uniform pore size;(Khayet, M. et al., 2004)

$$C_w^c = \frac{1}{RT\delta} \left[\frac{3}{2} \frac{\tau}{\varepsilon r} \left(\frac{\pi M}{8RT} \right)^{1/2} + \frac{P_a \tau}{\varepsilon PD} \right]^{-1} \qquad 2.26$$

2.6.2   Heat transfer

Membrane distillation is the non-isothermal process. There is the heat loss during the separation process from the hot side to the cold side. The latent heat of vaporization and the condensation of water vapor, and the conduction of heat through the membrane.

There are three regions for the heat transfer in the direct contact membrane distillation (DCMD).

(a) from the feed water in the hot side to the hot side boundary layer of membrane in the feed region, the heat transfer is Q_f. The convection takes place for this condition.(Lawson, K. W. and Lloyd, D. R., 1997; Khayet, M. et al., 2004; Belessiotis, V. et al., 2016)

$$Q_f = h_f \left(T_{bf} - T_{mf} \right) \qquad 2.27$$

(b) the heat transfer through the membrane layer, Q_m. The heat transfer through the membrane is by the latent heat of vaporization for the vapor flux, Q_v, and the heat is conducted across the membrane material and across the gas-filled pore, Q_c. (Lawson, K. W. and Lloyd, D. R., 1997; Khayet, M. et al., 2004; Belessiotis, V. et al., 2016)

$$Q_m = Q_v + Q_c \qquad 2.28$$

$$Q_m = J\Delta H_v + K_m \frac{dT}{dx} \qquad 2.29$$

$$Q_m = J\Delta H_v + \frac{K_m}{\delta} \left(T_{mf} - T_{mp} \right) \qquad 2.30$$

$$Q_m = \left(C_w \left(\frac{dP}{dT} \right) \Delta H_v + \frac{K_m}{\delta} \right) \Delta T_m \qquad 2.31$$

$$\Delta T_m = T_{mf} - T_{mp} \qquad \qquad 2.32$$

$$H = C_w \left(\frac{dP}{dT} \right) \Delta H_v + \frac{K_m}{\delta} \qquad \qquad 2.33$$

$$Q_m = H \left(T_{mf} - T_{mp} \right) \qquad \qquad 2.34$$

H is the effective heat transfer coefficient. Q_c can be considered as the heat loss. (Schofield, R. W. et al., 1987)

(c) from the cold side boundary layer of membrane to the permeate water in the cold side, the heat transfer is Q_p. The convection also takes place in this condition.(Lawson, K. W. and Lloyd, D. R., 1997; Khayet, M. et al., 2004; Belessiotis, V. et al., 2016)

$$Q_p = h_p \left(T_{mp} - T_{bp} \right) \qquad \qquad 2.35$$

At the steady state condition, the overall heat transfer through the membrane is given below.

$$Q_f = Q_p = Q_m \qquad \qquad 2.36$$

$$h_f \left(T_{bf} - T_{mf} \right) = h_p \left(T_{mp} - T_{bp} \right) = J \Delta H_v + \frac{K_m}{\delta} \left(T_{mf} - T_{mp} \right) \qquad \qquad 2.37$$

The temperature polarization coefficient is presented in (Schofield, R. W. et al., 1987) dealing with the heat transfer coefficient.

$$\left(T_{mf} - T_{mp} \right) = \frac{\left(T_f - T_p \right)}{\left(1 + H/h_f + H/h_p \right)} \qquad \qquad 2.38$$

$$TPC = 1/(1 + H/h_f + H/h_p) \qquad \qquad 2.39$$

K_m is the thermal conductivity coefficient of membrane material from the gas and solid conductivities of the "Isostrain" model. (Sarti, G. C. et al., 1985)

$$K_m = \varepsilon K_g + (1-\varepsilon)K_s \qquad 2.40$$

Where K_g is the thermal conductivity of gas diffusing in the membrane and K_s is the thermal conductivity of membrane material depending on the types of membrane. The unit is $Wm^{-1}K^{-1}$.

$$K_m = \left[\frac{\varepsilon}{K_g} + \frac{(1-\varepsilon)}{K_s} \right]^{-1} \qquad 2.41$$

K_g and K_s ($Wm^{-1}K^{-1}$) can be calculated by the function of temperature in Kelvin (K). The conductivities of water and air at atmospheric pressure are as below equations (Lawson, K. W. and Lloyd, D. R., 1997).

$$K_g^{water} = 2.72 \times 10^{-3} + 5.71 \times 10^{-5}\,T \qquad 2.42$$

$$K_g^{air} = 2.72 \times 10^{-3} + 7.77 \times 10^{-5}\,T \qquad 2.43$$

The conductivities of different polymeric membrane were introduced by (Ibrahim, S. S. and Alsalhy, Q. F., 2013).

$$K_s^{PVDF} = 9.23 \times 10^{-3} + 5.77 \times 10^{-4}\,T \qquad 2.44$$

$$K_s^{PTFE} = 0.087 + 6 \times 10^{-4}\,T \qquad 2.45$$

$$K_s^{PP} = -0.248 \times 10^{-3} + 1.3 \times 10^{-3}\,T \qquad 2.46$$

The surface temperature of membrane from feed and permeate sides can be obtained from Equation (2.42) and (2.43) that is obtained from Equation (2.37).

$$T_{mf} = \frac{K_m/\delta \left(T_p + h_f/h_p \, T_f \right) + h_f T_{bf} - J_w \Delta H_v}{\dfrac{K_m}{\delta} + h_f \left(1 + \dfrac{K_m}{\delta h_p} \right)} \qquad 2.47$$

$$T_{mp} = \frac{K_m/\delta \left(T_f + h_p/h_f \, T_p \right) + h_p T_p - J_w \Delta H_v}{\dfrac{K_m}{\delta} + h_p \left(1 + \dfrac{K_m}{\delta h_f} \right)} \qquad 2.48$$

Heat transfer coefficient from the feed and permeate sides (h_f and h_p) are estimated from the dimensionless Nusselt number for the correlation of temperature.

$$h_i = \frac{Nu_i k_i}{d_h}, \quad i = f,p \text{ (feed , permeate)} \qquad 2.49$$

k is the fluid thermal conductivity and the d_h is the hydraulic diameter. Nu is obtained from the flow types of conditions, Reynolds number and the Prandtl number.

For the laminar flow,

$$Nu = 1.86 \left(RePr \frac{d}{L} \right)^{0.33} \qquad 2.50$$

For the turbulent flow,

$$Nu = 0.023 Re^{0.8} Pr^{0.33} \left(\frac{\mu}{\mu_s} \right)^{0.14} \qquad 2.51$$

The Nusselt correlation for the heat transfer for the various membrane modules are described in Table 2.2. (Chiam, C.-K. and Sarbatly, R., 2013).

Table 2.2 Nusselt Empirical Correlations

Nusselt Empirical Correlations	Description
$Nu = 1.86\left(RePr\dfrac{d_h}{L}\right)^{1/3}$	Laminar flow (Re < 2100): For flat sheet and tubular membrane modules
$Nu = 3.66 + \dfrac{0.0668\left(RePrd_h/L\right)}{1+0.045\left(RePrd_h/L\right)^{2/3}}$	Laminar flow (Re < 2100): For hollow fiber membrane modules
$Nu = 0.116\left(Re^{2/3}-125\right)Pr^{1/3}\left(1+\left(\dfrac{d_h}{L}\right)^{2/3}\right)$	Transition flow (2100 < Re < 10,000): For flat sheet membrane modules
$Nu = 0.023Re^{0.8}Pr^n$ n = 0.4 for heating, n = 0.3 for cooling	Turbulent flow (Re > 2100): For flat sheet and tubular membrane modules
$Nu = 0.023Re^{0.8}Pr^{1/3}\left(1+\dfrac{6d_h}{L}\right)$	Turbulent flow (Re > 2100): For flat sheet and hollow fiber membrane modules

Where Pr is the Prandtl number and the Re is the Reynolds number.

$$Pr_i = \frac{\mu_i C_{p,i}}{k_i} \qquad\qquad 2.52$$

$$Re_i = \frac{\rho_i v_i d}{\mu_i} \qquad\qquad 2.53$$

$C_p(Jkg^{-1}K^{-1})$, $k_f(Wm^{-1}K^{-1})$, ρ (kgm^{-3}), μ $(kgm^{-1}s^{-1})$ and $v(ms^{-1})$ are the specific heat capacity, thermal conductivity, density, viscosity and the velocity of the respective solution. The above equation shows that the heat transfer coefficient depends on the different concentration of the solution from the experiment data. In the model of (Qtaishat, M. et al., 2008),both the heat transfer coefficients increased with the increase of temperature. The temperature is more effected on the h_f than the h_p.

2.7 Application of MD for wastewater treatment

Membrane Distillation (MD) can be applied in many applications. Most of the projects are still in laboratory unit. Membrane Distillation (MD) has already had an achievement in the water desalination field. This gives the satisfying result with the low energy requirement. Membrane Distillation can strike the point of the traditional desalination method. (Bui, V. A. et al., 2010)has set the optimal model of direct contact membrane distillation that can save the total energy consumption by 26.3%. They used the glucose solution of 1.5kg from 30 to 60 % wastewater for their simulation work. MD has also the potential for the food industry, dairy products, aromatic compounds and solutions of chemicals. This can be applied to the fields that is needed to get the high rejection treatment for the nuclear water and turbine water. And the heavy metal wastewater and textile wastewater is also convenient for this application.

MD has also been tested for the separation of saline wastewater into the concentrate (brine) and pure water (Gryta, M. et al., 2006). For the NaCl solution containing the natural organic matter present in intestinal mucous, the severe fouling occurred. (Gryta, M. et al., 2001)used the 2wt% solution of citric acid to remove the fouling. The membrane is obtained as the performance close to the initial efficiency. (Mokhtar, N. et al., 2015) also tried the treatment of wastewater from rubber industry. Although the water with high quality, the severe flux declination is still the problem.

2.8 Textile Wastewater

The contaminants including acids, bases, dissolved solids, toxic compounds and color are containing in the dye wastewater. The natural and synthetic dyes are used for the dyeing industry. Nowadays, the synthetic dyes are used in the textile, rubber, paper, plastic and leather industry.

Generally, there are four basic processing stages in the textile industry.

1. Fabric formation
2. formation
3. Yarn Wet processing
4. Fabrication

The most common processing techniques are also involved in the industry dealing with the dyeing material; sizing, desizing, scouring, bleaching, mercerizing and dyeing.

Sizing	• first preparation step
Desizing	• to remove sizing materials step prior to weaving
Scouring	• to remove impurities from the fibers step by using alkali solution
Bleaching	• to remove unwanted color by using chemicals
Mercerizing	• to increase dye-ability, lustre and fibre appearance by using alkaline solution (NaOH) and salt (NaCl)
Dyeing	• the adding color stage to fibres by using salt

Figure 2.3 Textile industry processes

The different amounts of dyes are required by the unit of fabric. The color and salts in wastewater are the concern for textile wastewater. The using of dyes is dependent on the required dyebath ratio which is the ratio of the units of dye required per unit of fabric and typically ranges from 5 to 50 depending on the type of dye, dyeing system and affinity of the dyes for the fibers. (Industry, T., 1997)

The consumption of water from textile industry in Thailand is shown in

Table 2.3. And the primary source of wastewater in textile industry is from dyebath and the wash water.

Table 2.3 Water Consumption of the Thai textile industry (Tubtimhin, S., 2002)

Type of Establishment	Water consumption (m3/ton of product)	
	minimum	maximum
Man-made fiber	4.4	30.7
Fabric making (dry processing) *	10.3	
Dyeing and finishing		
• Yarn	114.8	180
• Fabric	125	160
• Yarn + Fabric	73.1	166.7
Integrated textile**mills (all fabric)	107.7	183.3
Printing	11.9	62.4

* One factory data only

** The process requiring water in these mills is dyeing and finishing only and the dyed material is only fabric

The main waste stream from textile industry is the wastewater with color and other auxiliaries. The textile wastewater contains the complex mixtures of chemicals because of the various process steps. The color is prominent in the wastewater even at the low concentration in the water. Salt is also another problem for the textile wastewater. Itis used to aid the exhaustion of ionic dyes. It is used especially for the anionic dyes like the reactive and direct dyes on the cotton. (Agency, U. E. P., 1996)

2.8.1   Reactive dye wastewater characteristics

The textile wastewater has the complex structure of dyes chemicals. The textile dyes are mainly classified into two ways; based on their application characteristics (CI Generic Name such as acid, basic, disperse, mordant, reactive, Sulphur dye, pigment, vat, azo insoluble), and based on their chemical structure (CI Constitution Number such as nitro, azo, carotenoid, diphenylmethane, xanthene, inorganic pigment, etc.). Almost two-third of the organic dyes are azo dyes used in many different industrial processes. The textile dyes are also regarded as the anionic, nonionic and cationic dyes. (Carmen, Z. and Daniela, S., 2012)

The reactive dye is the anionic dye having the high-water solubility and strong covalent bond. The average presence of reactive dyes is about 30% as the hydrolyzed form in wastewater. the fixing degree is 50-90% and the loss of effluent percentage is 10-50. The salt such as sodium nitrate, potassium chloride, magnesium chloride, sodium sulfate and sodium chloride is used in large amount. The majority salt of total use is sodium chloride and sodium sulfate. For the pH, the sodium hydroxide is also used to the alkaline range. The quantity of salt is used 20 to 80 percent of the weight of goods dye and the concentration of wastewater is 2000 ppm to 3000ppm during the mercerizing process(Industry, T., 1997), (Carmen, Z. and Daniela, S., 2012).

2.8.2   The impacts of textile wastewater

The effluents of wastewater from the textile industry and dyeing processes are needed to consider for the environmental impacts because the presence of organic dye compounds in the textile wastewater retards the penetration of sunlight into the water when the wastewater is directly discharged to the waterbody. This situation makes the declination of oxygen transport into the water and the solubility of gases and toxic in the effluents can damage the environment. The wastewater containing dyes is one of the most dangerous effluents from the industrial waste because it makes the bad impacts not only to the accepting water body but also to the human health.

The textile industry is becoming bloom in the industrial field. The wastewater from textile industry is also considered as the severe pollution problem. The wastewater produces not only the undesirable color but also the breakdown products that are carcinogens and toxic. The dyes can remain in the environment for a long time if there is no adequate treatment before discharging to the receiving water bodies. The half-life of hydrolyzed Reactive Blue 19 is about 46 years at pH 7 and 25°C (Hao, O. J. et al., 2000). The decolorization process should be used for the environmental health. The wastewater containing dyes has to be cleaned before discharging into the receiving water because the regulations on the dyes are becoming more and more stringent in the recent years (Shi, B. et al., 2007), (Chu, W., 2001)

2.9 Previous research works on dyehouse wastewater treatment

There are also many treatments for the various kinds of textile wastewater. The chemical treatment, the physical treatment and the biological treatment can be classified as the wastewater treatment.

(Shi, B. et al., 2007) used purified Al_{13} for the coagulation treatment of direct dyes wastewater. Purified Al_{13} has the highest removal efficiency compared with the traditional Al and PACI. The other commercial inorganic adsorbents are also used besides of the activated carbon. For the electrochemical method, the result of the treatment gave the satisfied outcomes by using Ti/Pt as anode and Stainless Steel 304 as cathode. (Vlyssides, A. G. et al., 2000)

As the biological treatment, the reduction of chemical oxygen demand (COD) can make about 42%. The wastewater can be treated to be the standard of discharging level into the corresponding treatment plant. The application of Bacillus aryabhattai DC100 is also the bioremediation of the real textile wastewater for the decolorization efficiency and COD reduction (Paz, A. et al., 2017). For the advanced oxidation process, hydrogen peroxide is also viable for textile wastewater treatment. This concept may be the optimizing methodology with the economical and ecological importance in the future (Asghar, A. et al., 2015).

Membrane filtration is also applied to treat textile wastewater such as ultrafiltration, nanofiltration, forward osmosis and reverse osmosis. (Erkanlı, M. et al., 2017), (Ellouze, E. et al., 2012).There are also trying with industrial wastes and the agricultural wastes. For example, coal ashes, wood chips, groundnut shell powder, wood sawdust, grounded flower seed shells and other lingo-cellulosic wastes are used for the decolorization. The regeneration problem and the large amount of adsorbents are still the challenges(Carmen, Z. and Daniela, S., 2012).

Membrane filtration for the treatment of dye wastewater will be the limitations with the large scale for the high operation and cost, and the fouling problem. But the trying of new membrane and the effective system will be convenient for the textile industry. Membrane distillation with low energy consumption maybe one of the options for the treatment of industrial wastewater in future.

2.9.1   Treatment technologies for reactive dyehouse wastewater

There are many researches for the treatment of reactive dye wastewater. Many scientists are trying to solve the treatment of dye wastewater from different fields. The synthetic dye compound structures are very complex, and they are difficult to decolorize by conventional aerobic biological treatments, such as activated sludge process. The physical-chemical techniques such as coagulation, adsorption, membrane separation and advanced oxidation using chlorine and ozone are used conveniently. Each treatment method has advantages and disadvantages for the treatment results. (Gupta, V. K. et al., 2003; Shi, B. et al., 2007).

Solar pond reactors are one of the attractive methods for the treatment of textile wastewater in medium and small-scale industries. The dye reactive orange 16 (RO16) was decolorized to about 99% efficiency. The outcome result is compromising but the semi-industrial scale is still needed to conduct (Chavaco, L. C. et al., 2017) . The advanced oxidation technique is also the remediation of color waste. (Saharan, V. K. et al., 2011) used the hydrodynamic cavitation for the degradation of reactive dye red 120. For the adsorption of reactive dye, the granular activated carbon had a higher adsorption capacity than the coal-based bottom ash. The adsorption level was faster and can reach the higher equilibrium level. (Dinçer, A. R. et al., 2007)

The ozone technique is also another convenient process of the color wastewater. The concentration of reactive dyes of blue-19 and orange -13 can be reduced from 2000 to 200 ADMI within 30 minutes of reaction time (Chen, T. Y. et al., 2009). The results from that study will also aid in designing a system for the practical application.

Table 2.4 Some researches for the treatment of dyehouse wastewater

Method	Color	Reference
Photocatalytic Degradation (TiO$_2$)	Reactive Black 5	(Mahadwad, O. et al., 2011)
Coagulation	reactive dyes (Samofix red V-RBL) and (Samofix Green V-G)	(Najafi, H. and Movahed, H., 2009)
Ozonation	Reactive Blue 19	(Fanchiang, J.-M. and Tseng, D.-H., 2009)
Biodegradation	Reactive Black B (RBB)	(Liao, C.-S. et al., 2013)
Advanced Oxidation Processes	Reactive Black 5 (RB5) and industrial textile wastewater	(Bilińska, L. et al., 2016)
Nanofiltration	Reactive Black 5	(Tang, C. and Chen, V., 2002)
Reverse Osmosis	Torquise blue dye and Remozol golden yellow dye	(Sathiyamoorthy, M. et al., 2012)
Advanced Oxidation Processes	Reactive Blue 19	(Guimarães, J. R. et al., 2012)

2.9.2   Membrane technology for reactive dyehouse wastewater

The membrane can also be used for the treatment of reactive wastewater. There are many investigations for the reactive dyeing wastewater. Nanofiltration is also the alternative solution compared to the conventional processes for the textile wastewater. It has been undertaken since 1990 on dye bath wastewater. These membranes are ion-selective due to the negative surfaces. The portion of auxiliary chemicals can pass through the membrane into the permeate (Koyuncu, I. and Topacik, D., 2003).

The color and the auxiliary component (NaCl) in the reactive dye bath may affect the permeate flux and water quality. There is a good agreement of the salt rejection results. (Koyuncu, I. and Topacik, D., 2003) tested the operating conditions for the fouling and the salt rejection in the reactive dye and the salt mixtures. The

optimum conditions were set up with the cross-flow velocity for the rejection. (Ellouze, E. et al., 2012) used the microfiltration (MF) instead of coagulation-flocculation as a pretreatment. The rejection of salinity and COD retention can be enhanced with the performance of nanofiltration after the pretreatment.

Membrane filtration for the treatment of reactive textile wastewater will be the potential treatment method. The combination usage of other effective pretreatment or the membrane pretreatment system can also aid to the effect of membrane filtration reactor.

2.9.3   Direct Contact Membrane Distillation and textile wastewater

The effluent discharge to the water bodies and the purpose for reusing the water will be satisfied with the standard regulations. The system with different membrane materials are on the research unit with the different concentration color. The color removal is also satisfied for some projects as shown in section (2.9.2). As a new born research, direct contact membrane distillation will be the option of the potential treatment system for the textile wastewater. The limited energy consumption and the high performance are the features of the direct contact membrane distillation process. The textile wastewater is also tested with direct contact membrane distillation system (Calabro, V. et al., 1991; Li, F. et al., 2018).

Table 2.5 Some of the textile water treatment with direct contact membrane distillation

Mechanism	Color	Types of Membrane	Rejection Rate	Reference
Polyvinylidene Fluoride (PVDF)	Reactive Blue Dye	Hollow Fiber	Up to 96.2 %	(Chong, K. et al., 2016)
Polypropylene (PP)	Red E-4BA, Blue E-G and Blue E-BA	Hollow Fiber	Rejection coefficient 100%	(Calabro, V. et al., 1991)

CHAPTER 3

METHODOLOGY

3.1 Flow chart of overall research methodology

Reactive dye wastewater preparation with Reactive Black and Reactive Blue at color concentration of 400,600,800 ADMI

DCMD membrane experimental set-up

1- Operational parameters
- Driving temperature
- Cross-flow velocity
2- Wastewater parameters
- Concentrations of Reactive Black and Blue
- pH
- Concentrations of Anions

1. Investigation of color and initial concentration removal from synthetic reactive dye by DCMD process with varied temperatures and cross-flow velocities

2. Investigation of the flux condition by the affect of the scaling condition

3. Investigation the performance of DCMD for the treatment of textile wastewater

Compare overall results and discussion for the driving parameter of DCMD system that effect to the permeate quality of water and flux

Figure 3.1 Scope of overall experimental runs

3.2 Experimental Instrument and Equipment

1. PVDF Flat Sheet Membrane
2. Membrane Cell Casing
3. Waterbath
4. Pump
5. Pressure Gauge
6. Chiller
7. Thermometer
8. Weighing Balance

3.2.1   Membrane cell and sheet

The membrane cell is acrylic body included with the cell top, cell bottom, inner and outer O rings and the fastening bolts and washer.

Table 3.1 Operational Parameters and Technical Specifications of Direct Contact Membrane Distillation Cell

Parameters		Unit
Company Name	Sterlitech Corporation	-
Membrane Active Area	140	cm^2
Maximum Pressure	27	bar
Maximum Temperature	88	°C
Channel Depth	0.19	cm
Channel Width	9.53	cm
Channel Area	1.81	cm^2

The hydrophobic membrane sheet was used in flat sheet type. The flat sheet membrane is easier operation in lab scale setups.(Thomas, N. et al., 2017). The characteristics of the membrane sheet are shown in Table 3.2

Table 3.2 Membrane Sheet Characteristics

Features of Membrane		Unit
Product Manufacturer	Novamem	-
Module Configuration	Flat sheet membrane	
Material	Polyvinylidene fluoride (PVDF)	-
Type of Membrane	Hydrophobic microporous	-
Pore Size	0.1	µm
Effective Area	140	cm^2
Thickness	45	µm
Applicable Temperature Range	≤ 120	°C
pH	1-12	-
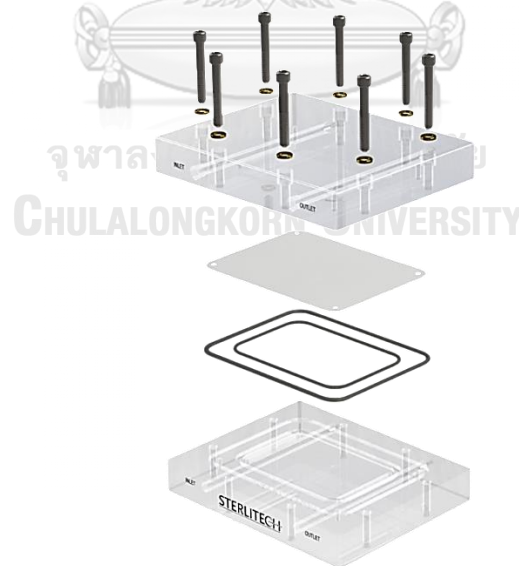
Figure 3.2 Membrane cell and membrane sheet

3.2.2 System appliances

The temperature of the feed water was maintained by the hot waterbath. The waterbath has thermostatics to detect and maintain the desired temperature of the water. The used waterbath is WNB-7 from memmert. It can be set the temperature range from 10°C to 95°C with the activation mode and the setting accuracy is ± 1°C. The water refrigerated chiller was used for the permeate cold side from Xi'an Heb Biotechnology Co.,Ltd (CCA-420).

The two peristaltic pumps were used to drive the flow rate to each side. The pressure gauge was used to watch the pressure of the system. The thermometer was also used to measure the water temperature. The permeate water was weighed by the electronic balance from A&D Company (GX-6100) with 0.01g accuracy. The computer was also connected with the data acquisition system to get the weight of water for every 10 minutes.

3.2.3 Membrane Unit Set up

The membrane sheet and its casing were set up. The cell bottom, the inner and outer O rings, the membrane sheet, and the cell top were assembled with the fastened bolts. The PP silicon pipe were connected to both feed and permeate sides.

The direct contact membrane distillation is the simplest one of the membrane distillation systems. The experiment was also set up as the lab-scale model. The circulating pump was for the recirculating of feed and permeate sides. The membrane cell and the other appliances were connected as the Figure 3.3.
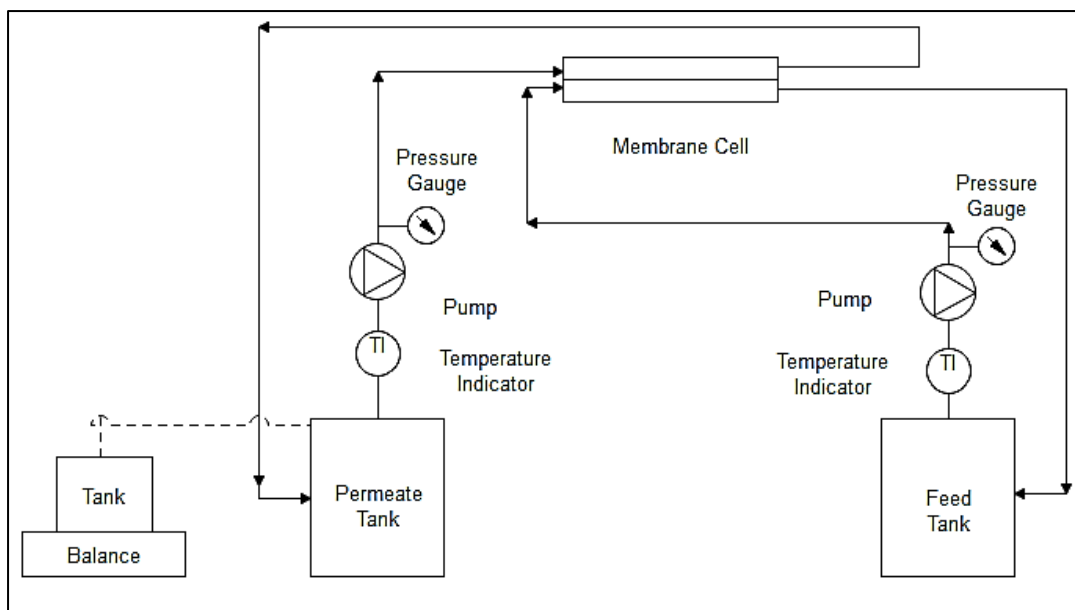
Figure 3.3 Membrane Distillation Laboratory Plant

3.3 Target Contaminants

    3.3.1   Reactive Dyes

      a.   Reactive Black
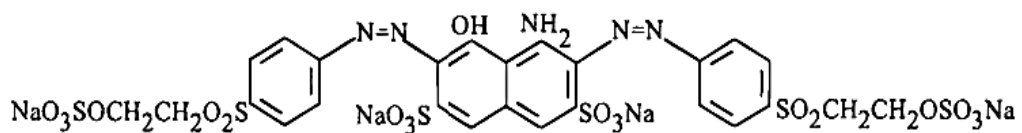
Figure 3.4 Structure of Reactive Black (MW = 991.82 gmol^{-1})
(Mahadwad, O. et al., 2011)

b. Reactive Blue
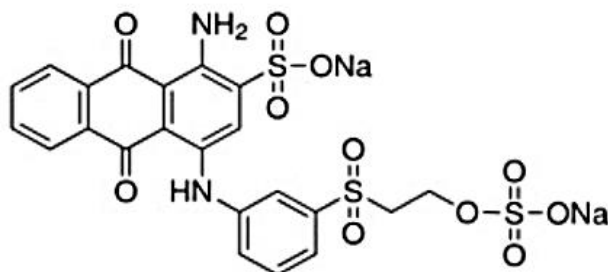
Figure 3.5 Structure of Reactive Blue (MW = 626.54 gmol^{-1})
(Lazaridis, N. K. et al., 2003)

Table 3.3 Characteristics of dyes

	Reactive Black	Reactive Blue
Molecular Formula	$C_{26}H_{21}N_5Na_4O_{19}S_6$	$C_{22}H_{16}N_2Na_2O_{11}S_3$
Molecular Weight (gmol^{-1})	991.82	626.54
CI	Reactive Black 5	Reactive Blue 19
Color Index Number	20505	61200
Molecular structure	Remazol	Anthraquinone
Maximum wavelength (nm)	597	590

The synthetic wastewater was prepared by reactive dyes (Reactive Black 5 and Reactive Blue 19). The concentrations of reactive dye water were varied with 400, 600, 800 ADMI (American Dye Manufacturers Institute) to know the effect of reactive dye concentration on the treatment performance of direct contact membrane distillation. Reactive Black 5 and Reactive Blue 19 were obtained from SIGMA-ALDRICH company.

3.3.2   Auxiliary Components for the Wastewater

In the real wastewater, there are not only color but also many chemical components. In this research, chloride, sulfate, phosphate, nitrate and pH will be considered as the auxiliary components. Sodium chloride, magnesium sulfate, potassium dihydrogen orthophosphate, sodium nitrate and sodium hydroxide were used for the synthetic wastewater. pH was also adjusted to 7.0, 8.5 and 10 using NaOH.

Table 3.4 Anions Chemical Concentrations

Anions chemicals	Concentration (mg/L)
Sulfate	100,200,300
Phosphate	5,10,15
Nitrate	5,10,20

3.4 Experimental Procedure

3.4.1   Temperature

The driving force is the partial pressure difference of membrane from the feed side to the permeate side of membrane surface in direct contact membrane distillation. According to the literature review, the increased feed temperature can make the higher flux level. However, the maximum allowable temperature is 88°C for this membrane sheet. If the higher temperature is used, the cost of energy will also be higher. So, the feed temperatures on the bulk feed side are set up to 40, 50, 60°C.

3.4.2   Flow rate

As the above mention, the flow rate is also the influencing factor on the flux rate. The higher flow rate can give the higher partial pressure between feed and permeate side. There is the restriction for the flow rate with liquid entry pressure (LEP). The suited flow rate should not be over for the pressure difference that is lower than the LEP value because of prevention for the membrane pore wetting. The feed flow rate will be used as 0.15 ms^{-1}, 0.1 ms^{-1} and 0.05 ms^{-1}.

3.4.3   Membrane Flux

The flux can be calculated from the accumulated mass of water from the permeate side, the effective area of the membrane and the accumulated time.

$$\text{Flux} = \frac{\text{acccumulated mass of water}}{\text{effective area x time}} \qquad 3.1$$

3.5 Experimental Scenarios

There are synthetic dye wastewater and the real textile effluent wastewater. The synthetic wastewater was prepared into two types of reactive dyes with different concentrations.

<u>Scenario A</u>

To know the effect of feed temperature on color removal and permeate flux, the temperature was ranged. The feed temperature was varied and the permeate temperature was remained constant.

Table 3.5 Effect of feed temperature on color removal and permeate flux

$SO_4^{2-} = 100$ mg/L, $Cl^- = 50$ mg/L, $PO_4^{2-} = 5$ mg/L, $NO^{3-} = 5$mg/L

Water Sample	Feed Temperature(°C)	Permeate Temperature (°C)	pH	Velocity (ms^{-1})	Duration (hr)
Black (400 ADMI)	40	20	7	0.1	4
	50				
	60				

Water Sample	Feed Temperature(°C)	Permeate Temperature (°C)	pH	Velocity (ms⁻¹)	Duration (hr)
Blue (400 ADMI)	40	20	7	0.1	4
	50				
	60				

Scenario B

For the effect of color removal, the result data can be used from the

Scenario- A.

Table 3.6 Effect of initial color concentration on MD performance

SO_4^{2-} = 100 mg/L, Cl^- = 50 mg/L, PO_4^{2-} = 5 mg/L, NO^{3-} = 5mg/L

Water Sample	Color Concentration (ADMI)	Feed Temperature (°C)	Permeate Temperature (°C)	Velocity (ms⁻¹)	pH	Duration (hr)
Black	400	The optimum temperature from Scenario A	20	0.1	7	4
	600					
	800					

Water Sample	Color Concentration (ADMI)	Feed Temperature(°C)	Permeate Temperature (°C)	Velocity (ms⁻¹)	pH	Duration (hr)
Blue	400	The optimum temperature from Scenario A	20	0.1	7	4
	600					
	800					

Scenario C

For the effect of cross flow rate on color removal and permeate flux, the high color concentration from this research was used.

Table 3.7 Effect of cross-flow velocity on color removal and permeate flux

SO_4^{2-} = 100 mg/L, Cl^- = 50 mg/L, PO_4^{2-} = 5 mg/L, NO^{3-} = 5mg/L, Color = 800 ADMI

Water Sample	Velocity (ms^{-1})	Feed Temperature(°C)	Permeate Temperature (°C)	pH	Duration (hr)
Black (800 ADMI)	0.15	The optimum temperature from Scenario A	20	7	4
	0.1				
	0.05				

Water Sample	Velocity (ms^{-1})	Feed Temperature(°C)	Permeate Temperature (°C)	pH	Duration (hr)
Blue (800 ADMI)	0.15	The optimum temperature from Scenario A	20	7	4
	0.1				
	0.05				

Scenario D

Table 3.8 Effect on pH value

SO_4^{2-} = 100 mg/L, Cl^- = 50 mg/L, PO_4^{2-} = 5 mg/L, NO^{3-} = 5mg/L, Color = 400 ADMI

Water Sample	pH	Feed Temperature(°C)	Permeate Temperature (°C)	Velocity (ms⁻¹)	Duration (hr)
Black (800 ADMI)	7	The optimum temperature from Scenario A	20	The optimum temperature from	4
	8.5				
	10				

Water Sample	pH	Feed Temperature(°C)	Permeate Temperature (°C)	Velocity (ms⁻¹)	Duration (hr)
Blue (800 ADMI)	7	The optimum temperature from Scenario A	20	The optimum temperature from	4
	8.5				
	10				

Scenario E

Table 3.9 Effect on the auxiliary component of textile effluent (Phosphorus)

SO_4^{2-} = 100 mg/L, Cl^- = 50 mg/L, NO^{3-} = 5mg/L, Color = 400 ADMI

Water Sample	Phosphorus mg/L	Feed Temperature(°C)	Permeate Temperature (°C)	Velocity (ms⁻¹)	pH	Duration (hr)
Black	10	The optimum temperature from Scenario A	20	The optimum velocity from	7	2
	15					

Water Sample	Phosphorus mg/L	Feed Temperature(°C)	Permeate Temperature (°C)	Velocity (ms^{-1})	pH	Duration (hr)
Blue	10	The optimum temperature from Scenario A	20	The optimum velocity from	7	2
	15					

Scenario F

Table 3.10 Effect on the auxiliary component of textile effluent (Sulfate)

$Cl^- = 50$ mg/L, $PO_4^{2-} = 5$ mg/L, $NO^{3-} = 5$mg/L, Color = 400 ADMI

Water Sample	Sulfate mg/L	Feed Temperature(°C)	Permeate Temperature (°C)	Velocity (ms^{-1})	pH	Duration (hr)
Black	200	The optimum temperature from Scenario A	20	The optimum velocity from	7	2
	300					

Water Sample	Sulphate mg/L	Feed Temperature(°C)	Permeate Temperature (°C)	Velocity (ms^{-1})	pH	Duration (hr)
Blue	200	The optimum temperature from Scenario A	20	The optimum velocity from	7	2
	300					

Scenario G

Table 3.11Effect on the auxiliary component of textile effluent (Nitrate)

$Cl^- = 50$ mg/L, $PO_4^{2-} = 5$ mg/L, $SO_4^{2-} = 100$ mg/L, Color = 400 ADMI

Water Sample	Nitrate mg/L	Feed Temperature(°C)	Permeate Temperature (°C)	Velocity (ms⁻¹)	pH	Duration (hr)
Black	10	The optimum temperature from Scenario A	20	The optimum velocity from	7	2
	20					

Water Sample	Nitrate mg/L	Feed Temperature(°C)	Permeate Temperature (°C)	Velocity (ms⁻¹)	pH	Duration (hr)
Black	10	The optimum temperature from Scenario A	20	The optimum velocity from	7	2
	20					

Scenario H

After getting up the satisfied feed temperature and the cross-flow velocity from the experiment, the effluent of textile wastewater from the pre-treatment will be also examined for the color removal, pH effect and the salt concentration removal.

3.6 Analytical Methods

3.6.1 Color removal

In this research, the color is represented by American Dye Manufacturer Institute (ADMI) unit. The color removal efficiencies can also be calculated from ADMI unit of the permeate water. The removal efficiency and the color level can get from the changes of specific wavelength (λ_{max}) and the absorbance.

$$\text{ADMI removal \%} = \frac{\text{Initial ADMI} - \text{Final ADMI}}{\text{Initial ADMI}} \times 100 \qquad 3.2$$

Spectroquant® Prove Spectrometer 100 was used to measure ADMI unit for the color. It can give the direct ADMI value by measuring the absorbance.

3.6.2 Salt rejection

For the removal of salt, the rejection efficiency can also be obtained. The non-volatile substance, NaCl will retained in the feed side and only vapor water can pass through the membrane material. The rejection efficiency can get the calculation of the concentration of solution from the feed and permeate side.

$$\text{Efficiency} = \frac{\text{feed concentration} - \text{permeate concentration}}{\text{feed concentration}} \times 100 \qquad 3.3$$

The removal efficiency can be calculated by %.

3.6.3 IC Analysis, pH, conductivity and TOC

Ion chromatography can be used to detect the anions in water. By measuring the anions from the wastewater and the permeate water, the working efficiency of the system can be known.

pH meter (INDEX- ID1000) and the conductivity meter (HANNA HI-98192) were used to measure pH and the conductivity. TOC was also measured with the TOC analyzer. Total carbon (TC) is the sum of organically and inorganically bound carbon present in water. TOC is a measurement of all carbon atoms that are covalently bound in organic molecules.

CHAPTER 4

RESULTS AND DISCUSSIONS

This chapter includes the discussion about effect of operating condition on the water quality and the permeate water flux from the direct contact membrane distillation system. The synthetic wastewater and the real wastewater (textile effluent) were used as the feed water, and the flat sheet hydrophobic material membrane was also used. The results and discussions are divided into the following sub-sections.

- Characterization of Membrane
- Operating Parameters of Direct Contact Membrane Distillation
- Water Quality Analysis by the varied concentrations

4.1 Characterization of Membrane

4.1.1 SEM Imaging

To investigate the morphology of membrane surfaces, Scanning Electron Microscope Imaging (SEM) was undertaken. The surface of membrane morphology was captured by SEM to know the fouling condition of the membrane surfaces and pore condition. After the treatment of reactive dye solution, the membrane surface showed the possible contaminants from wastewater, deposited on the surface. The prominent membrane fouling could be significant with the real textile effluent test due to various contaminant composition in the textile effluent as shown in Figure 4.1. This can make the flux reduction of the system and it can be seen in the discussion of operating parameters of the system.
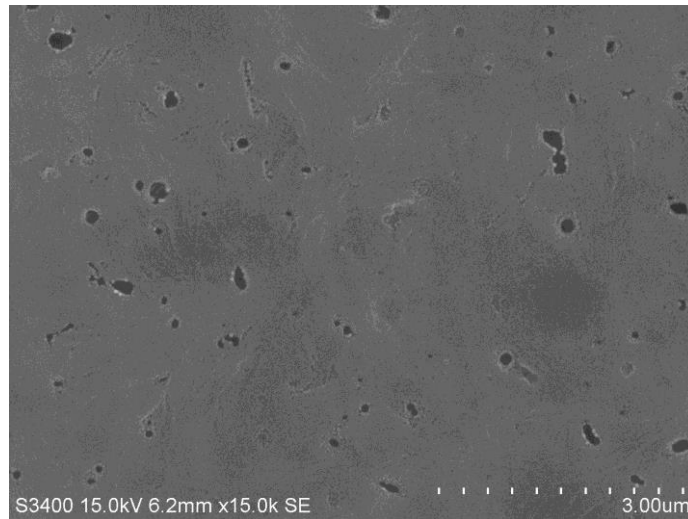
(a) SEM Imaging of used membrane after treatment of synthetic wastewater (reactive black dye solution)
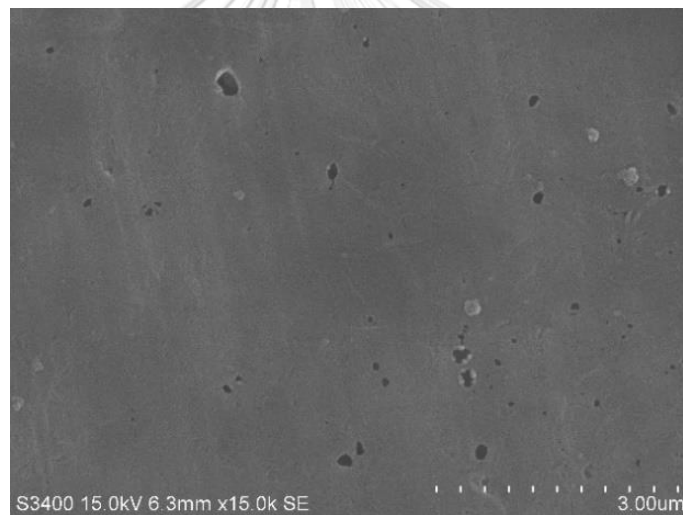
(b) SEM Imaging of used membrane after treatment of real textile effluent

Figure 4.1 SEM imaging of membrane morphology

4.1.2   Contact Angle Measurement

To investigate the hydrophobicity and wettability of the membrane, the contact angle measurement was also done to analyze the hydrophobicity of the membrane before and after treatment of reactive dye solution. The contact angle measurement for virgin membrane can be seen in Figure 4.2. The active layer has the angle that is more than 90 degrees, indicating the property of hydrophobicity of the membrane surface. The average hydrophobicity of membrane from three measurements is shown in Table 4.1.
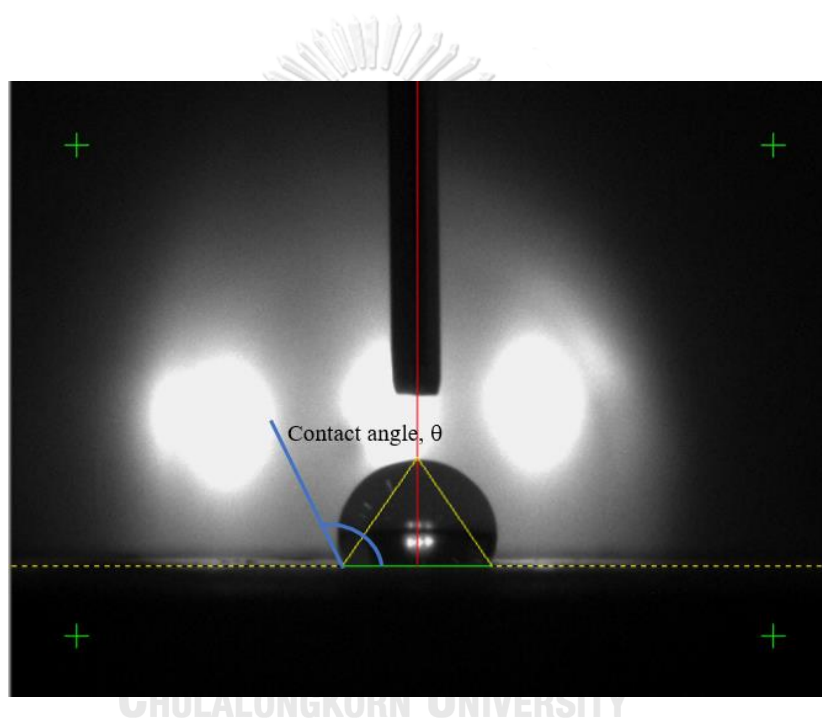
Figure 4.2 Contact angle measurement for virgin membrane

Table 4.1 Average Contact angle values for virgin membrane

Measurement	Contact Angle (degree)
1	110.75
2	104.06
3	107.79
Average value	**108**

The hydrophobic property of material can reject the water and non-volatile components and can allow the passage of the vapor. The hydrophobic nature that the contact angle is larger than 90 degrees for the membrane sheet (PVDF) can be seen in this system. According to the LEP equation in Section 2.5.2, the high values of LEP are obtained by using membrane material with high hydrophobicity and a small maximum pore size (Belessiotis, V. et al., 2016).
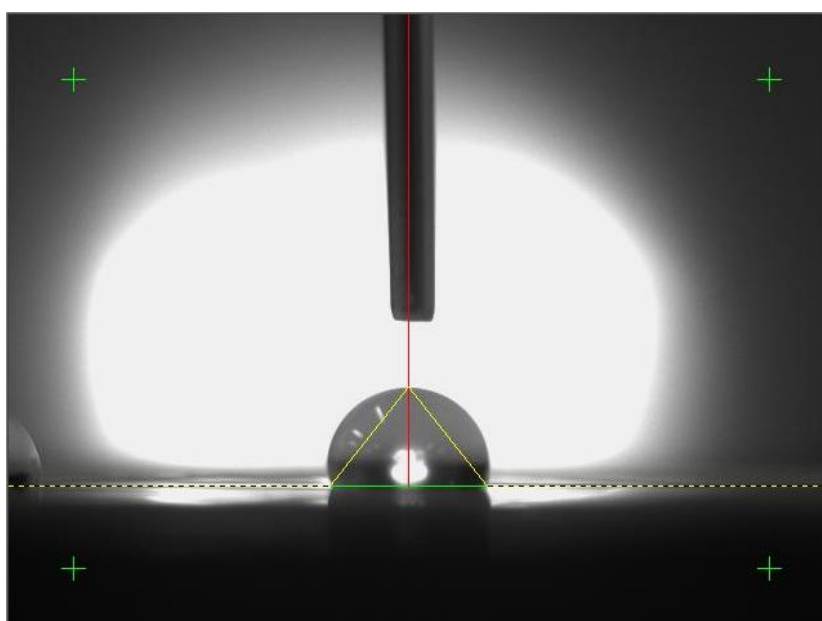
Figure 4.3 Contact angle measurement for used membrane

Also, the used membrane after the reactive dye removal test was taken for the contact angle measurement to investigate any change in condition of the material property in terms of surface hydrophobicity. Table 4.2 illustrates the average value of contact angle for the used membrane after the reactive dye removal.

Table 4.2 Average contact angle value for the used membrane

Measurement	Black	Blue	WW
1	104.86	100.39	111.65
2	93.14	100.81	105.08
3	96.54	104.86	101.42
Average value	**98**	**102**	**106**

In that data, the contact angles measurement larger than 90 degrees were obtained. This characteristic indicates that the property of hydrophobic material of membrane surface was remained after the operation of reactive dye wastewater treatment. While the hydrophilic material has the smaller angle, the larger angle represents the hydrophobicity that is larger than 90°C. Therefore, the membrane can be said that it still has the hydrophobic property after treatment of the reactive dye wastewater and the hydrophobic material is suitable for the removal of reactive dye wastewater.

4.1.3 Zeta Potential Measurement

To measure the charged surface of the membrane and the dispersion medium, the potential difference was measured by the zeta potential difference. The determination of zeta potential is used to evaluate the surface charge of a membrane, the possible interaction between the particles (foulants) and the membrane surface.

The results from Figure 4.4 show that the membrane surface has the zeta potential in the negative zeta potential ranges.
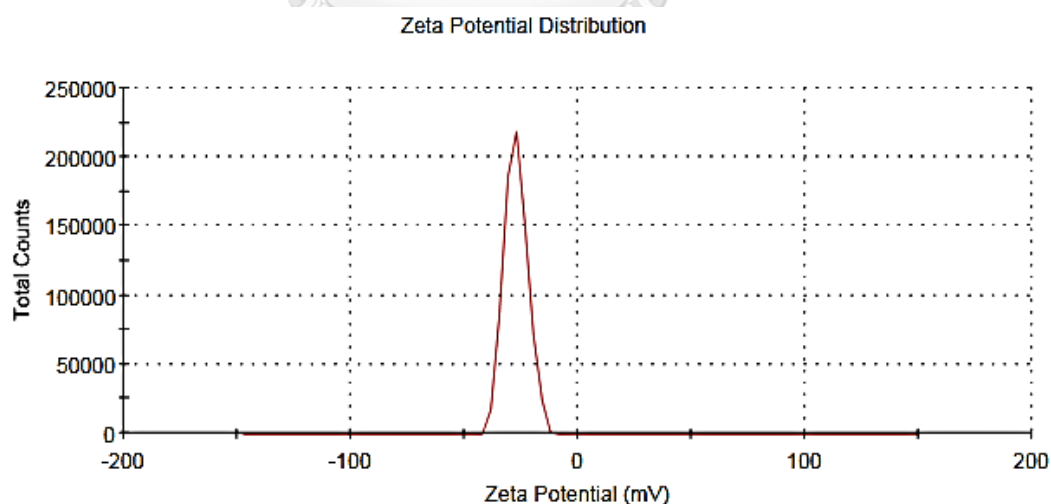
Figure 4.4 Zeta potential measurement of membrane surface

The measurement of membrane zeta potential values was done in the case of original membrane and the used membrane after the treatment of black 5 and blue 19 reactive dye wastewaters. The zeta potential values were presented as follows;

Table 4.3 Average zeta potential value for the membrane

	Origin	Black-5	Blue-19	Textile Effluent
Zeta potential (mV)	-27.2	-15.3	-27.6	-9.96
	-26.6	-25.4	-27	-6.34
	-26.3	-18.9	-21.1	-5.78
	-24.7	-14.9	-22.4	-8.27
	-25.8	-24.5	-23	-9.23
	-26.12	**-19.8**	**-24.22**	**-7.916**

According to the measurement, the membrane material has the negative potential value. It has the negative charged membrane material surface. The two reactive dyes: black 5 and blue 19 also have the negatively charged. (Rafiee, M. and Jahangiri-rad, M., 2014) (El-Bindary, A. et al., 2016) (Karadag, D. et al., 2007). There is the repulsion between the charged membrane material and the anion dyes. Therefore, the repulsive force between the anion contaminants and the negative zeta potential of membrane surface might help reduce the membrane fouling from anion adsorption on the membrane surface. The sulfonate group is repelled by the negatively charged membrane. In (An, A. K. et al., 2016) research, the negatively charged dye was repelled more than the positively and negatively charged group dye by the negative charge membrane surface.

The zeta potential values were changed with several types of contaminants in the case of real textile effluent after wastewater treatment. The membrane surface value after treatment with real textile effluent was decreased to the lowest value, compared with the synthetic dye wastewater. This means that the possible adsorption by the cations that were presented in the textile effluent. The membrane charge neutralization was significantly obtained in the case of real textile effluent, implying that membrane fouling could be highly risky.   The membrane

cleaning will be required in high frequency mode. As for another research, the detailed concepts and discussions about the zeta potential effect with the wastewater type will be interested.

4.1.4 Porosity test

The gravimetric method was used to measure the porosity of the membrane in this study. The weight of ethanol that was filled in the membrane pores is also determined in the porosity equation 4.1. (Li, Q. et al., 2011)

$$\varepsilon = \frac{(m_1 - m_2) / \rho_G}{(m_1 - m_2) / \rho_G + m_2 / \rho_p} \times 100\% \qquad 4.1$$

Where m_1 = the weight of wet membrane (g), m_2 = the weight of dry membrane (g), ρ_G = the density of ethanol (0.789 g/cm^3) and ρ_p = the density of polymer material (1.765 g/cm^3 for PVDF material) (Zhang, P.-Y. et al., 2012). The density of polymer material will be different depending on the material used. The difference is negligible as an assumption. The detailed calculation is shown in Appendix A.

Porosity = 76.2 % (approximately 76%)

The tortuosity can be also calculated by Equation 2.3.

$$\text{tortuosity} = \frac{(2 - \text{porosity})^2}{\text{porosity}} = \frac{(2 - 0.76)^2}{0.76} = 2.02$$

From the above data, the membrane has high porosity for promoting the vapor evaporation in large amount.

4.2 Operating Parameters of Direct Contact Membrane Distillation

The effect of the feed temperature and the cross-flow velocity are discussed as the effect of operating conditions of the direct contact membrane distillation system.

4.2.1 Effect of feed temperature on permeate flux

The temperature difference is one of the operating parameters for designing the direct contact membrane distillation system to govern the permeate flux.

(Manawi, Y. M. et al., 2014) indicates that the effect of feed temperature is much more significant than the effect of permeate temperature. Therefore, the permeate temperature was kept constant in this study. The feed temperatures were varied to investigate the performance of direct contact membrane distillation for synthetic dye wastewater treatment. The feed temperatures that were used in this study are 40°C, 50°C and 60°C to investigate the performance of direct contact membrane distillation for the synthetic dye wastewater treatment.

The flux was calculated as Equation (2.10). The fluxes are shown in Figure 4.5, Figure 4.6 and Figure 4.7. The permeate flux was increased up to about 2.5 times when the feed temperature changed from 40°C to 50°C whereas the temperature was increased to 60°C, the highest permeate flux was achieved by increasing up to 1.5 times, compared to that at 50°C. The increment of flux is trending like the increased temperature. Therefore, the permeate fluxes with the temperature changes in these data are under the Antoine equation. The recovered flux was slightly higher with the reactive blue wastewater.
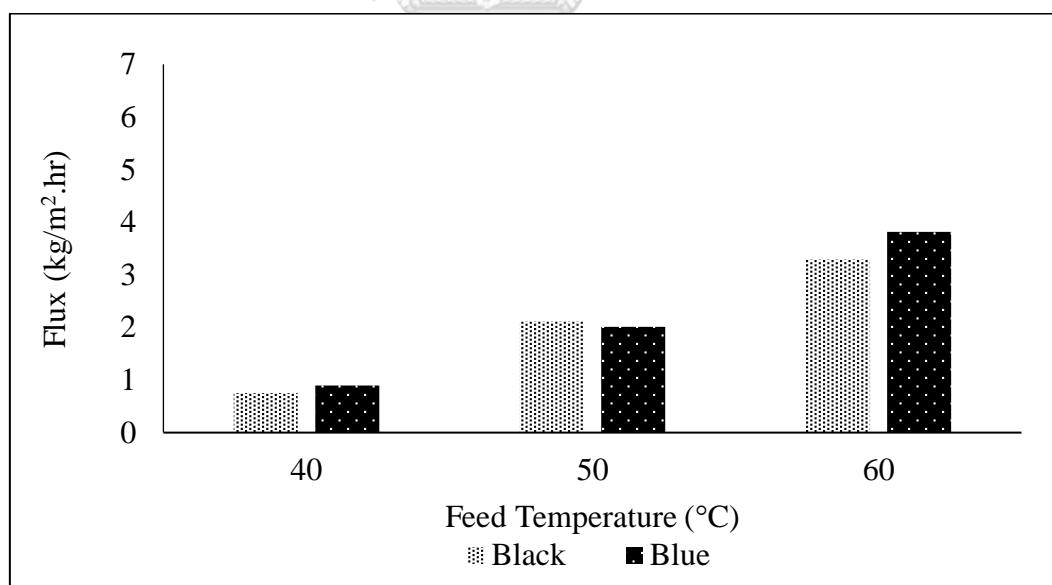
Figure 4.5 Flux with different feed temperatures for reactive dyes
($T_p = 20°C$, v = 0.1 m/s)
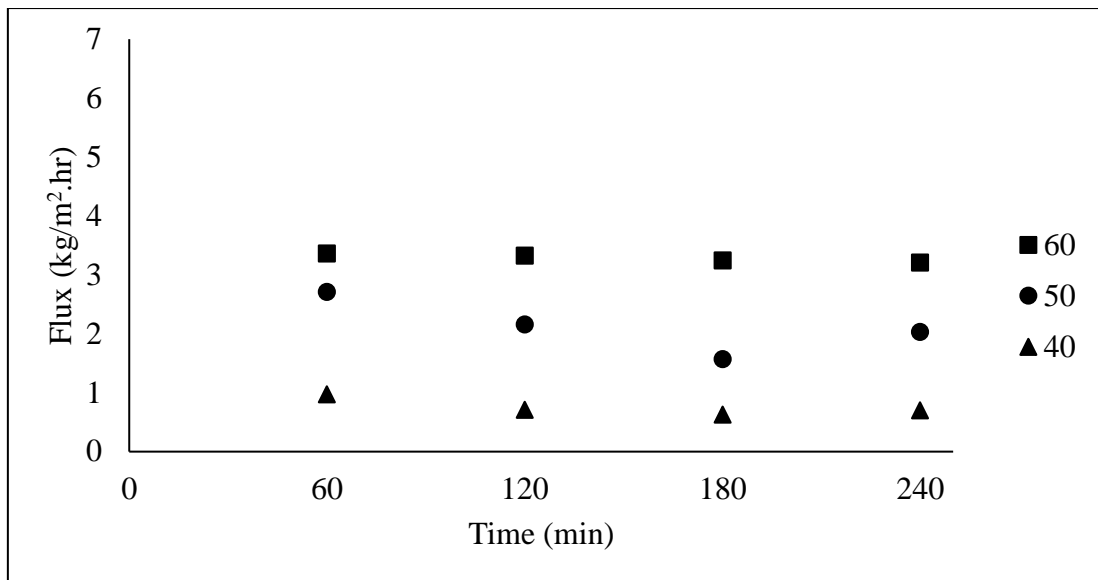
Figure 4.6 Flux of different feed temperatures (°C) for reactive black dye synthetic wastewater (v = 0.1 m/s)
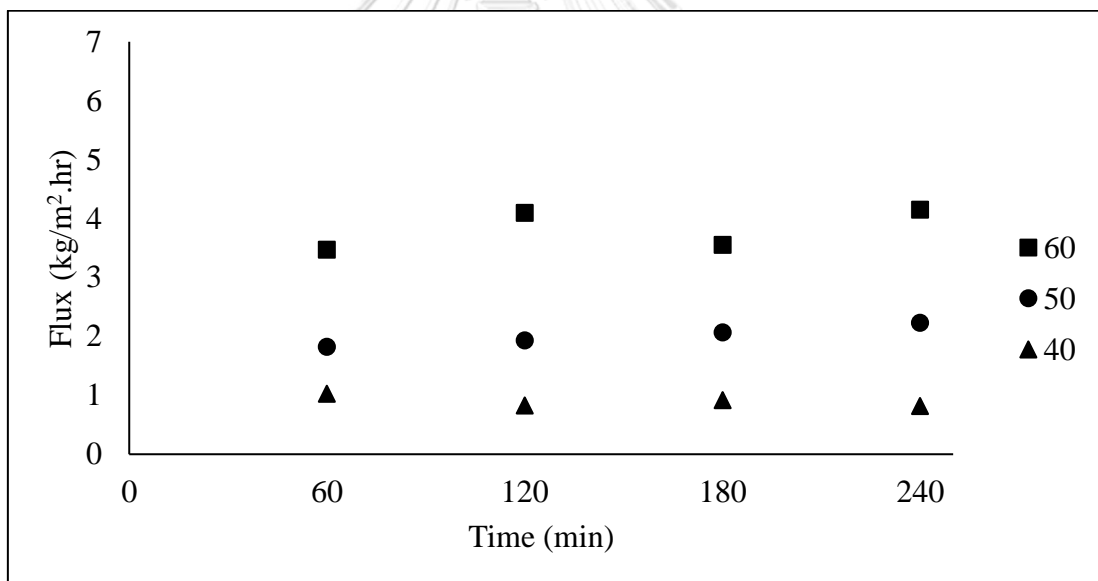
Figure 4.7 Flux with different feed temperatures (°C) for blue dye synthetic wastewater (v = 0.1 m/s)

The increased feed temperature can give the exponentially increment for the obtained flux. This research shows the similar result to those obtained with other wastewaters by other researchers (Khalifa, A. et al., 2017) and (Martínez-Díez, L. and Vázquez-González, M. I., 1999).

In this study, the governing of feed temperature to the flux can be seen significantly at the constant permeate temperature and crossflow velocity. The highest feed temperature (60°C) can give the highest flux rather than the lower temperature for both colors. The flux of the black color (400ADMI) and the blue color (400 ADMI) are 4.89 kg/m^2.hr and 4.75 kg/m^2.hr (cross-flow velocity = 0.1 m/s for both reactive dye wastewaters).

4.2.2   Effect of cross-flow velocity on permeate flux

There is also the relationship between the cross-flow velocity and the permeate flux. The cross-flow velocity can also affect the permeate flux as the temperature effect. The higher flow rate can reduce the boundary temperature and the bulk temperature difference as also discussed in Section 2.5.8. In this test, 0.05 m/s, 0.1 m/s and 0.15 m/s are used as the various trial cross-flow velocity testing. The calculations of each cross-flow velocity are shown in Appendix-A. The permeate flux can increase up to 80% (blue color) and 50% (black color) by the velocity from 0.05 m/s to 0.15m/s. The resulted flux at 0.15 m/s is nearly same for both colors.
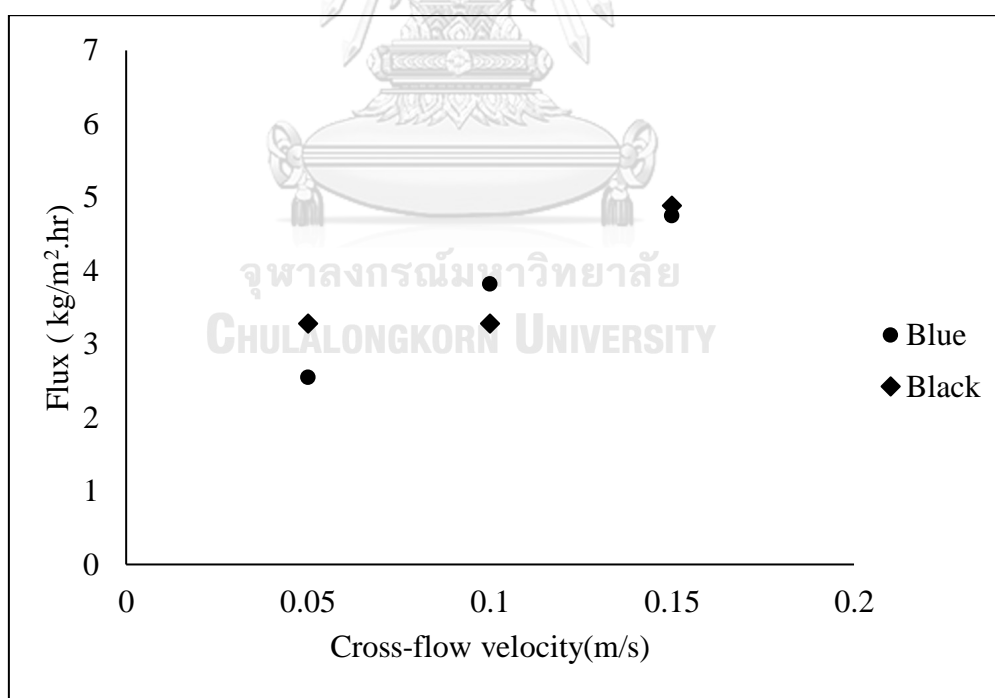
Figure 4.8 Effect of cross-flow velocity to the flux (reactive blue and black dye wastewater)
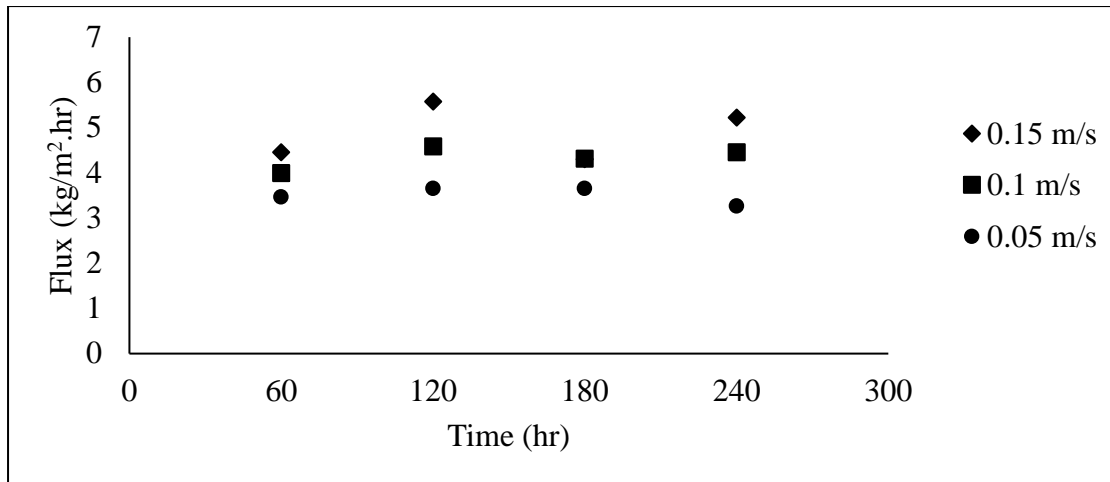
Figure 4.9 Effect of cross-flow velocity to the flux (reactive black dye)
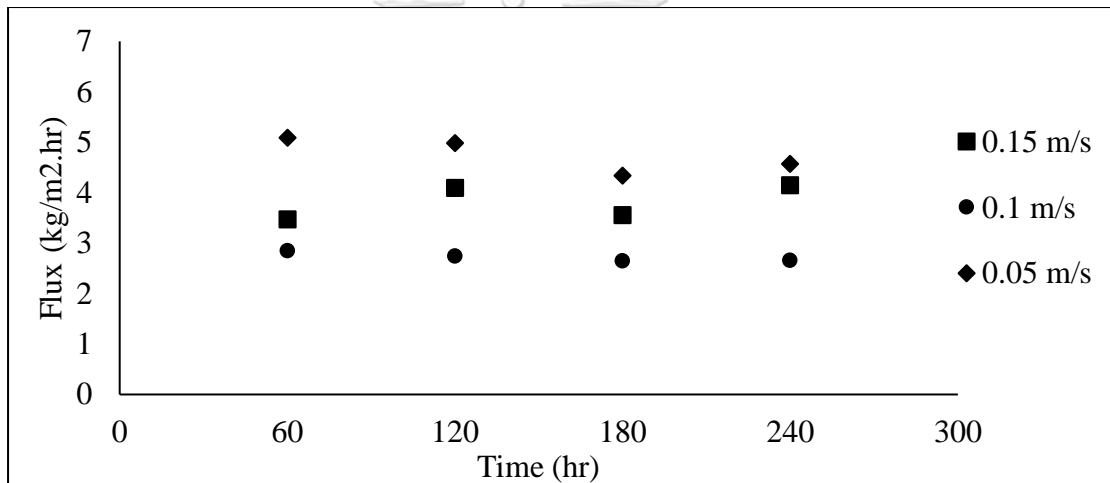
Figure 4.10 Effect of cross-flow velocity to the flux (reactive blue dye)

The cross-flow velocity can reduce the temperature polarization and concentration polarization of the system. The higher flow can affect the heat transfer coefficient at the membrane boundary surfaces and the increased circulation rate can reduce the concentration contacting time to the membrane surface. (Chen, T.-C. et al., 2009)

As the Reynolds number, the higher flow rate (cross-flow velocity) tends to the turbulent flow region. The larger Reynolds number can give the higher value of Nusselt number. This can promote the heat transfer coefficient. However, liquid entry pressure should be considered. In this study, the circulation flow rates (cross-flow velocity) are ranged in the laminar flow region. In Figure 4.8, the

relationship of the flow rate (cross-flow velocity) and the permeate flux can be seen. The flow rates between 0.5 l/min (0.05 m/s) to 1.5 l/min (0.15 m/s) are in the ranges of Reynolds number 185 to 1098 that is in the laminar flow region. But the higher Reynolds number can give the higher flow rate (cross-flow velocity). Laminar flow operation does not need the higher pumping pressure for the protection of membrane wettability and the reduction of energy cost. (Chen, T.-C. et al., 2009)

Temperature polarization coefficient is the dealing with the bulk temperature and the flow rate (cross-flow velocity). It is also influenced by the operating condition, the wastewater characteristics and the type of membrane material. The temperature at the boundary surfaces can govern to the flux conditions. The higher flow rate (cross-flow velocity) can reduce the higher temperature polarization coefficient value that can give the higher flux. The high temperature and cross flow velocity can promote to the permeate flux with the decreased heat loss and temperature polarization effect. (Martínez-Díez, L. et al., 1999). (Martínez, L. and Rodríguez-Maroto, J. M., 2007) recommended to consider for both the model design and the module characteristics for the high fluxes. To investigate the permeate water quality by the increased feed concentrations, the feed temperature (60°C) and cross-flow velocity (0.15 m/s) were used as the operating conditions.

4.2.3   Effect of operating parameters on color removal efficiency

The color removal efficiency was investigated by the operating parameters. The feed color was prepared as 400 ADMI for all that experiments. The effluent color ADMI value can be seen in Figure 4.11 and Figure 4.12 by the effect of feed temperature and cross-flow velocity. The color removal efficiency is over 96%. There are no prominent changes in removal efficiency for both operating parameters even there is the changes of effluent color value. The effluent color value of blue 19 is better than the reactive black 5. The effluent of Black 5 dye tends to increase in higher temperature. The cross-flow velocity (v = 0.05 m/s and 0.1 m/s) can give the approximately same results whereas the velocity (0.1 m/s). Therefore, the long-term operation should be examined to discuss about the prominent escaped components because there is a slight change of efficiency for 4 hours operating time and color concentration of 400 ADMI wastewater
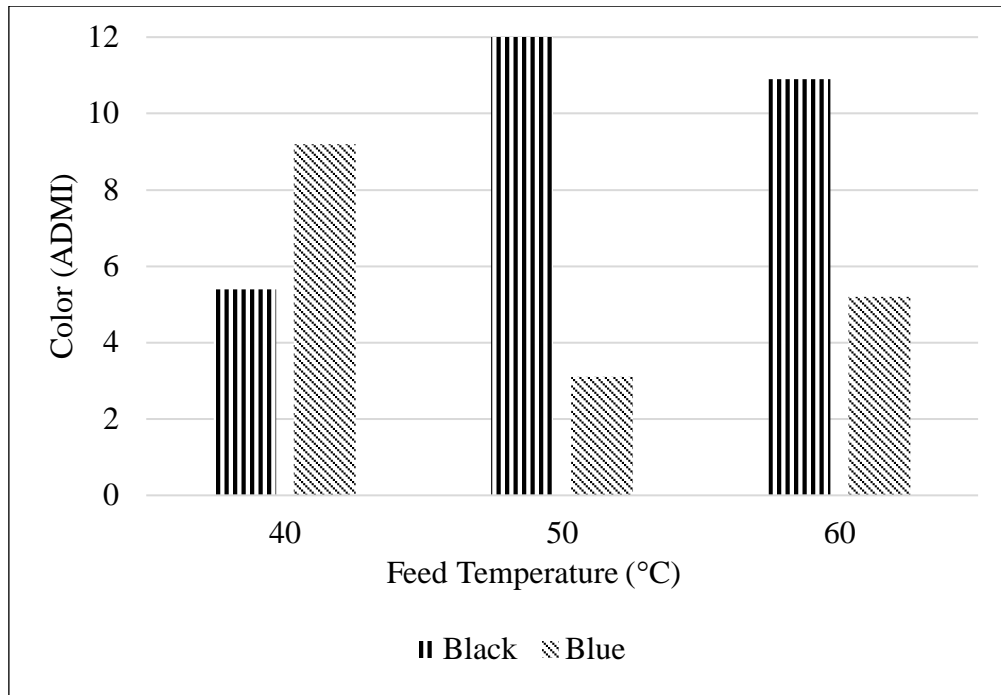
Figure 4.11 Color removal by feed temperature (v = 0.1m/s)
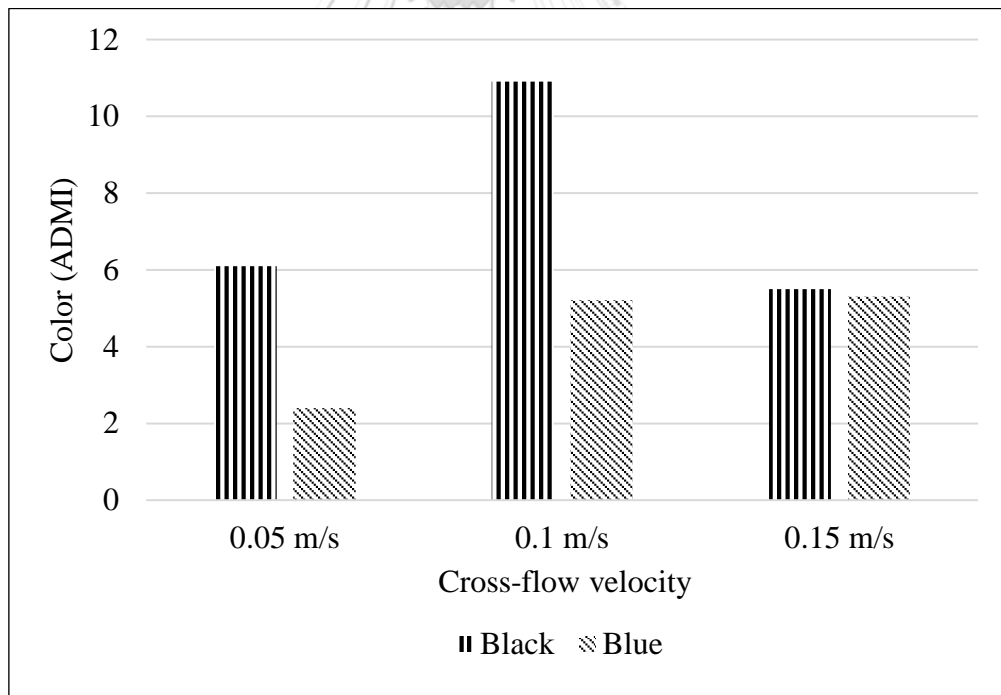
Figure 4.12 Color removal by cross-flow velocity (T$_f$ = 60°C)

4.2.4   Effect of color and auxiliary components concentrations on permeate
flux

At first, the effect of color concentration to the permeate flux was
investigated. The color concentration also can affect to the flux in Figure 4.13. The
binding between the ion of membrane surface and the color materials might also
result in the amount of permeate water. In general, due to the higher boiling point of
dye substance, the reactive dye substance cannot pass through the membrane surface
that can give the good water color removal. The determination of flux is difficult to
describe a result of various factors such as the complex chemical structure, ion effect
and the other effect of auxiliary chemicals. In this research, the blue color flux was
decreased, and the increased black color flux can be seen. There may be the short
operating time and for the long operation time, the results may be changed because of
the fouling condition.
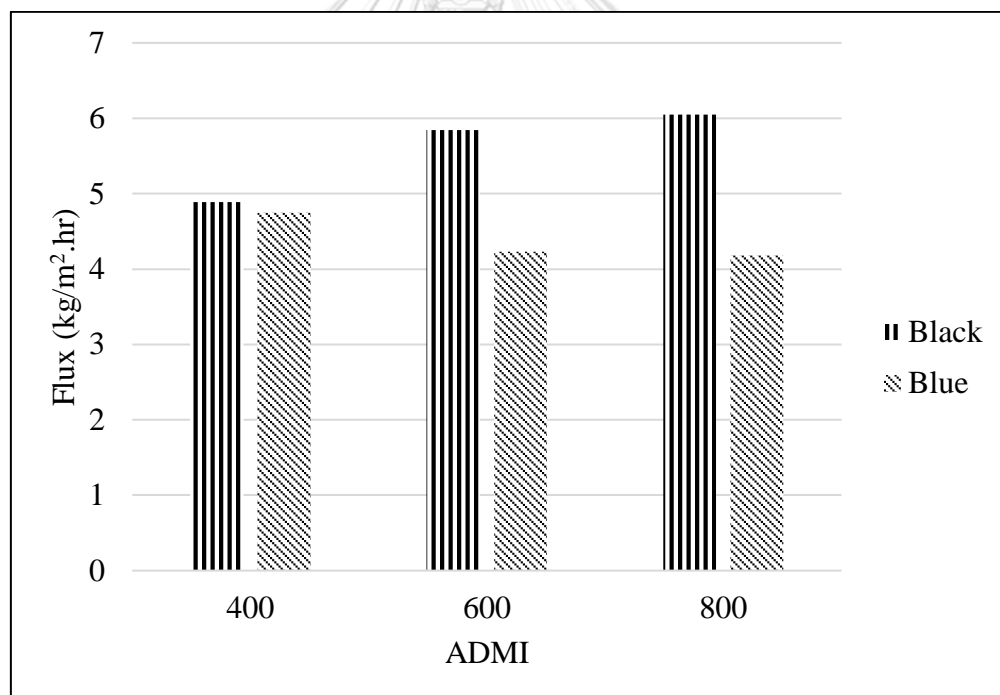
Figure 4.13 Flux with color concentration

As with the considerations of auxiliary component concentrations, the
flux conditions are described in Figure 4.14, Figure 4.15, Figure 4.16 and Figure 4.17.
The pH is increased to the alkaline range, the flux is approximately stable for the
black dye whereas the decreased flux for the blue dye. There may be the correlation

between the membrane surface properties and the pH range. In (An, A. K. et al., 2016) research, the zeta potential of PVDF membrane is increased in higher pH range. When the phosphorus concentration was changed to 5mg/l, 10mg/l and 15 mg/l. There are no significant flux changes for black dye and the decreased flux is occurred in the treatment of blue dye wastewater. According to the detection of Ion Chromatography, the phosphate value is low in some stock. For the changing of nitrate and sulfate value, the flux tends to decrease in black dye and the unstable flux is occurred in blue dye. (Boubakri, A. et al., 2017) explained that the ionic strength has no significant effect on the permeate flux as that observed in the case of transmembrane temperature difference or Reynolds number.
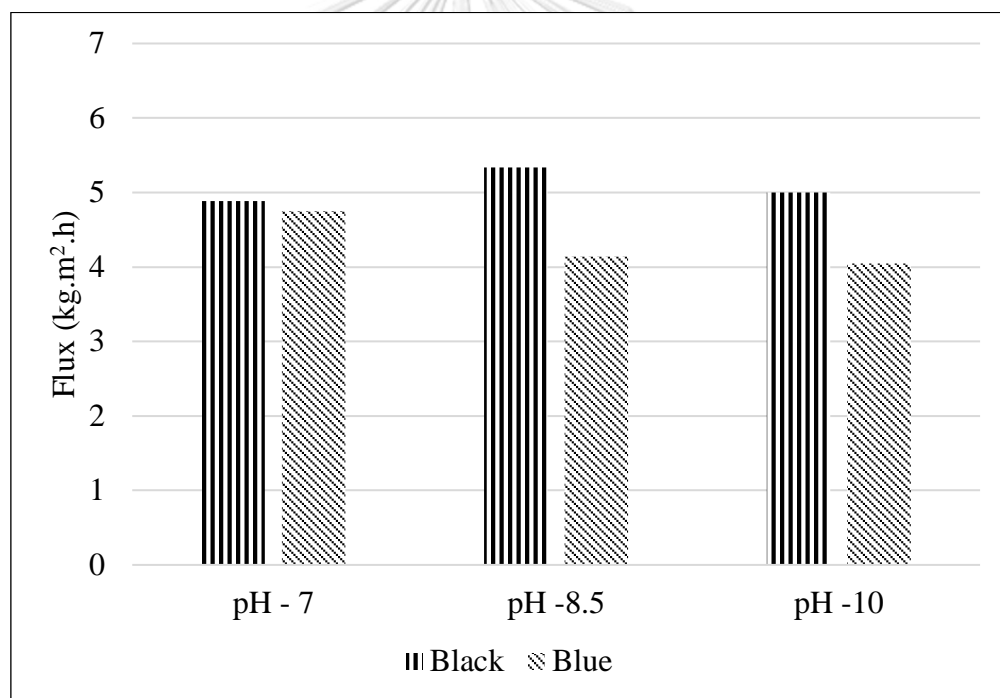
Figure 4.14 Flux with pH changes
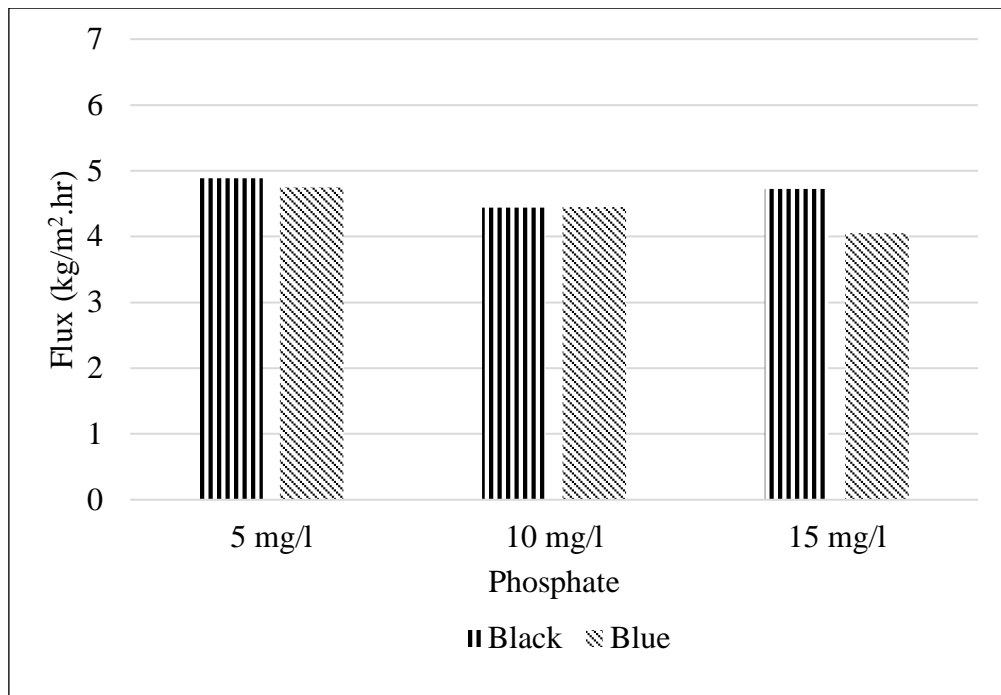
Figure 4.15 Flux with phosphate concentration
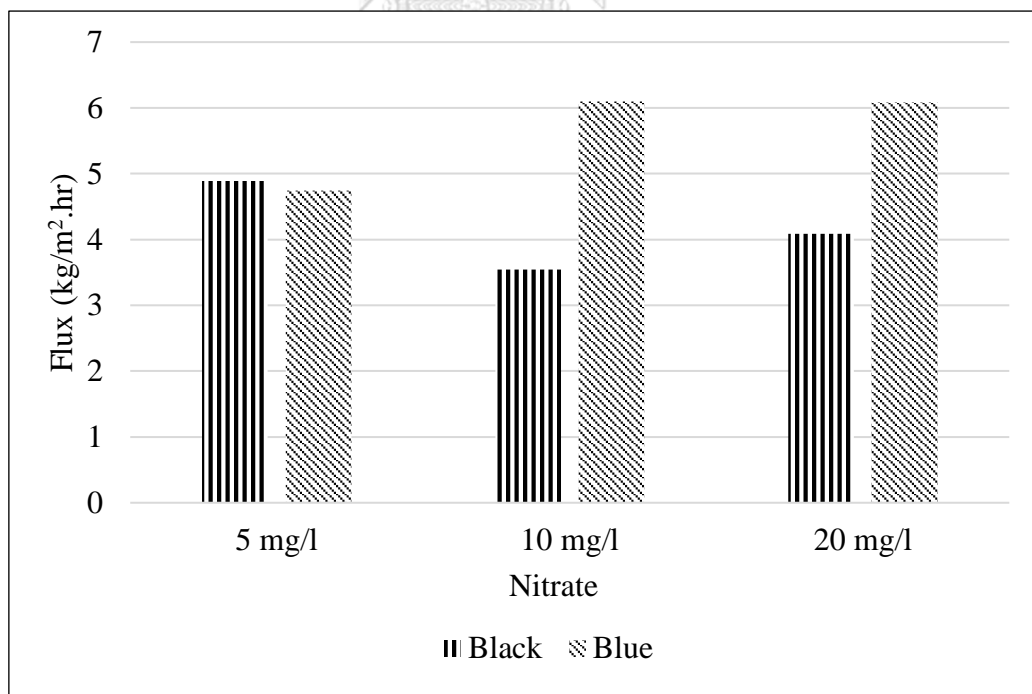
Figure 4.16 Flux with nitrate concentration
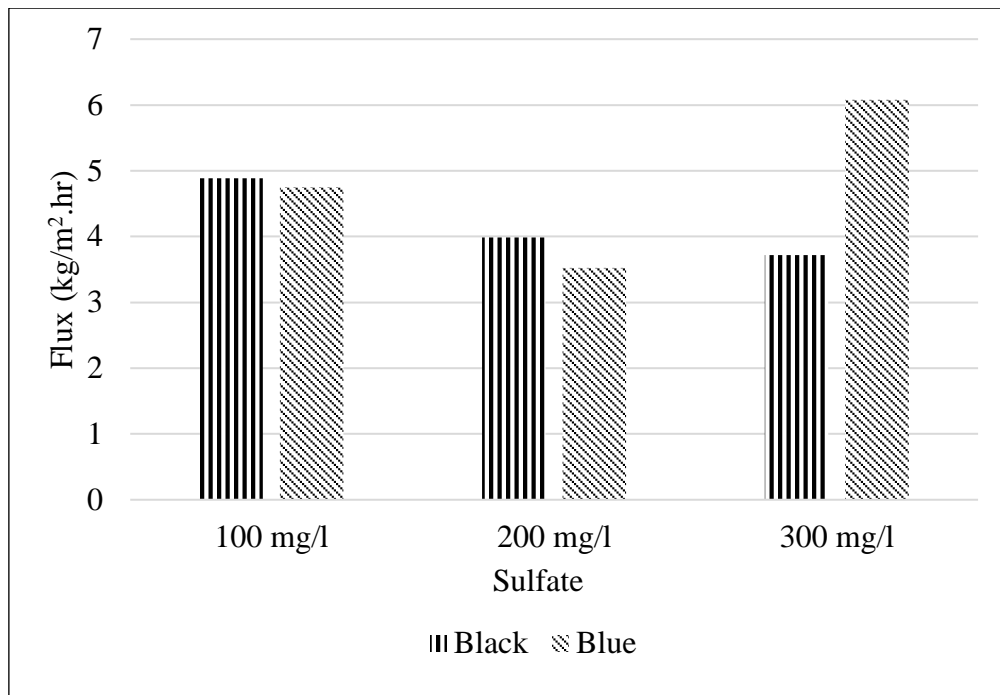
Figure 4.17 Flux with sulfate concentration

The flux of the real textile effluent was significantly decreased to 2.53 kg/m^2.hr. The reduction was about 48% under the operating parameters (feed temperature, permeate temperature and cross-flow velocity = 0.15 m/s). In Figure 4.18, the reducing flux of the real textile effluent can be seen by the time. After 5 hours treatment, the flux was decreased to 0.35 kg/m^2.hr. Besides of the operating parameters, the concentration can affect to the system efficiency.
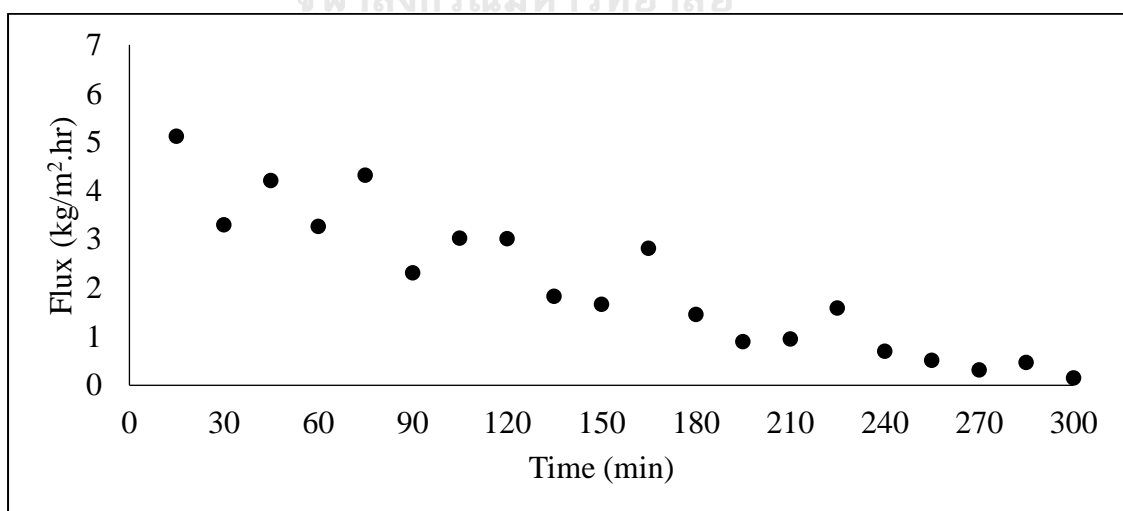
Figure 4.18 The flux with textile effluent (T$_f$ = 60°C, T$_p$ = 20°C, v = 0.15 m/s)

4.3 Water Quality Analysis

    4.3.1   Effect of color removal by the different pollutant concentrations
(synthetic and real wastewater)

The water treatment efficiencies of the direct contact membrane distillation
system with the effects of color concentration, anion concentrations and pH changes
were operated at the optimal operating condition: feed temperature (60°C), the
permeate temperature (20°C) and cross-flow velocity (0.15 m/s), that was obtained
from our previous experiments. The effluent water was measured for the parameters;
pH, conductivity, TOC, color (ADMI) and the ion analysis.

Table 4.4 Water quality of synthetic black dye wastewater treatment

wastewater	Color (ADMI)		pH		Conductivity (μS/cm)			TOC (mg/l)	
	Inf.	Eff.	Inf.	Eff.	Inf.	Eff.	Rejection (%)	Inf.	Eff.
Effect of color concentration changes									
Black	400	5.50	7.0	7.3	388	15.99	96	1.561	0.10
Black	600	3.20	6.9	7.2	407.9	15.13	97	2.506	0.28
Black	800	2.80	6.9	7.0	550.27	15	98	1.974	0.41
Effect of pH value changes									
pH - 7	400	5.40	7.0	7.3	388	15.99	96	1.561	0.10
pH -8.5	400	3.73	8.5	7.1	448	14	97	16.35	2.9
pH -10	400	2.87	10.0	7.0	389	11	98	1.826	0.93
Effect of phosphate (mg/l) changes									
5 mg/l	400	5.40	7.0	7.3	388	15.99	96	1.561	0.10
10 mg/l	400	4.03	6.4	6.5	376.17	12.25	97	1.646	0.20
15 mg/l	400	7.23	7.2	7.2	360.57	14.85	96	3.301	0.99

Effect of nitrate (mg/l) changes									
5 mg/l	400	5.40	7.0	7.3	388	15.99	96	1.561	0.10
10 mg/l	400	6.1	7.4	8.0	376.07	11.94	97	3.039	1.25
20 mg/l	400	6.7	6.9	7.4	386	17	96	3.993	2.10
Effect of sulfate(mg/l) changes									
100 mg/l	400	5.40	7.0	7.3	388	15.99	96	1.561	0.10
200 mg/l	400	6.2	7.4	7.4	508.87	10.56	98	2.102	1.82
300 mg/l	400	7.3	7.4	7.2	712.5	15.32	98	2.403	2.19

 * All the changes values of wastewater are that mentioned in the experimental scenarios section. Inf. = feed water side (Influent water), Eff. = permeate water side (Effluent water)

Table 4.5 Water quality of blue color synthetic wastewater

	Color (ADMI)		pH		Conductivity (µS/cm)			TOC (mg/l)	
wastewater	Inf.	Eff.	Inf.	Eff.	Inf.	Eff.	Rejection (%)	Inf.	Eff.
Effect of color concentration changes									
Blue	400	5.3	7.0	7.4	406.5	13.1	97	4.755	0.72
Blue	600	2.7	6.9	7.3	361.7	9.3	98	6.705	0.60
Blue	800	6.2	6.9	7.4	340.0	16.4	96	8.227	0.12
Effect of pH value changes									
pH - 7	400	5.3	7.0	7.4	406.5	13.1	97	4.755	0.72
pH -8.5	400	5.4	8.5	7.3	355.8	9.6	98	9.174	2.64
pH -10	400	5.5	10.0	7.2	380.1	10.8	98	4.856	2.95

Effect of phosphate (mg/l) changes									
5 mg/l	400	5.3	7.0	7.4	406.5	13.1	97	4.755	0.72
10 mg/l	400	<2	6.7	7.3	343.4	9.6	98	6.426	1.3
15 mg/l	400	3.4	6.7	7.4	443.1	9.7	98	4.629	0.14
Effect of nitrate (mg/l) changes									
5 mg/l	400	5.3	7.0	7.4	406.5	13.1	97	4.755	0.72
10 mg/l	400	2.0	7.2	7.0	370.6	12.2	97	4.26	0.49
20 mg/l	400	3.0	6.9	7.3	396.4	11.4	98	4.472	0.13
Effect of sulfate(mg/l) changes									
100 mg/l	400	5.3	7.0	7.4	406.5	13.1	97	4.755	0.72
200 mg/l	400	<2	7.2	7.3	579.6	13.8	98	3.99	0.30
300 mg/l	400	4.6	7.1	7.1	649.4	17.8	98	4.494	0.17

 * All the changes values of wastewater are that mentioned in the experimental scenarios section. Inf. = feed water side (Influent water), Eff. = permeate water side (Effluent water)

Table 4.6 Water quality of real textile effluent

	Color (ADMI)		pH		Conductivity (µS/cm)			TOC (mg/l)	
	Inf.	Eff.	Inf.	Eff.	Inf.	Eff.	Rejection (%)	Inf.	Eff.
Textile effluent	319	11	10.5	8.2	2167	145	94	250.8	4.6

Inf. = feed water side (Influent water), Eff. = permeate water side (Effluent water)

- Color removal and pH changes by different concentrations

	400	600	800
‖ Black Dye	5.4	3.2	2.8
⊠ Blue Dye	5.3	2.7	6.2

Color (ADMI)

‖ Black Dye　⊠ Blue Dye
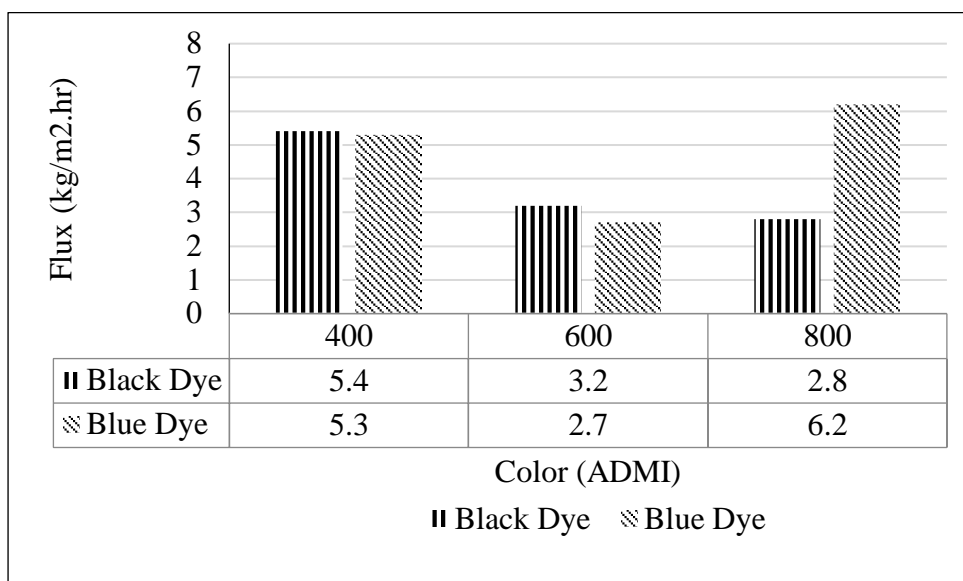
Due to the data from the experiment, the color removal efficiency is not too much different even though the feed concentration is changed. The overall maximum effluent color concentration is about 11 ADMI. The overall effluent is acceptable to dispose to the water body. (Chong, K. et al., 2016) investigated also reactive blue dye by hollow fiber membrane as the direct contact membrane and showed that the color rejection is up to 96.2 %. (Calabro, V. et al., 1991) also tested Red E-4BA, Blue E-G and Blue E-BA with same system and different membrane material and the rejection 100% is very attractive for that test. The rejection of dye reactive black 5 (>99.75%) was achieved by using of a modified PVDF hollow fiber membrane with direct contact membrane distillation system. (Mokhtar, N. M. et al., 2015)

It can be said that the concentration of feed side can influence to the effect of flux more than the effect of permeate quality. The average color removal was in the range from 96% to 98% whereas the concentration of color, ions and pH were changed. The auxiliary components cannot affect to the dye removal. The melting points of black 5 and blue 2 (>300°C) are higher than the operating temperature that can retentate the color dye only in the feed side. Therefore, the dye concentration was repelled by the membrane ion surface and the water vapor only can pass through the hydrophobic membrane. The permeate color from the real textile effluent treatment was the highest value, compared to that of the synthetic wastewater; even though the feed color concentration is lower than that of the synthetic colors. There may be the

escaped volatile components for this because pH value, conductivity and TOC investigations were also higher than the effluent of synthetic colors.

The permeate pH values are 7 ±0.4 for all the synthetic color wastewater. However, the real wastewater is 8.2 that is still in alkaline region, the feed wastewater is 10.5.

- Conductivity removal by different concentrations

The conductivity rejection was in the range from 96% to 98% for the synthetic wastewater. The rejection efficiencies of both colors were not different. The auxiliary components of salts mainly influence to the conductivity of the solutions. The color cannot affect the conductivity and then, high salt reduction could be obtained. The conductivity of synthetic reactive dye wastewater was 650 µS/cm in maximum value, whereas the real textile effluent had 2167 µS/cm more than threefold of the synthetic wastewater. The permeate conductivity might not be satisfied for the real wastewater as compared with the synthetic wastewater, however, the percentage of rejection was 94%. (Gryta, M. et al., 2006) studied that the conductivity of permeate water by direct contact membrane distillation was in the range of 2-4 µS/cm from the treatment of saline wastewater concentration. The conductivity was 3-5 µS/cm for the treatment of NaCl solution containing natural organic matter by PP material and direct contact membrane distillation system in the research of (Gryta, M. et al., 2001). The investigation of brackish water and sea water showed that the conductivity of distilled water 1.1 to 107 µS/cm after 62 hours of direct contact membrane distillation system (Boubakri, A. et al., 2017).
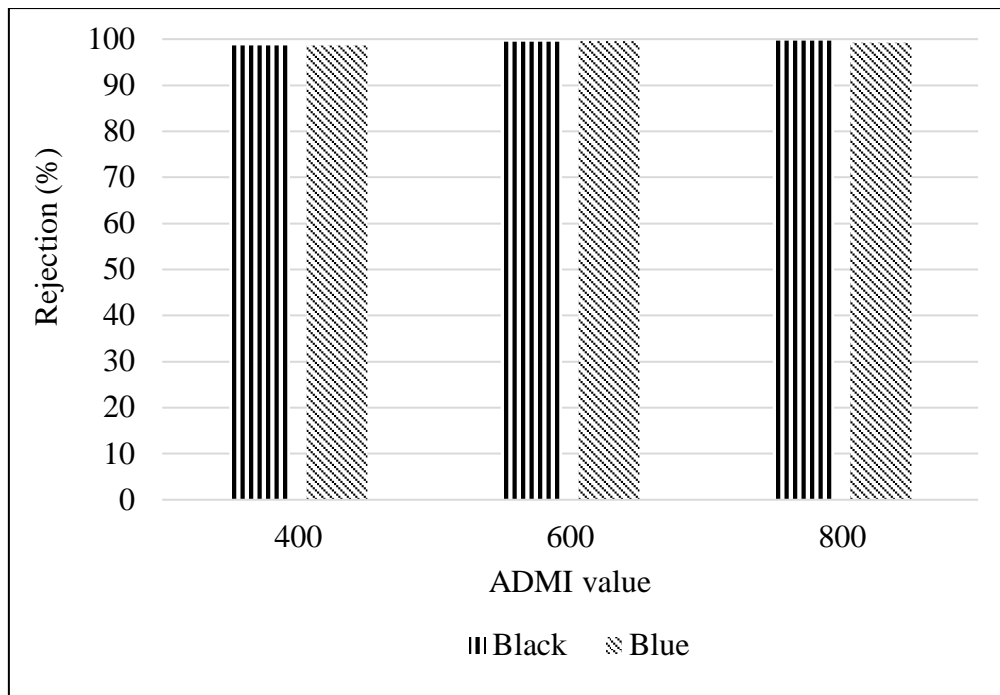
Figure 4.19 Color removal efficiency by the feed color concentrations

(black and blue color)
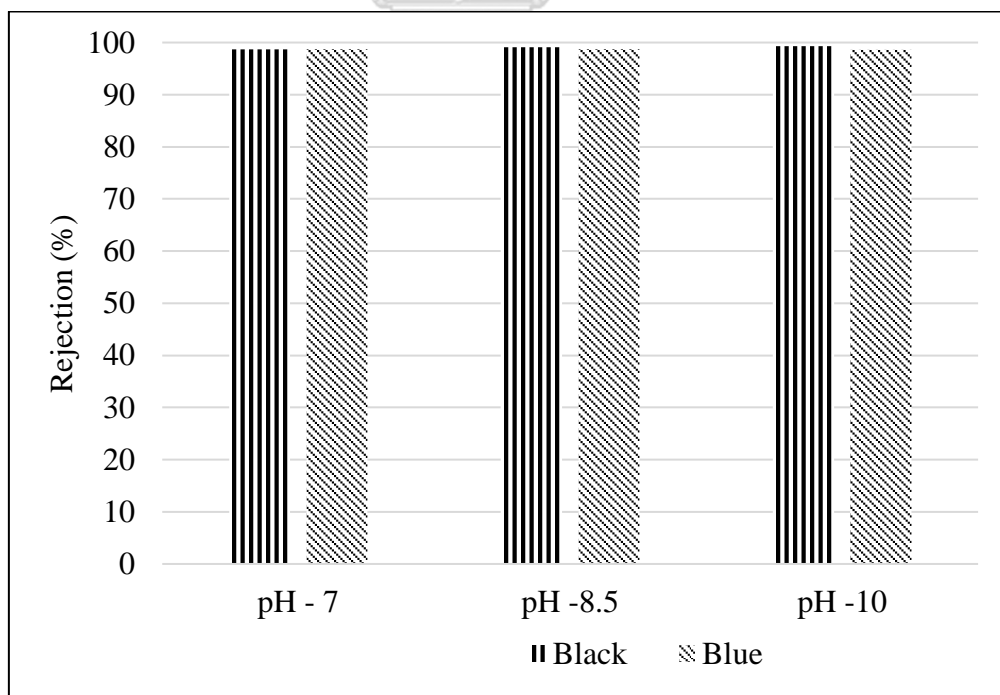
Figure 4.20 Color removal efficiency as a function of pH
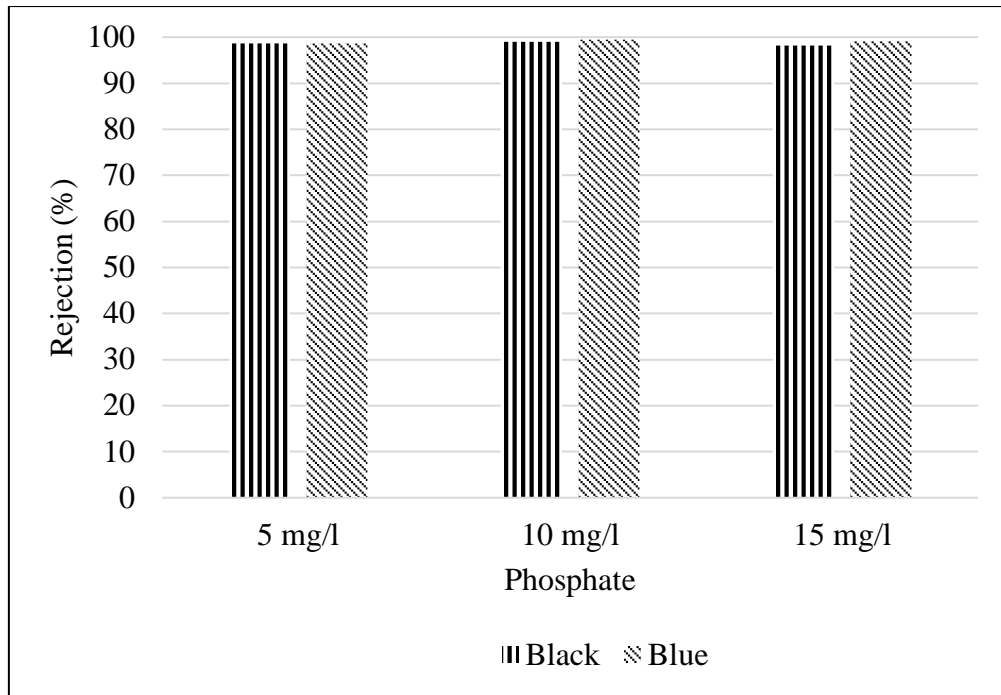
Figure 4.21 Color removal efficiency by the effect of phosphate
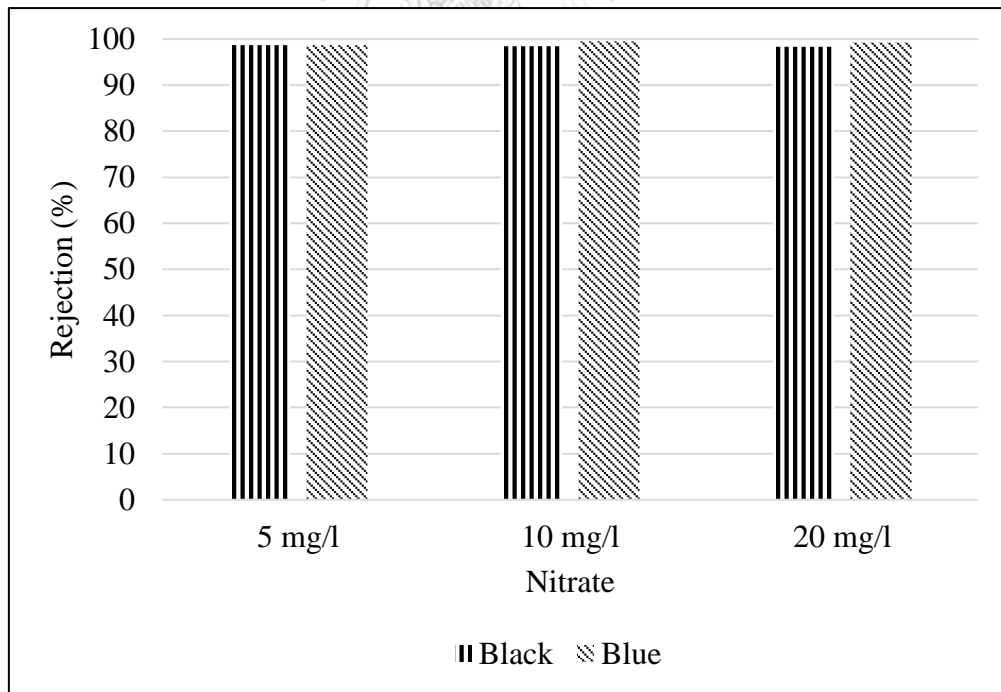
Figure 4.22 Color removal efficiency by the effect of nitrate
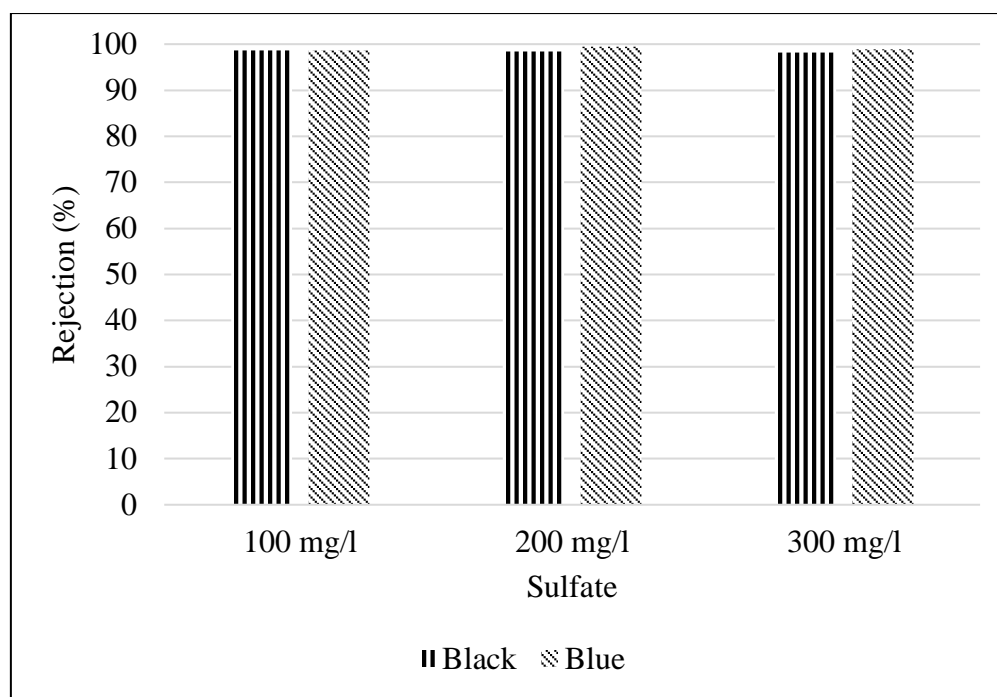
Figure 4.23 Color removal efficiency by the effect of sulfate

- TOC removal by different concentrations

The anions auxiliary substance can slightly interference to the TOC effect. The permeate concentration is lower than the feed concentration. The organic carbon effect is significantly seen in case of real wastewater experiment. The permeate TOC effect of the organic carbon in real textile effluent that was higher than the synthetic wastewater is not different from the synthetic wastewater. The permeate TOC (4.59 mg/l) for the real textile effluent might contain some volatile organic matters, that can pass through the membrane sheet.

However, the fouling condition is more impact to the membrane. The high TOC value is dealing with the membrane surface fouling as organic carbon fouling. The real textile effluent has greater TOC value than the synthetic wastewater (not more than 16 mg/l). The declination of flux can be seen significantly in the Figure 4.18 for 5 hours. After one hour, the flux was getting decreased by time whereas the synthetic wastewater flux is nearly stable during the operation time (4 hours). The pretreatment for TOC removal is recommended before the direct contact membrane distillation system to prevent the fouling conditions.

As the other treatment system, the combination of ozonation and anaerobic treatment can give TOC removal of 84% for the Reactive Black-5 (Venkatesh, S. et al., 2017). TOC from reactive dyes (Samofix red V-RBL and Samofix Green V-G) could be removed by coagulation from 99.8 and 99.2% (Najafi, H. and Movahed, H., 2009). For the direct contact membrane distillation, the quality of permeate water is not changed in large amount. Therefore, the membrane cannot reject some of the volatile organic compounds.

4.3.2 Effect of Anions removal by the different concentrations (synthetic and real wastewater)

From the overall results from the studies on effects of reactive dye concentrations, each anion concentration and pH on the anion pollutant removal, the results are shown in Table 4.7.

Table 4.7 Effects of reactive dye concentrations, each anion concentrations and pH on the anion pollutant removal

	Cl (ppm)		NO_3 (ppm)		PO_4 (ppm)		SO_4 (ppm)	
	Inf.	Eff.	Inf.	Eff.	Inf.	Eff.	Inf.	Eff.
Effect of color concentration changes								
Black (400ADMI)	51.72	1.17	6.21	0.31	5.66	-	76.72	0.78
Black (600ADMI)	42.58	1.06	3.9	0.23	3.98	-	85.23	0.67
Black (800ADMI)	46.14	1.29	4.02	0.24	4.21	-	93.74	0.34
Effect of phosphate (mg/l) changes (Black)								
5 mg/l	51.72	1.17	6.21	0.31	5.66	-	76.72	0.78
10 mg/l	51.57	0.98	5.1	0.3	10.59	-	73.72	0.46
15 mg/l	53.4-	1.26	4	0.28	15.6	0.05	72.1	0.83

Effect of nitrate (mg/l) changes (Black)								
5 mg/l	51.72	1.17	6.21	0.31	5.66	-	76.72	0.78
10 mg/l	53.63	1.03	10.94	0.33	8.26	-	76.72	1.05
20 mg/l	57.1	1.36	23.2	0.49	4.41	-	76.72	0.71
Effect of sulfate(mg/l) changes (Black)								
100 mg/l	51.72	1.17	6.21	0.31	5.66	-	76.72	0.78
200 mg/l	47.13	1.07	5.285	0.22	4.64	-	179.72	0.61
300 mg/l	42.54	1.23	4.36	0.29	3.62	-	282.72	1.27
Effect of pH value changes								
pH -7	51.72	1.17	6.21	0.31	5.66	-	76.72	0.78
pH -8.5	48.25	0.97	4.57	0.4	3.7	-	97.42	0.39
pH -10	71.54	0.91	5.4	0.34	4.98	-	118.12	0.46
Effect of color concentration changes								
Blue (400ADMI)	52.06	1.05	5.6	0.31	4.21	-	105.65	0.61
Blue (600ADMI)	50.6	2.04	4.8	0.39	4.01	-	105.11	8.4
Blue (800ADMI)	48.05	1.16	4.6	0.39	3.85	-	104.25	0.84
Effect of phosphate (mg/l) changes (Blue)								
5 mg/l	52.06	1.05	5.6	0.31	4.21	-	105.65	0.61
10 mg/l	48.5	0.81	4.6	0.34	7.92	-	104.53	0.27
15 mg/l	50.74	1.03	4.78	0.4	12.56	-	103.41	0.42
Effect of nitrate (mg/l) changes (Blue)								
5 mg/l	52.06	1.05	5.6	0.31	4.21	-	105.65	0.61

10 mg/l	50.04	1.07	9.04	0.44	4.22	-	103.56	0.45
20 mg/l	51.22	1	18.32	0.47	3.92	-	101.47	0.48
Effect of sulfate(mg/l) changes (Blue)								
100 mg/l	52.06	1.05	5.6	0.31	4.21	-	105.65	0.61
200 mg/l	48.67	0.8	4.79	0.35	3.45	-	205.65	0.41
300 mg/l	50.3	0.93	3.98	0.37	-	-	305.65	0.36
Effect of pH value changes								
pH -7	52.06	1.05	5.6	0.31	4.21	-	105.65	0.61
pH -8.5	49.4	1.51	4.6	0.37	4.45	0.08	126.35	0.63
pH -10	50.13	1.13	1.1	0.32	4.83	-	147.05	0.42
Real wastewater	69.12	5.21	-	0.31	1.77	-		2.3

* All the changes values of wastewater are that mentioned in the experimental scenarios section. Inf. = feed water side (Influent water), Eff. = permeate water side (Effluent water)

จุฬาลงกรณ์มหาวิทยาลัย

CHULALONGKORN UNIVERSITY
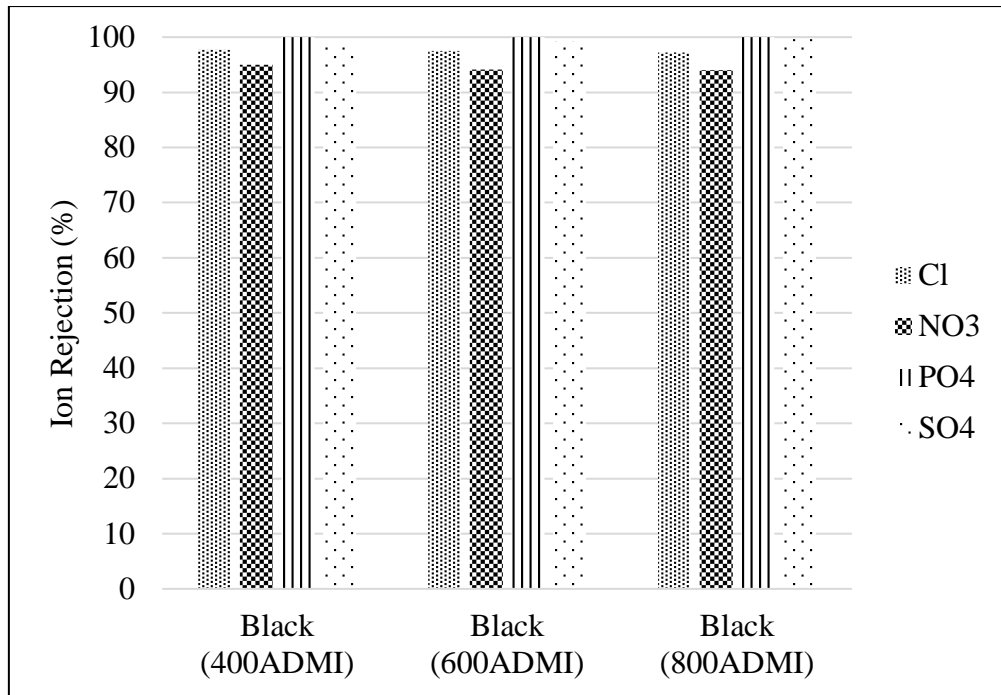
Figure 4.24 Anions removal by the effect of color concentration (Black)
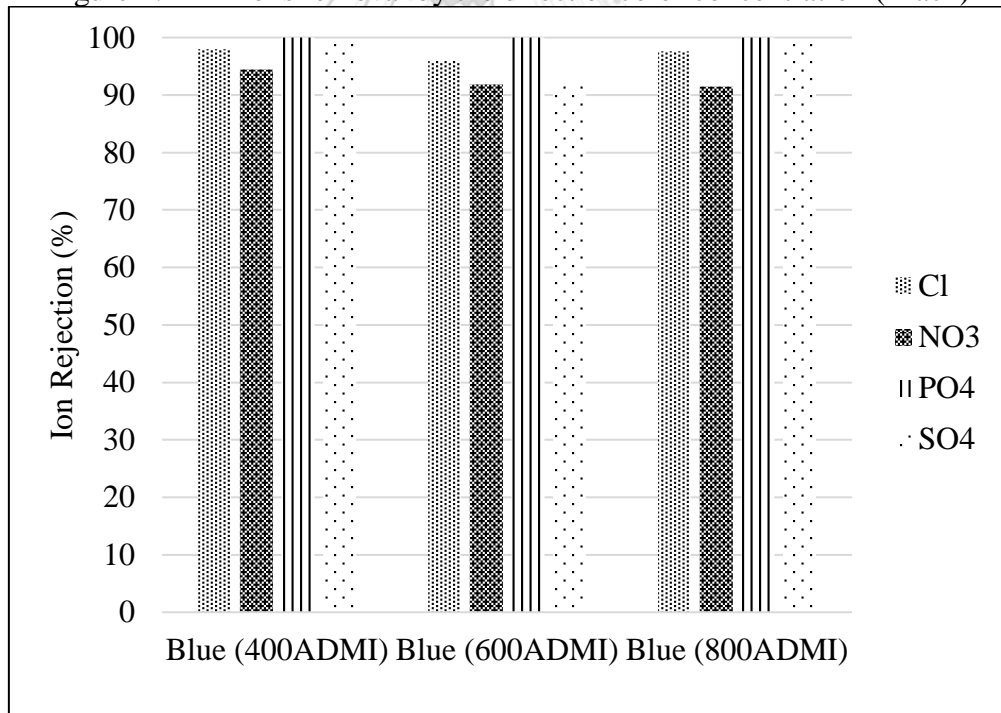
Figure 4.25 Anions removal by the effect of color concentration (Blue)

The anion rejection was not changed too much even though the changes of the color concentration. The color concentration did not affect to the anion removal of the

system. The efficiencies for all anions rejection were over 90 %. The anion removal of the direct contact membrane distillation system is highly satisfied.
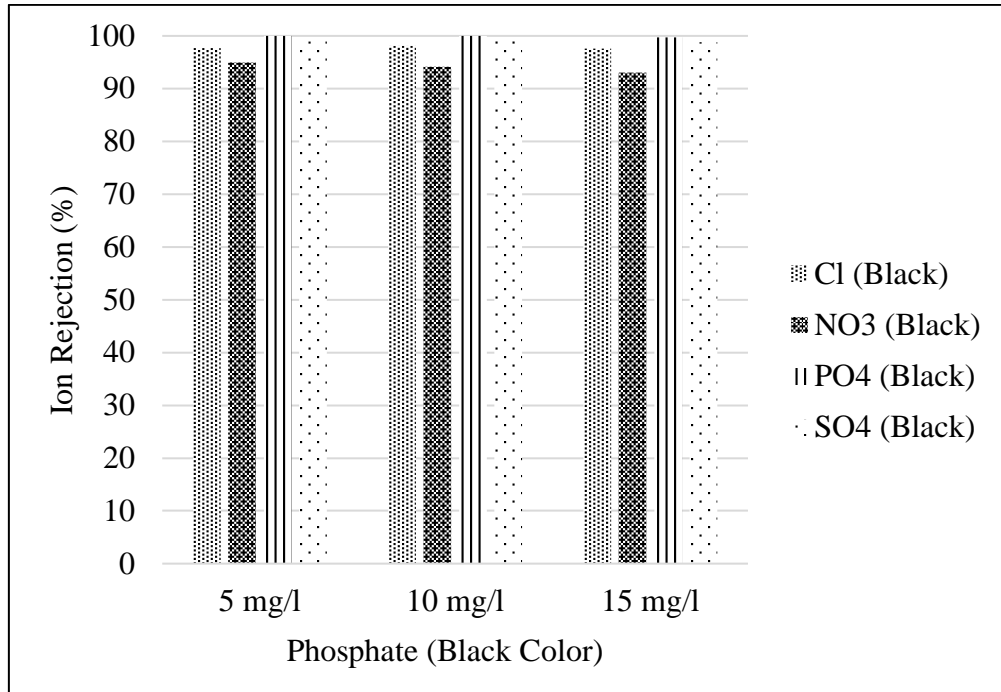
Figure 4.26 Anions removal by the effect of phosphate concentration (Black)
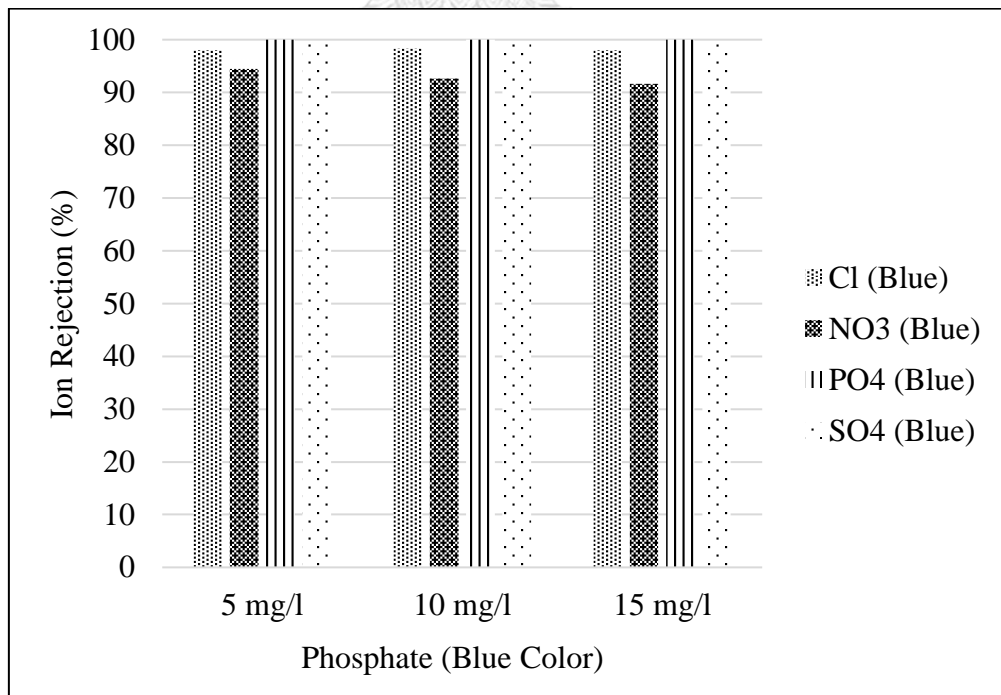
Figure 4.27 Anions removal by the effect of phosphate concentration (Blue)

According to the measurement of ion chromatography, the phosphate concentration of feed synthetic dye wastewater was very low, and the concentration of phosphate could not be detected as low concentration level. As with the concentration of phosphate in the given synthetic wastewater, the removal efficiency is so satisfied for this direct contact membrane distillation system.
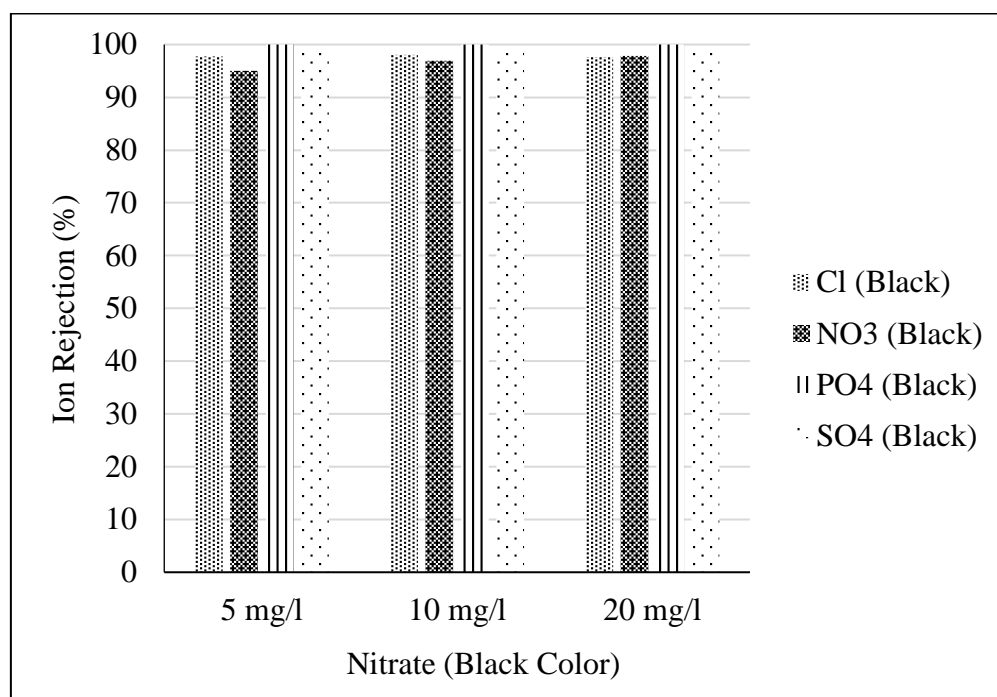
Figure 4.28 Anions removal by the effect of nitrate concentration (Black)

จุฬาลงกรณ์มหาวิทยาลัย

CHULALONGKORN UNIVERSITY
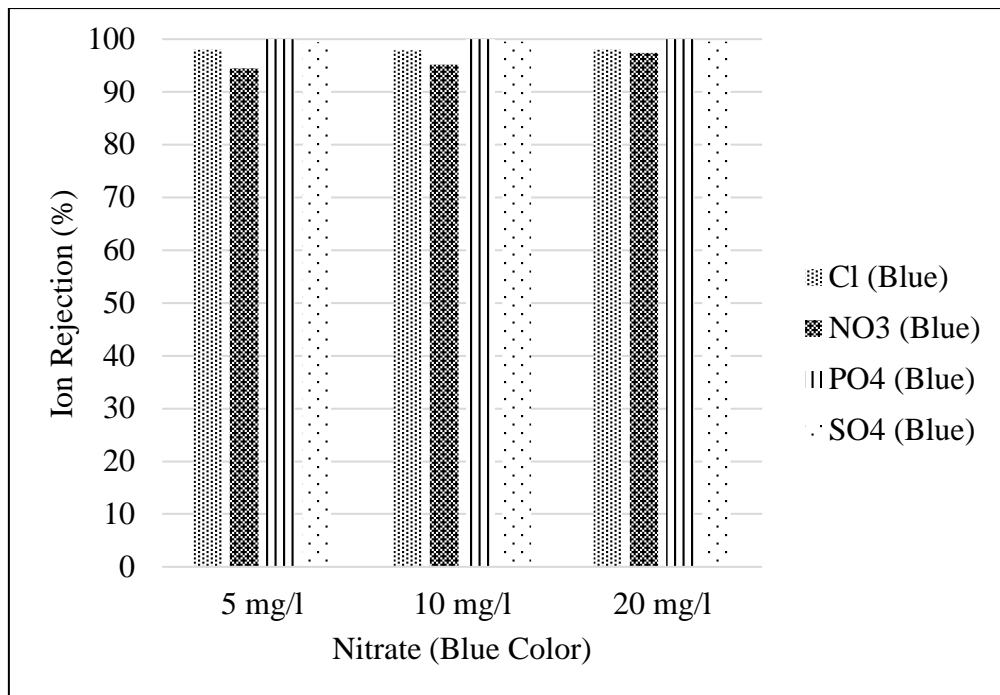
Figure 4.29 Anions removal by the effect of nitrate concentration (Blue)

The detection of nitrate in the effluent is lower than 5ppm despite increasing nitrate value. Therefore, the rejection seems to be more in higher concentration as shown in Figure 4.28 and Figure 4.29. A previous research work with the use of PP and PVDF membranes. It can be found that the permeate nitrate concentration increased slightly when the initial nitrate concentration increased from 50 to 1,000 mg/L for two studied membranes. For PP membrane, the permeate nitrate concentration was kept under 0.2 mg/L, which means almost 99.96% of nitrate rejection, and for PVDF membrane, the permeate concentration was kept under 0.4 mg/L, (Boubakri, A. et al., 2015)

Table 4.8 Nitrate rejection with membrane distillation configurations

Influent Concentration	Effluent Concentration	Membrane Material	Configuration	
50 to 1000 mg/l	Under 0.2 mg/l	PP	DCMD (FS)	(Boubakri, A. et al., 2015)
50 to 1000 mg/l	Under 0.4 mg/l	PVDF	DCMD (FS)	(Boubakri, A. et al., 2015)
200 to 1500 mg/l	97-100% rejection	PTFE	VMD (FS)	(Jain, J. et al.)

*FS = Flat Sheet, DCMD = direct contact membrane distillation,

VMD = vacuum membrane distillation
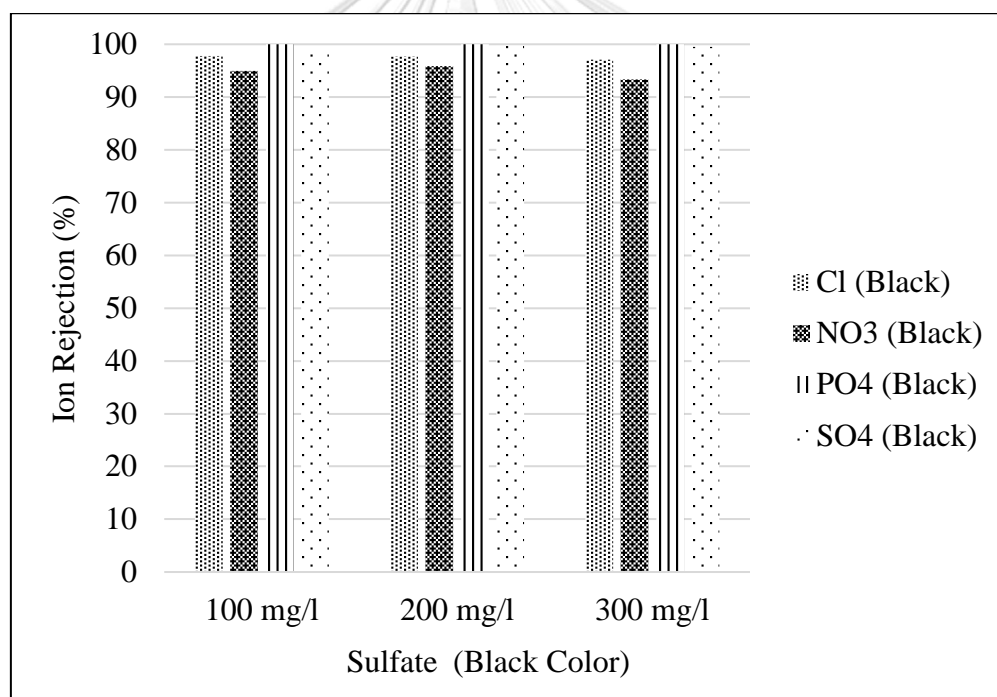
Figure 4.30 Anions removal by the effect of sulfate concentration (Black)
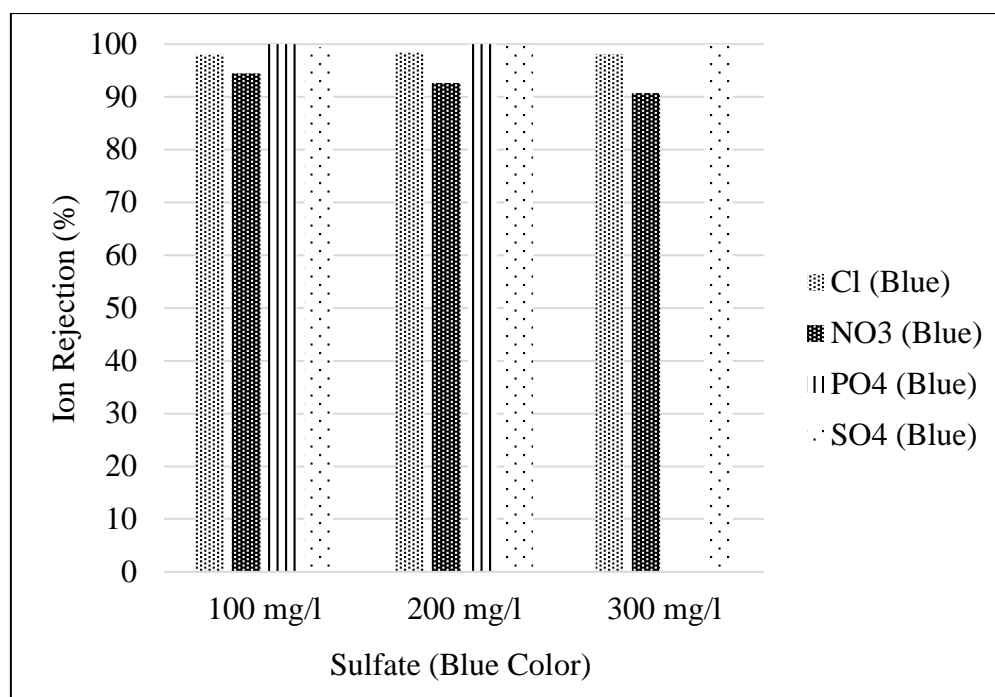
Figure 4.31 Anions removal by the effect of sulfate concentration (Blue)

The sulfate concentration in effluent was also not changed as the other experiments though the feed concentration was changed. From the research of (Fersi, C. et al., 2009), the textile wastewater treatment efficiency with other processes are shown in below table, as compared to our study.

Table 4.9 Comparison with other processes

	MF	UF	NF	This study
Conductivity	3.6%	12.1%	55.5%	96~98%
Color	44.2%	39.7%	93.3%	96~98%
SO_4^{2-}	10.6%	37.3%	96.2%	>92%

*MF = Micro filtration, *UF = Ultra-filtration, *NF = Nano filtration

For the ion concentration, conductivity and color, the direct contact membrane distillation system is more efficient than MF and UF. As the comparison with NF, the treatment efficiency depends on the ion conditions and the concentration type of solution.
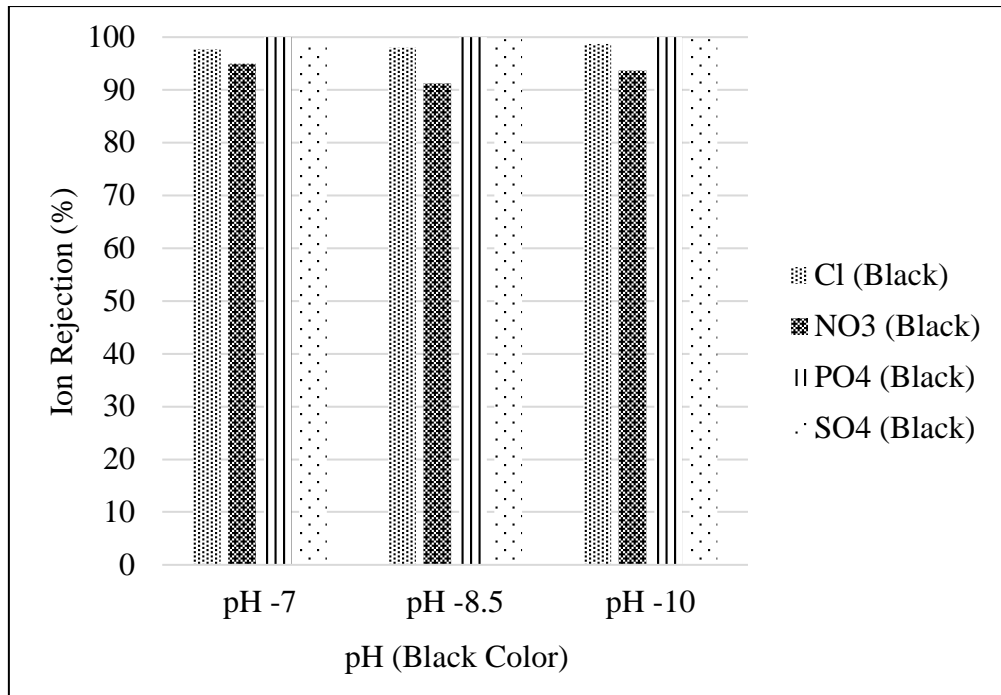
Figure 4.32 Anions removal by the effect of pH (Black)
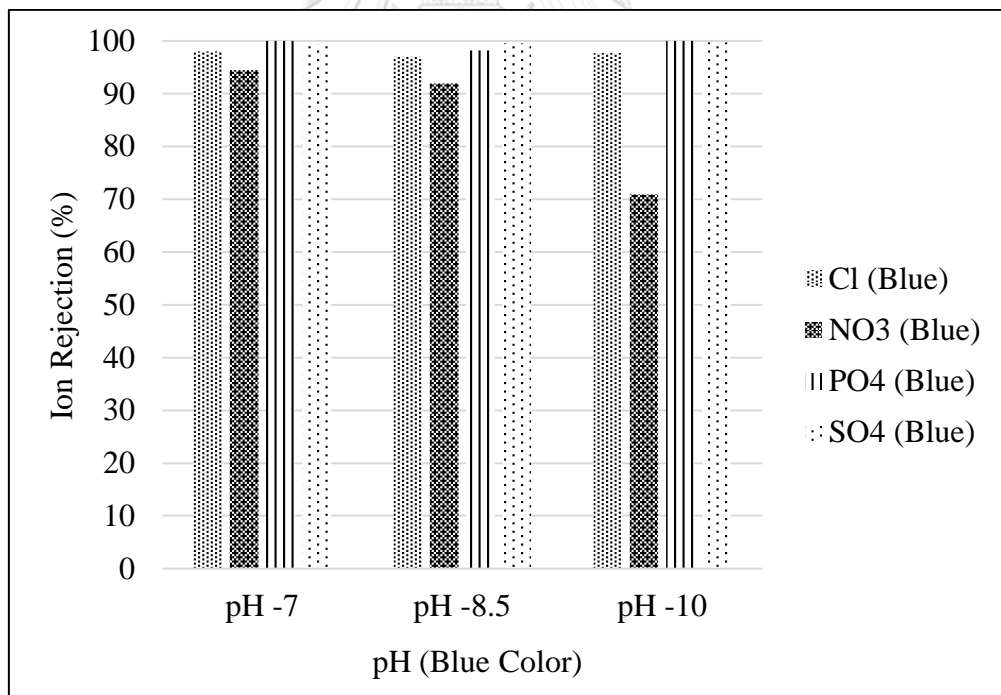
Figure 4.33 Anions removal by the effect of pH (Blue)

The pH effect of feed wastewater indicates that pH change did not affect the anion rejection for both color solutions. The anion concentration in real wastewater was very low except the chloride concentration. The treated effluent

concentration was about 5 ppm. So, the reuse of water in the industry could be considerable. To summarize of the ion removal, there is no influence of black color and blue color. The removal efficiency is not governed by the pH. pH value can favor to the presence of ammonia by adding to the NaOH. In the removal of ammonia, pH is the crucial factor that the increased pH can enhance to the removal efficiencies of ammonia in VMD. (El-Bourawi, M. et al., 2007) In this research, the ion concentration of the real wastewater is lower than that of the synthetic wastewater. According to this research, direct contact membrane distillation system can remove the non-volatile substance above 90% efficiency.

As for the overall removal of ions, the removal efficiency of phosphate (PO_4^{3-}) and sulfate (SO_4^{2-}) are higher than others; Cl^- and NO_3^-. These two has the stronger ionic charge density and the negative property of membrane surface can repel and reject between the ions and surface. (An, A. K. et al., 2016) tested about the zeta potential of membrane with color ions. The negative charged membrane surface can reject the negative charged dye than that the positive charged dye. There was the stronger attraction of the membrane surface and the lower permeate flux for the positive dye compared with the negative dye.

- Overall discussions of synthetic and real textile effluent treatment

According to the above discussion, the synthetic colors concentrations are changed into (400,600 and 800 ADMI), the permeate effluent was not over 8 ADMI that was lower than that of the real textile effluent. The synthetic color concentrations are twice of the real wastewater (300 ADMI), whereas the effluent value is nearly stable than the real textile effluent.

The effluent pH value of real wastewater was still in the alkaline range. The influent conductivity and TOC values were still higher than the synthetic wastewater. Therefore, the rejections efficiency is nearly same as with the synthetic black and blue concentrations. However, the effluent from the real wastewater is still above the synthetic ones.

The anions composition in real wastewater contained high content of chloride ion. Cl value is a little higher than that in the synthetic wastewater. The effluent quality could achieve more than 90% rejection efficiency. So, the use of direct contact

membrane distillation system is suitable after the pretreatment of organic compounds. The sulfate removal is so excellent for the anion removal and the opposite charge removal can be given by this direct contact membrane distillation system.

By comparing with the industrial effluent standards, the effluent from the direct contact membrane distillation system is acceptable for discharging into water environment as shown in Table 4.10. Also, the treated effluent has good water quality for further reused.

Table 4.10 Comparison with the industrial effluent standards

	Industrial Effluent Standards B.E. 2560 by the Ministry of Industry	Black	Blue	Real Wastewater
pH	5.5 - 9	Acceptable	Acceptable	Acceptable
Color	300 ADMI	<300	<300	<300
EC	-	<16 µS/cm	<18 µS/cm	<145 µS/cm

CHAPTER 5

CONCLUSIONS

This study was conducted by the direct contact membrane distillation system to treat the textile wastewater. The overall results can be summarized as follows;

1) To investigate the system efficiency, the membrane characterization, the driving parameters and the water quality were examined. The membrane was observed by the SEM, contact angle, porosity and the zeta potential. The SEM results indicated some foulants on membrane surface after system operation. The contact angle measurement shows the hydrophobic properties of the membrane. The used membrane still has the hydrophobic properties.

2) There is the lesser clogging effect on membrane with synthetic wastewater rather than with the real wastewater. The fouling can cause the reduction of membrane workability and the reduction of permeate flux. So, the combination of use of other pretreatment can give the better efficiency of the membrane.

3) The operating parameter experiment showed that by increasing temperature and the variable by the flow rate. The increasing feed temperature could give the significantly increment of permeate flux. The highest temperature (60°C) that is used in this study could give the highest flux. The higher flow rate could also give the higher permeate flux. The vapor temperature difference could give the flux changes by the Antoine equation. These two effects can give to the temperature polarization effect that can affect to the heat transfer, membrane permeability and the thermal conductivity, and give the real permeate flux. The synthetic wastewater flux can be said as the stable condition whereas the real wastewater flux was decreasing time by time. So, the fouling condition should be considered by the type of wastewater.

4) The water quality was analyzed by the Ion Chromatography, conductivity, color measurement, TOC and pH. The resulted permeate water is very satisfied to discharge the treated effluent by comparing with the Industrial Effluent Standards as well as to reuse the treated effluent for various water use purposes.

5) The color concentration cannot affect the removal efficiency of anion and the permeate water. The concentration of feed water that used in this study can affect to the flux of permeate water.

6) With many advantages, the direct contact membrane distillation system is a promising system to reduce the pollution and will be an assistance system to reuse water usage in the industry. For the treatment of industrial pollution, the system will be an assistance to reduce the environmental problems with the consideration of renewable energy and the availability of membrane material.
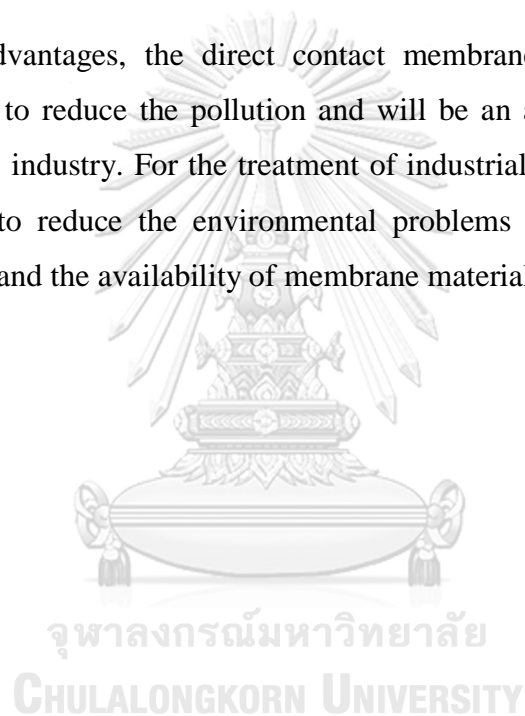
Recommendations for Future Works

To be conveniently used in practical site, some of the following recommendations are suggested for the future works for this study.

- To reduce the fouling condition and to increase the flux, the use of spacer that can increase the flow condition is recommended. And, the pretreatment of the wastewater is required to reduce the clogging of membrane pores. The combination work with other pretreatment systems could be used in the real projects.

- The simulation and computation of the system is needed to modify for the expected flux and to optimize for the temperature and the flow rate that can affect to the operating parameters for the system.

- For the long-termed use in real site, the feasibility of fouling condition and the wettability of the membrane material should be modified or the aided material like a spacer should be used.

- The working temperature should be analyzed for the energy efficiency to determine the use of the energy source.

- To be economical use of membrane distillation, the low heat loss condition and the less use of energy should be considered and investigated. In practical use, the cheap and reused energy from the waste and solar energy should be considered as one of the energy usage.

- The economical consideration, the renewable energy should be considered as the energy source. The project should be conducted with pilot project with the countability of implementation cost, the operating cost and the maintenance cost.

- Other configurations should be investigated to treat the textile wastewater to examine the efficiency of the system and to get the reliable system that is suited with the certain wastewater.

REFERENCES

Agency, U. E. P. (1996). Best management practices for pollution prevention in the textile industry.

Alkhudhiri, A., Darwish, N. and Hilal, N. (2012). Membrane distillation: a comprehensive review. Desalination, 287, 2-18.

An, A. K., Guo, J., Jeong, S., Lee, E.-J., Tabatabai, S. A. A. and Leiknes, T. (2016). High flux and antifouling properties of negatively charged membrane for dyeing wastewater treatment by membrane distillation. Water Research, 103, 362-371.

Asghar, A., Abdul Raman, A. A. and Wan Daud, W. M. A. (2015). Advanced oxidation processes for in-situ production of hydrogen peroxide/hydroxyl radical for textile wastewater treatment: a review. Journal of Cleaner Production, 87, 826-838.

Ashoor, B. B., Mansour, S., Giwa, A., Dufour, V. and Hasan, S. W. (2016). Principles and applications of direct contact membrane distillation (DCMD): A comprehensive review. Desalination, 398(Supplement C), 222-246.

Belessiotis, V., Kalogirou, S. and Delyannis, E. (2016). Chapter Four - Membrane Distillation. In *Thermal Solar Desalination* (pp. 191-251): Academic Press.

Bilińska, L., Gmurek, M. and Ledakowicz, S. (2016). Comparison between industrial and simulated textile wastewater treatment by AOPs–biodegradability, toxicity and cost assessment. Chemical Engineering Journal, 306, 550-559.

Boubakri, A., Hafiane, A. and Al Tahar Bouguecha, S. (2015). Nitrate removal from aqueous solution by direct contact membrane distillation using two different commercial membranes. Desalination and Water Treatment, 56(10), 2723-2730.

Boubakri, A., Hafiane, A. and Bouguecha, S. A. T. (2017). Direct contact membrane distillation: capability to desalt raw water. Arabian journal of chemistry, 10, S3475-S3481.

Bui, V. A., Vu, L. T. T. and Nguyen, M. H. (2010). Simulation and optimisation of direct contact membrane distillation for energy efficiency. Desalination, 259(1), 29-37.

Calabro, V., Drioli, E. and Matera, F. (1991). Membrane distillation in the textile wastewater treatment. Desalination, 83(1-3), 209-224.

Carmen, Z. and Daniela, S. (2012). Textile organic dyes–characteristics, polluting effects and separation/elimination procedures from industrial effluents–a critical overview. Paper presented at the Organic pollutants ten years after the Stockholm convention-environmental and analytical update.

Chavaco, L. C., Arcos, C. A. and Prato-Garcia, D. (2017). Decolorization of reactive dyes in solar pond reactors: Perspectives and challenges for the textile industry. Journal of Environmental Management, 198, 203-212.

Chen, T.-C., Ho, C.-D. and Yeh, H.-M. (2009). Theoretical modeling and experimental analysis of direct contact membrane distillation. Journal of Membrane Science, 330(1), 279-287.

Chen, T. Y., Kao, C. M., Hong, A., Lin, C. E. and Liang, S. H. (2009). Application of ozone on the decolorization of reactive dyes — Orange-13 and Blue-19. Desalination, 249(3), 1238-1242.

Chiam, C.-K. and Sarbatly, R. (2013). Vacuum membrane distillation processes for aqueous solution treatment—A review. Chemical Engineering and Processing: Process Intensification, 74, 27-54.

Chong, K., Lai, S., Thiam, H., Lee, S., Lau, W. and Mokhtar, N. (2016). Reactive Blue Dye Removal by Membrane Distillation using PVDF Membrane. Indian Journal of Science and Technology, 9(S1).

Chu, W. (2001). Dye Removal from Textile Dye Wastewater Using Recycled Alum Sludge. Water Research, 35(13), 3147-3152.

Dinçer, A. R., Güneş, Y., Karakaya, N. and Güneş, E. (2007). Comparison of activated carbon and bottom ash for removal of reactive dye from aqueous solution. Bioresource Technology, 98(4), 834-839.

Ding, Z., Ma, R. and Fane, A. G. (2003). A new model for mass transfer in direct contact membrane distillation. Desalination, 151(3), 217-227.

El-Bindary, A., Abd El-Kawi, M., Hafez, A., Rashed, I. and Aboelnaga, E. (2016). Removal of reactive blue 19 from aqueous solution using rice straw fly ash. Journal of Materials and Environmental Sciences, 7(3), 1023-1036.

El-Bourawi, M., Khayet, M., Ma, R., Ding, Z., Li, Z. and Zhang, X. (2007). Application of vacuum membrane distillation for ammonia removal. Journal of Membrane Science, 301(1-2), 200-209.

El-Bourawi, M. S., Ding, Z., Ma, R. and Khayet, M. (2006). A framework for better understanding membrane distillation separation process. Journal of Membrane Science, 285(1), 4-29.

Ellouze, E., Tahri, N. and Amar, R. B. (2012). Enhancement of textile wastewater treatment process using Nanofiltration. Desalination, 286, 16-23.

Erkanlı, M., Yilmaz, L., Çulfaz-Emecen, P. Z. and Yetis, U. (2017). Brackish water recovery from reactive dyeing wastewater via ultrafiltration. Journal of Cleaner Production, 165, 1204-1214.

Fanchiang, J.-M. and Tseng, D.-H. (2009). Degradation of anthraquinone dye CI Reactive Blue 19 in aqueous solution by ozonation. Chemosphere, 77(2), 214-221.

Fersi, C., Gzara, L. and Dhahbi, M. (2009). Flux decline study for textile wastewater treatment by membrane processes. Desalination, 244(1-3), 321-332.

Gryta, M., Tomaszewska, M., Grzechulska, J. and Morawski, A. W. (2001). Membrane distillation of NaCl solution containing natural organic matter. Journal of Membrane Science, 181(2), 279-287.

Gryta, M., Tomaszewska, M. and Karakulski, K. (2006). Wastewater treatment by membrane distillation. Desalination, 198(1), 67-73.

Guimarães, J. R., Maniero, M. G. and de Araújo, R. N. (2012). A comparative study on the degradation of RB-19 dye in an aqueous medium by advanced oxidation processes. Journal of Environmental Management, 110, 33-39.

Gupta, V. K., Ali, I., Suhas and Mohan, D. (2003). Equilibrium uptake and sorption dynamics for the removal of a basic dye (basic red) using low-cost adsorbents. Journal of Colloid and Interface Science, 265(2), 257-264.

Hao, O. J., Kim, H. and Chiang, P.-C. (2000). Decolorization of wastewater. Critical reviews in environmental science and technology, 30(4), 449-505.

Ibrahim, S. S. and Alsalhy, Q. F. (2013). Modeling and simulation for direct contact membrane distillation in hollow fiber modules. AIChE Journal, 59(2), 589-603.

Industry, T. (1997). Profile of the Textile Industry.

Jain, J., Singh, J. K. and Chaurasia, S. Experimental Analysis of Process Parameters on Energy Consumption for Nitrate Removal from Water Using VMD.

Jönsson, A. S., Wimmerstedt, R. and Harrysson, A. C. (1985). Membrane distillation - a theoretical study of evaporation through microporous membranes. Desalination, 56, 237-249.

Karadag, D., Turan, M., Akgul, E., Tok, S. and Faki, A. (2007). Adsorption equilibrium and kinetics of reactive black 5 and reactive red 239 in aqueous solution onto surfactant-modified zeolite. Journal of Chemical & Engineering Data, 52(5), 1615-1620.

Khalifa, A., Ahmad, H., Antar, M., Laoui, T. and Khayet, M. (2017). Experimental and theoretical investigations on water desalination using direct contact membrane distillation. Desalination, 404, 22-34.

Khayet, M. (2011). Membranes and theoretical modeling of membrane distillation: A review. Advances in Colloid and Interface Science, 164(1), 56-88.

Khayet, M., Velázquez, A. and Mengual Juan, I. (2004). Modelling mass transport through a porous partition: Effect of pore size distribution. In *Journal of Non-Equilibrium Thermodynamics* (Vol. 29, pp. 279).

Koyuncu, I. and Topacik, D. (2003). Effects of operating conditions on the salt rejection of nanofiltration membranes in reactive dye/salt mixtures. Separation and Purification Technology, 33(3), 283-294.

Lawal, D. U. and Khalifa, A. E. (2014). Flux prediction in direct contact membrane distillation. Int. J. Mater. Mech. Manuf, 2(4), 302-308.

Lawson, K. W. and Lloyd, D. R. (1997). Membrane distillation. Journal of Membrane Science, 124(1), 1-25.

Lazaridis, N. K., Karapantsios, T. D. and Georgantas, D. (2003). Kinetic analysis for the removal of a reactive dye from aqueous solution onto hydrotalcite by adsorption. Water Research, 37(12), 3023-3033.

Li, F., Huang, J., Xia, Q., Lou, M., Yang, B., Tian, Q. and Liu, Y. (2018). Direct contact membrane distillation for the treatment of industrial dyeing wastewater and characteristic pollutants. Separation and Purification Technology, 195, 83-91.

Li, Q., Xu, Z. L. and Liu, M. (2011). Preparation and characterization of PVDF microporous membrane with highly hydrophobic surface. Polymers for Advanced Technologies, 22(5), 520-531.

Liao, C.-S., Hung, C.-H. and Chao, S.-L. (2013). Decolorization of azo dye reactive black B by Bacillus cereus strain HJ-1. Chemosphere, 90(7), 2109-2114.

Mahadwad, O., Parikh, P., Jasra, R. and Patil, C. (2011). Photocatalytic degradation of reactive black-5 dye using TiO 2 impregnated ZSM-5. Bulletin of Materials Science, 34(3), 551-556.

Manawi, Y. M., Khraisheh, M., Fard, A. K., Benyahia, F. and Adham, S. (2014). Effect of operational parameters on distillate flux in direct contact membrane distillation (DCMD): Comparison between experimental and model predicted performance. Desalination, 336, 110-120.

Martínez-Díez, L., Florido-Díaz, F. J. and Vázquez-González, M. I. (1999). Study of evaporation efficiency in membrane distillation. Desalination, 126(1), 193-198.

Martínez-Díez, L. and Vázquez-González, M. I. (1999). Temperature and concentration polarization in membrane distillation of aqueous salt solutions. Journal of Membrane Science, 156(2), 265-273.

Martínez, L. and Rodríguez-Maroto, J. M. (2007). Effects of membrane and module design improvements on flux in direct contact membrane distillation. Desalination, 205(1), 97-103.

Mokhtar, N., Lau, W., Ismail, A. and Veerasamy, D. (2015). Membrane distillation technology for treatment of wastewater from rubber industry in Malaysia. Procedia CIRP, 26, 792-796.

Mokhtar, N. M., Lau, W. J. and Ismail, A. F. (2015). Dye wastewater treatment by direct contact membrane distillation using polyvinylidene fluoride hollow fiber membranes. Journal of Polymer Engineering, 35(5), 471-479.

Najafi, H. and Movahed, H. (2009). Improvement of COD and TOC reactive dyes in textile wastewater by coagulation chemical material. African Journal of Biotechnology, 8(13).

Onsekizoglu, P. (2012). Membrane distillation: principle, advances, limitations and future prospects in food industry. In *Distillation-Advances from Modeling to Applications*: InTech.

Paz, A., Carballo, J., Pérez, M. J. and Domínguez, J. M. (2017). Biological treatment of model dyes and textile wastewaters. Chemosphere, 181, 168-177.

Phattaranawik, J., Jiraratananon, R. and Fane, A. G. (2003). Effect of pore size distribution and air flux on mass transport in direct contact membrane distillation. Journal of Membrane Science, 215(1), 75-85.

Qtaishat, M., Matsuura, T., Kruczek, B. and Khayet, M. (2008). Heat and mass transfer analysis in direct contact membrane distillation. Desalination, 219(1), 272-292.

Rafiee, M. and Jahangiri-rad, M. (2014). Adsorption of Reactive Blue 19 from Aqueous Solution by Carbon Nano Tubes: Equilibrium, Thermodynamics and Kinetic Studies. Research Journal of Environmental Sciences, 8(4), 205.

Saharan, V. K., Badve, M. P. and Pandit, A. B. (2011). Degradation of Reactive Red 120 dye using hydrodynamic cavitation. Chemical Engineering Journal, 178, 100-107.

Sarti, G. C., Gostoli, C. and Matulli, S. (1985). Low energy cost desalination processes using hydrophobic membranes. Desalination, 56, 277-286.

Sathiyamoorthy, M., Gashaw, M., Tesfaye, M., Yilma, M., Tasew, T. and Fantahun, N. (2012). The removal of colour from synthetic textile dye effluent using Cellulose acetate reverse osmosis membrane. International Journal of Advanced Research in IT and Engineering, 1, 25-42.

Schofield, R. W., Fane, A. G. and Fell, C. J. D. (1987). Heat and mass transfer in membrane distillation. Journal of Membrane Science, 33(3), 299-313.

Shi, B., Li, G., Wang, D., Feng, C. and Tang, H. (2007). Removal of direct dyes by coagulation: The performance of preformed polymeric aluminum species. Journal of Hazardous Materials, 143(1), 567-574.

Shirazi, A., Mahdi, M. and Kargari, A. (2015). A review on applications of membrane distillation (MD) Process for Wastewater Treatment. Journal of Membrane Science and Research, 1(3), 101-112.

Srisurichan, S., Jiraratananon, R. and Fane, A. G. (2006). Mass transfer mechanisms and transport resistances in direct contact membrane distillation process. Journal of Membrane Science, 277(1), 186-194.

Tang, C. and Chen, V. (2002). Nanofiltration of textile wastewater for water reuse. Desalination, 143(1), 11-20.

Thomas, N., Mavukkandy, M. O., Loutatidou, S. and Arafat, H. A. (2017). Membrane distillation research & implementation: Lessons from the past five decades. Separation and Purification Technology, 189, 108-127.

Tubtimhin, S. (2002). Pollution minimization and energy saving potentials in the cotton dyeing industry. In: School of Environmental Resources and Development, Asian Institute of Technology, Thailand.

Venkatesh, S., Venkatesh, K. and Quaff, A. R. (2017). Dye decomposition by combined ozonation and anaerobic treatment: Cost effective technology. Journal of Applied Research and Technology, 15(4), 340-345.

Vlyssides, A. G., Papaioannou, D., Loizidoy, M., Karlis, P. K. and Zorpas, A. A. (2000). Testing an electrochemical method for treatment of textile dye wastewater. Waste Management, 20(7), 569-574.

Zhang, P.-Y., Yang, H. and Xu, Z.-L. (2012). Preparation of polyvinylidene fluoride (PVDF) membranes via nonsolvent induced phase separation process using a Tween 80 and H2O mixture as an additive. Industrial & Engineering Chemistry Research, 51(11), 4388-4396.

APPENDIX A

Calculation of LEP

Assume cylindrical pore, $B = 1$,

Surface tension of pure water, $\gamma = 72 \times 10^{-3}$ Nm^{-1},

Pore size, $d_{max} = 0.1 \times 10^{-6}$ m,

Contact angle, $\theta = 108°C$,

$$LEP = \frac{-2\,B\,\gamma\cos(\theta)}{d_{max}} = \frac{-2 \times 1 \times 72 \times 10^{-3} \times \cos(108)}{0.1 \times 10^{-6}}$$

LEP = 445 kPa = 4.4bar

Calculation of porosity

Density of polymer = 1765 kg/m^3,

Density of ethanol = 789 kg/m^3,

Weight of membrane damped condition = 0.0382 g,

Weight of dry membrane = 0.0157 g,

According to Equation 2.10,

$$Porosity = \frac{(0.0382-0.0157)\times 10^{-3}/789}{(0.0382-0.0157)\times 10^{-3}/789 + 0.0157\times 10^{-3}/1765} \times 100\%,$$

Porosity = 76.2 % (approximately 76%),

$$tortuosity = \frac{(2\text{-porosity})^2}{porosity} = \frac{(2-0.68)^2}{0.68} = 2.56$$

Calculation of cross-flow velocity

$$Cross\text{-}flow\ velocity = \frac{Flow\ rate}{Channel\ area}$$

Channel area is according to the Table 3.1

Channel Depth	0.19	cm
Channel Width	9.53	cm
Channel Area	1.81	cm^2

$$\text{Cross-flow velocity} = \frac{1 \text{ l/min}}{1.81 \text{cm}^2} = 0.1 \text{ m/s}$$

Reynolds Number

$$\text{Hydraulic diameter,} \quad d_h = \frac{4 \text{ A}}{\text{P}}$$

$$d_h = \frac{4 \times 9.53 \times 0.19}{2 \times (9.53 + 0.19)} = 0.3726 \text{ cm} = 3.726 \times 10^{-3} \text{m}$$

Table 5.1 Water properties with different temperatures

Temperature (°C)	Density (kg/m^3)	Viscosity (kg/m.s)
20	998.29	0.001003
40	992.2	0.000653
50	988.1	0.000547
60	983.2	0.000467

In this study, the characteristics of water were taken to estimate the data.

$$\text{Re} = \frac{\rho \, v \, d_h}{\mu}$$

Reynold's Number at 60°C, v = 0.1 m/s;

$$\text{Re} = \frac{983.2 \text{ kg/m}^3 \times 0.1 \text{m/s} \times 3.726 \times 10^{-3} \text{ m}}{0.000467 \text{ kg/m.s}} = 784.45$$

Table 5.2 Velocity and Reynold Number

Flow rate (l/min)	Velocity (m/s)	20°C Re	40°C Re	50°C Re	60°C Re
0.5	0.05	185	283	337	392
1	0.1	371	566	673	784
1.6	0.15	519	793	942	1098

จุฬาลงกรณ์มหาวิทยาลัย

CHULALONGKORN UNIVERSITY

APPENDIX B

Table 5.3 Black color data, ADMI (400), $T_f = 60°C$, $T_p = 20°C$, $v = 0.15$ m/s

Time (min)	Mass of water (g)	Permeate water (g)	Flux (kg/m2.hr)
	615.13		
15	628.66	13.53	3.865714
30	638.97	10.31	2.945714
45	652.06	13.09	3.74
60	662.18	10.12	2.891429
75	674.31	12.13	3.465714
90	685.76	11.45	3.271429
105	695.84	10.08	2.88
120	708.74	12.9	3.685714
135	719.97	11.23	3.208571
150	730.23	10.26	2.931429
165	743.83	13.6	3.885714
180	754.2	10.37	2.962857
195	764.38	10.18	2.908571
210	777.51	13.13	3.751429
225	789.65	12.14	3.468571
240	799.09	9.44	2.697143

Table 5.4 Black color data, ADMI (400), $T_f = 60°C$, $T_p = 20°C$, $v = 0.15$ m/s

Time (min)	Mass of water (g)	Permeate water (g)	Flux (kg/m2.hr)
	717.4		
15	728.06	10.66	3.045714
30	738.07	10.01	2.86
45	756.52	18.45	5.271429

60	765.8	9.28	2.651429
75	775.33	9.53	2.722857
90	791.22	15.89	4.54
105	805.36	14.14	4.04
120	816.98	11.62	3.32
135	831.13	14.15	4.042857
150	845.97	14.84	4.24
165	852.5	6.53	1.865714
180	868.15	15.65	4.471429
195	877.54	9.39	2.682857
210	890.27	12.73	3.637143
225	901.93	11.66	3.331429
240	913.81	11.88	3.394286

Table 5.5 Black color data, ADMI (400), $T_f = 60°C$, $T_p = 20°C$, v = 0.15 m/s

Time (min)	Mass of water (g)	Permeate water (g)	Flux (kg/m2.hr)
	1184.83		
15	1197.43	12.6	3.6
30	1217.77	20.34	5.811429
45	1235.88	18.11	5.174286
60	1247.23	11.35	3.242857
75	1274.47	27.24	7.782857
90	1289.34	14.87	4.248571
105	1307.76	18.42	5.262857
120	1330.33	22.57	6.448571
135	1329.97	-0.36	-0.10286
150	1348.15	18.18	5.194286
165	1365.32	17.17	4.905714

	180	1380.52	15.2	4.342857
	195	1395.01	14.49	4.14
	210	1425.32	30.31	8.66
	225	1425.34	0.02	0.005714
	240	1458.53	33.19	9.482857

Table 5.6 Black color data, ADMI (600), $T_f = 60°C$, $T_p = 20°C$, v = 0.15 m/s

Time (min)	Mass of water (g)	Permeate water (g)	Flux (kg/m2.hr)
	574.84		
15	587.37	12.53	3.58
30	609.04	21.67	6.191429
45	630.84	21.8	6.228571
60	651.66	20.82	5.948571
75	673.13	21.47	6.134286
90	695.54	22.41	6.402857
105	718.34	22.8	6.514286
120	737.16	18.82	5.377143
135	756.27	19.11	5.46
150	774.74	18.47	5.277143
165	795.49	20.75	5.928571
180	816.59	21.1	6.028571
195	840.7	24.11	6.888571
210	861.84	21.14	6.04
225	882.22	20.38	5.822857
240	901.9	19.68	5.622857

Table 5.7 Black color data, ADMI (800), $T_f = 60°C$, $T_p = 20°C$, v = 0.15 m/s

Time (min)	Mass of water (g)	Permeate water (g)	Flux (kg/m2.hr)
	714.69		
15	733.97	19.28	5.508571
30	751.23	17.26	4.931429
45	773.16	21.93	6.265714
60	799.51	26.35	7.528571
75	820.57	21.06	6.017143
90	847.49	26.92	7.691429
105	866.42	18.93	5.408571
120	889.86	23.44	6.697143
135	910.31	20.45	5.842857
150	929.63	19.32	5.52
165	950.73	21.1	6.028571
180	973.75	23.02	6.577143
195	990.81	17.06	4.874286
210	1011.69	20.88	5.965714
225	1034.53	22.84	6.525714
240	1053.3	18.77	5.362857

Table 5.8 Black color data, Phosphate (10 mg/l), ADMI (400), $T_f = 60°C$, $T_p = 20°C$, v = 0.15 m/s

Time (min)	Mass of water (g)	Permeate water (g)	Flux (kg/m2.hr)
	604.13		
15	615.01	10.88	3.108571
30	632.84	17.83	5.094286
45	652.48	19.64	5.611429
60	669.89	17.41	4.974286
75	687.97	18.08	5.165714

90	700.31	12.34	3.525714
105	717.8	17.49	4.997143
120	728.52	10.72	3.062857

Table 5.9 Black color data, Phosphate (15 mg/l), ADMI (400), $T_f = 60°C$, $T_p = 20°C$, v = 0.15 m/s

Time (min)	Mass of water (g)	Permeate water (g)	Flux (kg/m2.hr)
	731.78		
15	750.88	19.1	5.457143
30	766.98	16.1	4.6
45	784.95	17.97	5.134286
60	798.9	13.95	3.985714
75	815.78	16.88	4.822857
90	834.63	18.85	5.385714
105	846.8	12.17	3.477143
120	864.01	17.21	4.917143

Table 5.10 Black color data, Sulfate (200 mg/l), ADMI (400), $T_f = 60°C$, $T_p = 20°C$, v = 0.15 m/s

Time (min)	Mass of water (g)	Permeate water (g)	Flux (kg/m2.hr)
	630.09		
15	641.17	11.08	3.165714
30	654.17	13	3.714286
45	668.79	14.62	4.177143
60	683.64	14.85	4.242857
75	696.51	12.87	3.677143
90	711.77	15.26	4.36
105	726.46	14.69	4.197143
120	741.58	15.12	4.32

Table 5.11 Black color data, Sulfate (300 mg/l), ADMI (400), $T_f = 60°C$, $T_p = 20°C$, v = 0.15 m/s

Time (min)	Mass of water (g)	Permeate water (g)	Flux (kg/m2.hr)
	646.9		
15	657.75	10.85	3.1
30	671.8	14.05	4.014286
45	683.05	11.25	3.214286
60	693.85	10.8	3.085714
75	708.53	14.68	4.194286
90	724.6	16.07	4.591429
105	738.91	14.31	4.088571
120	751.01	12.1	3.457143

Table 5.12 Black color data, Nitrate (10 mg/l), ADMI (400), $T_f = 60°C$, $T_p = 20°C$, v = 0.15 m/s

Time (min)	Mass of water (g)	Permeate water (g)	Flux (kg/m2.hr)
	69.26		
15	81.66	12.4	3.542857
30	91.86	10.2	2.914286
45	104.08	12.22	3.491429
60	120.3	16.22	4.634286
75	128.78	8.48	2.422857
90	145.17	16.39	4.682857
105	160.82	15.65	4.471429
120	168.39	7.57	2.162857

Table 5.13 Black color data, Nitrate (20 mg/l), ADMI (400), $T_f = 60°C$, $T_p = 20°C$, v = 0.15 m/s

Time (min)	Mass of water (g)	Permeate water (g)	Flux (kg/m2.hr)
	997.6		
15	1010.54	12.94	3.697143
30	1027.34	16.8	4.8
45	1042.17	14.83	4.237143
60	1058.91	16.74	4.782857
75	1071.67	12.76	3.645714
90	1089.25	17.58	5.022857
105	1103.17	13.92	3.977143
120	1111.94	8.77	2.505714

Table 5.14 Blue color data, ADMI (400), $T_f = 60°C$, $T_p = 20°C$, v = 0.15 m/s

Time (min)	Mass of water (g)	Permeate water (g)	Flux (kg/m2.hr)
	569.85		
15	584.02	14.17	4.048571
30	598.06	14.04	4.011429
45	609.41	11.35	3.242857
60	618.47	9.06	2.588571
75	633.39	14.92	4.262857
90	648.79	15.4	4.4
105	663.17	14.38	4.108571
120	675.75	12.58	3.594286
135	687.73	11.98	3.422857
150	700.09	12.36	3.531429
165	713.06	12.97	3.705714
180	725.51	12.45	3.557143
195	740.73	15.22	4.348571

	210	755.34	14.61	4.174286
225	767.68	12.34	3.525714
240	783.63	15.95	4.557143

Table 5.15 Blue color data, ADMI (400), $T_f = 60°C$, $T_p = 20°C$, v = 0.15 m/s

Time (min)	Mass of water (g)	Permeate water (g)	Flux (kg/m2.hr)
	556.72		
15	568.85	12.13	3.465714
30	575.87	7.02	2.005714
45	588.19	12.32	3.52
60	596.59	8.4	2.4
75	606.19	9.6	2.742857
90	616.3	10.11	2.888571
105	626.68	10.38	2.965714
120	635	8.32	2.377143
135	644.38	9.38	2.68
150	654.53	10.15	2.9
165	661.77	7.24	2.068571
180	672.04	10.27	2.934286
195	681.14	9.1	2.6
210	689.13	7.99	2.282857
225	699.51	10.38	2.965714
240	913.81	9.78	3.394286

Table 5.16 Blue color data, ADMI (400), $T_f = 60°C$, $T_p = 20°C$, v = 0.15 m/s

Time (min)	Mass of water (g)	Permeate water (g)	Flux (kg/m2.hr)
	693.14		
15	719.82	26.68	7.622857
30	728.5	8.68	2.48

45	747.5	19	5.428571
60	764.42	16.92	4.834286
75	780.3	15.88	4.537143
90	800.98	20.68	5.908571
105	814.74	13.76	3.931429
120	834.11	19.37	5.534286
135	849.99	15.88	4.537143
150	863.49	13.5	3.857143
165	880.06	16.57	4.734286
180	894.88	14.82	4.234286
195	910.97	16.09	4.597143
210	922.44	11.47	3.277143
225	939.74	17.3	4.942857
240	958.89	19.15	5.471429

Table 5.17 Blue color data, ADMI (600), $T_f = 60°C$, $T_p = 20°C$, v = 0.15 m/s

Time (min)	Mass of water (g)	Permeate water (g)	Flux (kg/m2.hr)
	774.76		
15	792.24	17.48	4.994286
30	807.79	15.55	4.442857
45	822.38	14.59	4.168571
60	835.51	13.13	3.751429
75	845.7	10.19	2.911429
90	860.18	14.48	4.137143
105	874.04	13.86	3.96
120	886.22	12.18	3.48
135	902.71	16.49	4.711429
150	917.93	15.22	4.348571
165	932.03	14.1	4.028571

180	948.98	16.95	4.842857
195	958.17	9.19	2.625714
210	971.48	13.31	3.802857
225	988.04	16.56	4.731429
240	1003.54	15.5	4.428571

Table 5.18 Blue color data, ADMI (800), $T_f = 60°C$, $T_p = 20°C$, v = 0.15 m/s

Time (min)	Mass of water (g)	Permeate water (g)	Flux (kg/m2.hr)
	563.42		
15	578.24	14.82	4.234286
30	594.55	16.31	4.66
45	610.51	15.96	4.56
60	626.77	16.26	4.645714
75	643.86	17.09	4.882857
90	658.17	14.31	4.088571
105	670.85	12.68	3.622857
120	686.75	15.9	4.542857
135	702.46	15.71	4.488571
150	711.26	8.8	2.514286
165	726.73	15.47	4.42
180	743.14	16.41	4.688571
195	755.17	12.03	3.437143
210	766.23	11.06	3.16
225	781.34	15.11	4.317143
240	797.68	16.34	4.668571

Table 5.19 Blue color data, Phosphate (10 mg/l), ADMI (400), $T_f = 60°C$, $T_p = 20°C$, $v = 0.15$ m/s

Time (min)	Mass of water (g)	Permeate water (g)	Flux (kg/m2.hr)
	1145.76		
15	1160.57	14.81	4.231429
30	1181.08	20.51	5.86
45	1190.14	9.06	2.588571
60	1210.69	20.55	5.871429
75	1225.93	15.24	4.354286
90	1244.64	18.71	5.345714
105	1260.76	16.12	4.605714
120	1270.21	9.45	2.7

Table 5.20 Blue color data, Phosphate (15 mg/l), ADMI (400), $T_f = 60°C$, $T_p = 20°C$, $v = 0.15$ m/s

Time (min)	Mass of water (g)	Permeate water (g)	Flux (kg/m2.hr)
	830.7		
15	844.11	13.41	3.831429
30	858.38	14.27	4.077143
45	877.74	19.36	5.531429
60	891.38	13.64	3.897143
75	906.31	14.93	4.265714
90	919.17	12.86	3.674286
105	930.54	11.37	3.248571
120	944.2	13.66	3.902857

Table 5.21 Blue color data, Sulfate (200 mg/l), ADMI (400), $T_f = 60°C$, $T_p = 20°C$,

v = 0.15 m/s

Time (min)	Mass of water (g)	Permeate water (g)	Flux (kg/m2.hr)
	1054.33		
15	1067.1	12.77	3.648571
30	1081.85	14.75	4.214286
45	1091.18	9.33	2.665714
60	1104.13	12.95	3.7
75	1118.46	14.33	4.094286
90	1132.65	14.19	4.054286
105	1142.99	10.34	2.954286
120	1152.89	9.9	2.828571

Table 5.22 Blue color data, Sulfate (300 mg/l), ADMI (400), $T_f = 60°C$, $T_p = 20°C$,

v = 0.15 m/s

Time (min)	Mass of water (g)	Permeate water (g)	Flux (kg/m2.hr)
	1033.47		
15	1055.12	21.65	6.185714
30	1075.99	20.87	5.962857
45	1097.78	21.79	6.225714
60	1124.4	26.62	7.605714
75	1143.79	19.39	5.54
90	1164.15	20.36	5.817143
105	1183.9	19.75	5.642857
120	1203.7	19.8	5.657143

Table 5.23 Blue color data, Nitrate (10 mg/l), ADMI (400), $T_f = 60°C$, $T_p = 20°C$,

v = 0.15 m/s

Time (min)	Mass of water (g)	Permeate water (g)	Flux (kg/m2.hr)
	714.6		
15	734.39	19.79	5.654286
30	756.31	21.92	6.262857
45	778.28	21.97	6.277143
60	798.99	20.71	5.917143
75	819.1	20.11	5.745714
90	841.19	22.09	6.311429
105	863.94	22.75	6.5
120	885.27	21.33	6.094286

Table 5.24 Blue color data, Nitrate (20 mg/l), ADMI (400), $T_f = 60°C$, $T_p = 20°C$,

v = 0.15 m/s

Time (min)	Mass of water (g)	Permeate water (g)	Flux (kg/m2.hr)
	1119.25		
15	1141.15	21.9	6.257143
30	1163.29	22.14	6.325714
45	1184.38	21.09	6.025714
60	1204.23	19.85	5.671429
75	1223.27	19.04	5.44
90	1247.32	24.05	6.871429
105	1278.44	31.12	8.891429
120	1289.43	10.99	3.14

Table 5.25 Flux with color and temperature

| Color	Tf	Tp	ADMI	Flow rate (l/min)	Flux (kg/m2.hr)
Blue	40	20	400	1	0.899821
Blue	50	20	400	1	2.013393
Blue	60	20	400	1	3.8175
Blue	60	20	400	1.5	4.745536
Blue	60	20	400	0.5	2.549821
Blue	60	20	400	1.5	4.745536
Blue	60	20	600	1.5	4.228214
Blue	60	20	800	1.5	4.183214
Black	40	20	400	1	0.750893
Black	50	20	400	1	2.115714
Black	60	20	400	1	3.285
Black	60	20	400	1.5	4.8875
Black	60	20	400	0.5	3.507321
Black	60	20	400	1.5	4.8875
Black	60	20	600	1.5	5.840357
Black	60	20	800	1.5	6.046607

APPENDIX C
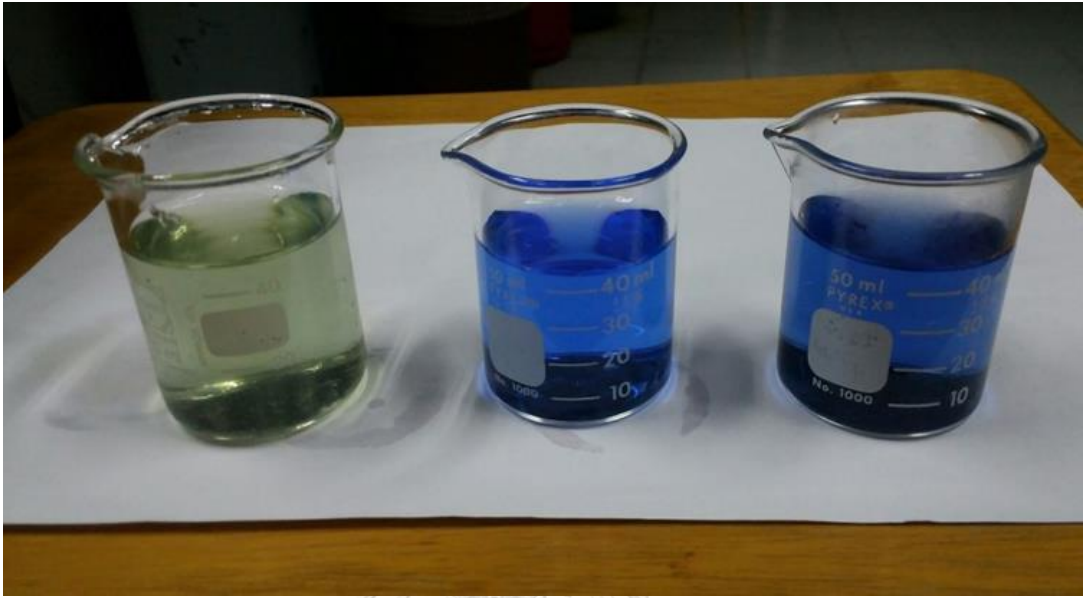
Figure 5.1 Figure of real wastewater, blue color and black color

Figure 5.2 Virgin membrane flat sheet (PVDF)

Figure 5.3 Condition of membrane sheet after treatment of wastewater
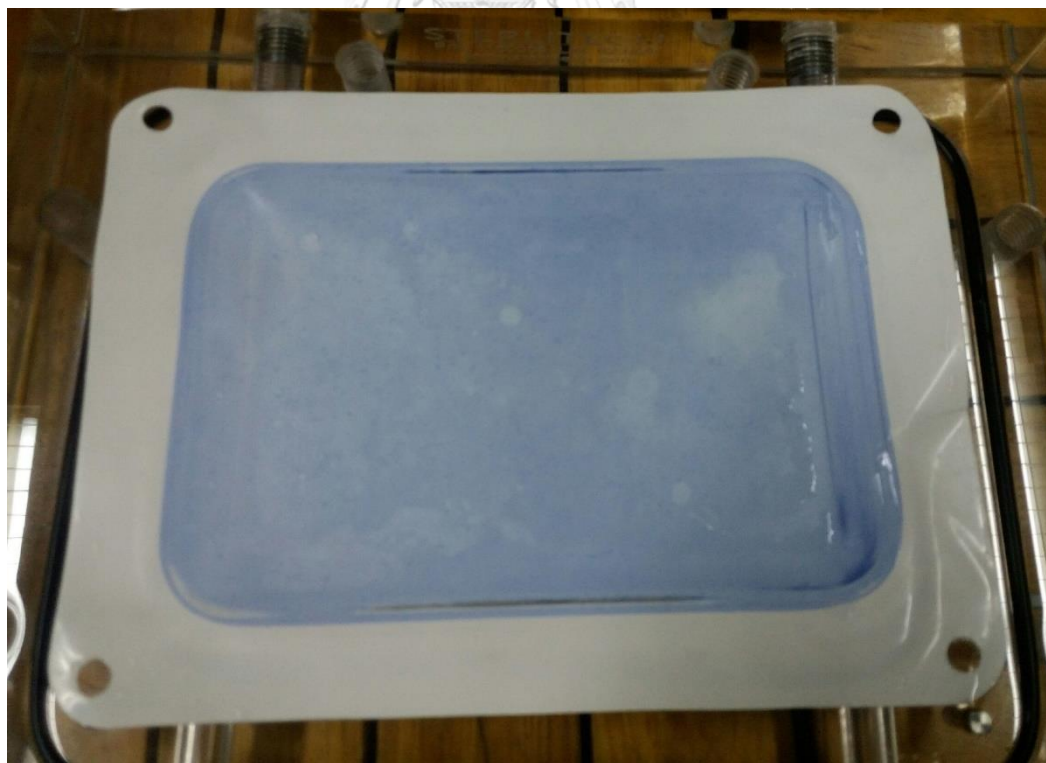

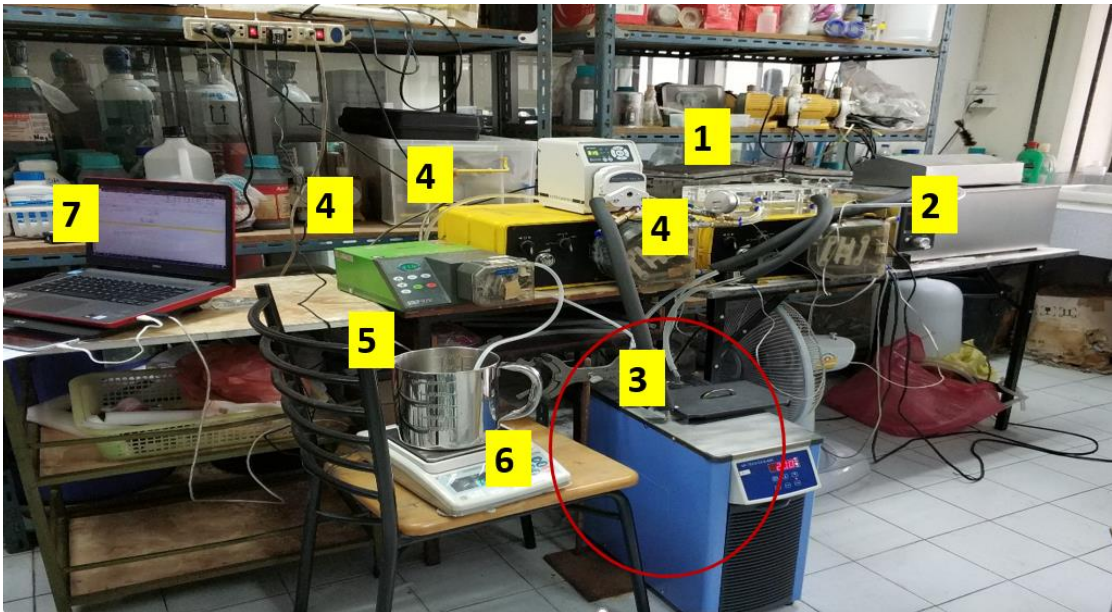Figure 5.4 Condition of membrane sheet after treatment of synthetic wastewater

Figure 5.5 Direct contact membrane distillation system layout (1 = membrane cell, 2 = hot water bath, 3 = chiller, 4 = pumps, 5 = water collecting beaker, 6 = balance, 7 = data collection system)

APPENDIX D

TOC-L Cal Curve Information
C:\TOC-L\CalCurves\Phyo\IC phyo1 17.10.18.2018 10 17 12 19 41.cal

Date of Creation	17/10/2561 12:46:10
User	
System	TOC+ASI+TN

Cal. Curve

Sample Name:	Untitled
Sample ID:	Untitled
Object ID	0L-10400100344-H54435300889-133F0191BE24-0000
Cal. Curve:	IC phyo1 17.10.18.2018 10 17 12 19 41.cal
Status	Completed
Comment:	

Type	Anal.
Standard	IC

Conc: 1.000mg/L

No.	Area	Inj. Vol.	Aut. Dil.	Rem.	Ex.	Date / Time
1	22.14	50uL	1.000	******S		17/10/2561 12:26:13
2	22.34	50uL	1.000	*******		17/10/2561 12:28:25

Sparge Gas Flow	80ml
Mean Area	22.24
SD Area	0.1414
CV Area	0.64%
Vial	4
No Washes	2

Conc: 5.000mg/L

No.	Area	Inj. Vol.	Aut. Dil.	Rem.	Ex.	Date / Time
1	28.68	50uL	1.000	*******		17/10/2561 12:34:52
2	28.20	50uL	1.000	*******		17/10/2561 12:37:13

Sparge Gas Flow	80ml
Mean Area	28.44
SD Area	0.3394
CV Area	1.19%
Vial	5
No Washes	2

Conc: 20.00mg/L

No.	Area	Inj. Vol.	Aut. Dil.	Rem.	Ex.	Date / Time
1	90.93	50uL	1.000	*******		17/10/2561 12:43:40
2	90.33	50uL	1.000	*******		17/10/2561 12:46:10

Sparge Gas Flow	80ml
Mean Area	90.63
SD Area	0.4243
CV Area	0.47%
Vial	6
No Washes	2

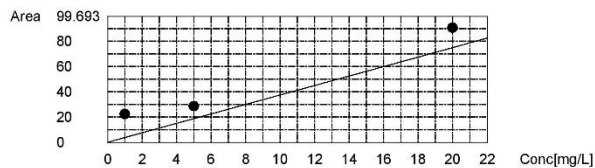|	
Slope:	3.749
Intercept	0.000
r^2	0.9859
r	0.9929
Zero Shift	Yes

1/1

Figure 5.6 Calibration curve of IC measurement

TOC-L Cal Curve Information
C:\TOC-L\CalCurves\Phyo\TC Phyo1 17.10.18..2018 10 17 11 55 00.cal

Date of Creation	17/10/2561 12:19:41
User	
System	TOC+ASI+TN

Cal. Curve

Sample Name:	Untitled
Sample ID:	Untitled
Object ID	0L-10400100344-H54435300889-133F0191BE18-0000
Cal. Curve:	TC Phyo1 17.10.18..2018 10 17 11 55 00.cal
Status	Completed
Comment:	

Type	Anal.
Standard	TC

Conc: 1.000mg/L

No.	Area	Inj. Vol.	Aut. Dil.	Rem.	Ex.	Date / Time
1	8.083	50uL	1.000	*******		17/10/2561 11:59:58
2	6.872	50uL	1.000	*******		17/10/2561 12:02:35

Acid Add.	0.000%
Sparge Gas Flow	80ml
Mean Area	7.478
SD Area	0.8563
CV Area	11.45%
Vial	1
No Washes	2

Conc: 5.000mg/L

No.	Area	Inj. Vol.	Aut. Dil.	Rem.	Ex.	Date / Time
1	23.71	50uL	1.000	*******		17/10/2561 12:08:07
2	24.24	50uL	1.000	*******		17/10/2561 12:11:00

Acid Add.	0.000%
Sparge Gas Flow	80ml
Mean Area	23.98
SD Area	0.3748
CV Area	1.56%
Vial	2
No Washes	2

Conc: 20.00mg/L

No.	Area	Inj. Vol.	Aut. Dil.	Rem.	Ex.	Date / Time
1	93.39	50uL	1.000	*******		17/10/2561 12:16:47
2	94.68	50uL	1.000	*******		17/10/2561 12:19:41

Acid Add.	0.000%
Sparge Gas Flow	80ml
Mean Area	94.03
SD Area	0.9122
CV Area	0.97%
Vial	3
No Washes	2

Slope:	4.587
Intercept	0.000
r^2	0.9996
r	0.9998
Zero Shift	Yes
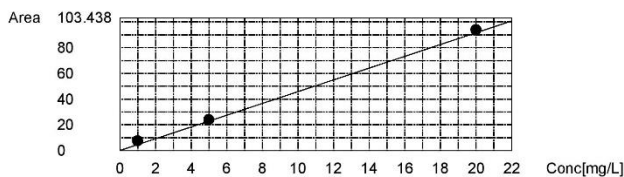
Figure 5.7 Calibration curve of TC measurement

VITA

จุฬาลงกรณ์มหาวิทยาลัย
CHULALONGKORN UNIVERSITY

REFERENCES

VITA

NAME   Miss Pyae Phyo Kywe

DATE OF BIRTH   15 November 1990

PLACE OF BIRTH   Yangon, Myanmar

INSTITUTIONS
ATTENDED   West Yangon Technological University

PUBLICATION   "Direct Contact Membrane Distillation for Decolorization of Reactive Dye Wastewater", proceeding of The 3rd Environment and Natural Resources International Conference Global Development with Environmental Sustainability on 22nd -23rd of November 2018, Chonburi, Thailand.

จุฬาลงกรณ์มหาวิทยาลัย
CHULALONGKORN UNIVERSITY